Universidad
Carlos III de Madrid

Ph.D THESIS

Design and optimization of new nanomaterials for the conservation of cultural heritage

Author:
Aránzazu Sierra Fernández

Supervisors:
Dr. Luz Stella Gómez Villalba
Dr. María Eugenia Rabanal Jiménez
Dr. Rafael Fort González

A Dissertation submitted for the degree of Doctor of Phylosophy at the
Department of Materials Science and Engineering and Chemical Engineering

University Carlos III of Madrid

Leganés, September, 2017

Universidad Carlos III de Madrid

TESIS DOCTORAL

Design and optimization of new nanomaterials for the conservation of cultural heritage

Autor:
Aránzazu Sierra Fernández

Directores:
Dr. Luz Stella Gómez Villalba
Dr. María Eugenia Rabanal Jiménez
Dr. Rafael Fort González

FIRMA DEL TRIBUNAL CALIFICADOR

Presidente:

Firma

Vocal:

Secretario:

Suplente:

CALIFICACIÓN

Leganés, Septiembre, 2017

Universidad
Carlos III de Madrid

Ph.D THESIS

Design and optimization of new nanomaterials for the conservation of cultural heritage

Author:
Aránzazu Sierra Fernández

Supervisors:
Dr. Luz Stella Gómez Villalba
Dr. María Eugenia Rabanal Jiménez
Dr. Rafael Fort González

To my family,

To my mother

"I never see what has been done; I only see what remains to be done"
Marie Curie

"Every great dream begins with a dreamer. Always remember, you have within you the strength, the patience, and the passion to reach for the stars to change the world"

H. Tubman

La presente tesis cumple los requisitos necesarios para obtener la Mención Internacional en el Título de Doctor que se describen en la normativa de enseñanzas universitarias de doctorado de la Universidad Carlos III de Madrid y que han sido establecidos en el artículo 15 del Real Decreto 99/2011 que establece la Ordenación de las Enseñanzas Universitarias Oficiales (B.O.E nº 35 del 28 de Enero de 2011, Págs. 13909-13926). Asimismo, la presente memoria de tesis ha sido informada por tres doctores pertenecientes a instituciones de educación superior de Estados miembros de la Unión Europea distintos de España:

- Dr. Angela Calia
  Italian National Council of Research-Institute of Archaeological Heritage
  CNR-IBAM
  Lecce, Italy

- Dr. Konstantinos Sotiriadis
  Institute of Theoretical and Applied Mechanics AS CR, Centre of Excellence Telč
  ITAM AS CR
  Batelovská, Czechia

- Dr. Olivera Milosevic
  Institute of Technical Sciences of the Serbian Academy of Sciences and Arts
  ITS SASA
  Belgrade, Serbia

Además, la presente memoria de tesis ha sido informada por tres doctores pertenecientes a instituciones internacionales:

- Dr. Patricia Quintana Owen
  Centro de Investigación y de Estudios Avanzados del Instituto Politécnico Nacional
  CINVESTAV
  Mérida, Yucatán, México

- Dr. Sergio Gómez Cornelio
  Laboratorio de Microbiología Aplicada, División de Ciencias Biológicas
  UJAT
  Tabasco, México

- Dr. Susana De la Rosa García
  Laboratorio de Microbiología Aplicada, División de Ciencias Biológicas
  UJAT
  Tabasco, México

Agradecimientos/Acknowledgements

Abrazando un rayo de luz es posible sentirse una estrella

Llega una de las partes más difíciles de esta tesis. Resumir en unas pocas hojas los agradecimientos que estaría dando en decenas, cientos, miles de ellas. Y es que he tenido la grandísima suerte de rodearme de gente maravillosa, generosa, que aman lo que hacen, y desde el amor y respeto lo comparten. Me siento profundamente afortunada y agradecida a todos esos rayos de luz que he tenido la suerte de abrazar, sentir y que han hecho de mi lo que hoy en día soy.

El primer agradecimiento va a mis directores de tesis, la *Dr. Luz Stella Gómez Villalba*, la *Dr. María Eugenia Rabanal Jiménez* y el *Dr. Rafael Fort González*. Trabajar con vosotros ha sido un sueño. Gracias infinitas por vuestro entusiasmo, confianza, por permitirme trabajar siempre con total libertad y por vuestra disposición cuando lo he necesitado:

Luz, *mi Luz*. Nos encontramos un 11/11/11 y míranos hoy, compartiendo este momento. GRACIAS, no sólo por haber confiado en mí, por tus conocimientos científicos, por tu forma de mirar haciendo de la escala atómica la mayor de las bellezas, sino por enseñarme además, grandes lecciones de vida. Eres una luchadora, y tienes el don de compartir tu fuerza, tu energía incansable y tu experiencia con todos los que te rodean. Nunca has perdido esta energía tan característica tuya ni en el pulso más importante de tu vida. GRACIAS por dejarme acompañarte, GRACIAS por tanto, todo y más.

Maru, GRACIAS por tu confianza, tu amor a los "rayitos", así como tu enseñanza en el campo de la Ciencia e Ingeniería de materiales siempre desde el cariño y vocación docente. Por recordarme que tan importante es el trabajo como saber parar, descansar, reflexionar y verlo todo desde otro ángulo. Nunca olvidaré las primeras emociones que sentí en los momentos de laboratorio de esta tesis. GRACIAS infinitas.

Rafa, GRACIAS por todo tu conocimiento sobre geomateriales, tu ejemplo de dedicación y trabajo siempre con la mejor de las sonrisas. Aún recuerdo una de nuestras primeras reuniones de tesis. Te encontré concentrado, cámara en mano, fotografiando el deterioro de una escultura, desde una vocación, dedicación y amor hacia el patrimonio que es ejemplar. GRACIAS por tu apoyo constante. Por tu ejemplo.

Esta tesis ha sido llevada a cabo gracias a la sinergia entre dos grupos de investigación: el grupo de investigación *Petrología Aplicada a la Conservación del Patrimonio* del Instituto de Geociencias (CSIC, UCM) y el *Grupo de Tecnología de Polvos* (GTP) del Departamento de Ciencia e Ingeniería de Materiales de la Universidad Carlos III de Madrid. GRACIAS infinitas a ambos por su inestimable ayuda siempre que lo he necesitado. Ambos grupos siempre han valorado el trabajo bien hecho por encima del resto de cosas, permitiéndome con ello crecer como investigadora. Me siento enormemente afortunada de haber formado parte de ambos.

Agradecimientos/Acknowledgements

Especialmente, mi más profundo agradecimiento:

Dentro del grupo de *Petrología Aplicada a la Conservación del Patrimonio* del Instituto de Geociencias (CSIC, UCM), liderado por Rafael Fort. GRACIAS: A la *Dr. Mónica Álvarez de Buergo*, por tus ánimos constantes, por tener siempre una sonrisa preparada, por tu profesionalidad. A la *Dr. María José Varas Muriel*, por tu apoyo, dedicación e interés hacia mi trabajo. Al *Dr. David Freire Lista* por tu entusiasmo, vocación y dedicación. A la *Dr. Elena Mercedes Pérez Montserrat* por tu energía, saber hacer y ánimo. A la *Dr. Mª Carmen Vázquez Calvo* por tu apoyo y dedicación explicando cada una de las técnicas del laboratorio. Al *Dr. Miguel Gómez Heras*, por tu calma y por ser un ejemplo a seguir. A la *Dr. Mª Inmaculada Martínez Garrido,* por tu humor, forma de ver la vida y profesionalidad. A la *Dr. Natalia Perez Ema* por tu saber hacer y apoyo. A la *Dr. Duygu Ergenç*, mi compañera en esta preciosa batalla, por tu energía y apoyo continuo. A la *Dr. Beatriz Cámara Gallego*, por tu profesionalidad y ánimo. A la *Dr. Arianna Murru*, por tu apoyo y ejemplo. A la *Dr. Nevin Mohamed*, al *Dr. Mauro F. La Russa,* a la *Dr. Giulia Forestieri*, a *Manuela Martino* y a *Vincenzo Renda*, con los que he tenido la gran suerte y lujo de compartir tiempo de laboratorio y grandes momentos. Me siento enormemente orgullosa de tener la suerte de aprender día a día de un grupo con una calidad humana y profesional incalculable. Somos una gran familia (¡Vivan los desayunos de los viernes!).
Asimismo, parte crucial integrante del grupo es el *Laboratorio de Petrofísica del Instituto de Geociencias* (CSIC, UCM), cuya directora es Mónica Álvarez de Buergo. Doy unas gracias especiales por toda la asistencia técnica en el estudio y caracterización de las muestras pétreas que conforman esta tesis doctoral a *Blanca Gallardo López*, *Cristián Zapatero Martín*, *Silvia Santos*, *Andrés Lira Aguado* e *Iván Serrano*. Asimismo, doy las gracias a *Marían Barajas*, por la realización de láminas delgadas con sumo "mimo" y dedicación, así como a *Pedro Lozano* y *Carmen Valdehita* del Laboratorio de Petrología y Geoquímica de la Facultad de Ciencias Geológicas, de la Universidad Complutense de Madrid (UCM).

Dentro del Grupo de *Tecnología de Polvos* de la Universidad Carlos III de Madrid, quiero expresar mi más sincero agradecimiento por dejarme formar parte de un grupo excepcional en todos los sentidos. Gracias al *Dr. José Manuel Torralba*, *Dr. Elena Gordo*, *Dr. Antonia Jiménez Morales*, *Dr. Mónica Campos*, *Dr. Sophia Tsipas*, *Dr. Elisa Mª Ruiz Navas, Dr. Paula Alvaredo Olmos*, *Dr. Andrea García*, así como a todas las generaciones de doctores con los que he tenido la gran suerte de compartir este increíble sueño: *Dr. Javier Hidalgo García*, *Dr. Roberto García Das Neves*, *Dr. Nerea García Rodríguez*, *Dr. Mohammad Ali Jabbari Taleghani* (Mo), *Dr. Elena Bernardo Quejido*, *Dr. Ignacio Barroso Benavente*, *Dr. Carolina Abajo Clemente*, *Dr. Alicia Paéz Pavón, Dr. Gregorio Flores Carrasco...* y, a las futuras generaciones: *Beatriz Velasco Nuñez*, *Lidia Muñoz Fernández*, *Andrea Galán Salazar*, *Julia Mª Ureña Alcazar*, *Miguel de Dios Pérez*, *Amaya García Casas*, *Marta Cartón*, *Rafael Casas Ferreras*, *Eric Macia Rodríguez*, *Andrea Alcántara García*, *Estela Prieto Muñoz*. ¡Gracias por todo GTPeros!.
Esta gratitud se extiende a los técnicos de laboratorio, quienes con su asistencia y dedicación nos facilitan enormemente el trabajo diario: *Dr. Cristina Moral Gil*, *Juan Carlos Nieto Sierra* y *Luis Alberto López Muñoz*. Gracias por la gran ayuda recibida todas las veces que lo he necesitado.
Quisiera agradecer a los demás miembros del área de *Ciencia e Ingeniería de Materiales e Ingeniería Química*, quienes siempre con una sonrisa han mostrado interés hacia mi trabajo. En especial:

Agradecimientos/Acknowledgements

Dr. Alejandro Várez Álvarez, *Dr. Belén Levenfeld Laredo*, *Carmen de la Torre Gamarra*, *Dr. Asunción Bautista Arija*, *Dr. Francisco J. Velasco López, Dr. Yahya Agzenai Ben Salem*, por tu continuo apoyo y sabios consejos (¡Viva África!), *Dr. Dania Olmos Díaz.* Así como a todos los que estuvieron y después se marcharon. Especialmente, al *Dr. Dušan K Božanić*, gracias por cuidarme, por tus *crazy ideas*, por estar siempre. ¡Cuánto se te ha echado de menos en esta última etapa de tesis!, toda mi admiración.

During the course of this Ph.D thesis, I have had the immense privilege of working in fascinating research institutions in different parts of the world, where part of this research work was made.

Firstly, I should like to express my deep gratitude to *Dr. Levente Csóka,* who opened up the doors of the *Institute of Wood based Products and Technologies* at the *University of West Hungary.* Thank you so much for all your confidence, help, support, and for introducing me in the amazing field of cellulose and paper technology and processes. It has been a complete honour working with you. I also sincerely thank all the members of the research group, especially *Dr. Dimitrios Tsalagkas* and *Dr. Katalin Halàsz,* thank you for your great help, support and all the good times! Thanks also to *Niki* and *Peter.* I wish you all the best family! I will never forget our trip to one of the most beautiful areas of the Austrian Alps. the nature is amazing! Thank you guys! I promise re-take the ukelele lessons :) *KÖSZÖNÖM!*

My gratitude also goes to *Dr. Carlos Guerrero Sánchez,* who gave me the opportunity of joining the *Laboratory of Organic and Macromolecular Chemistry*, part of the *Jena Center for Soft Matter* and the *Friedrich Schiller Universität of Jena* (Germany). Gracias Carlos por todo tu apoyo. Fue un placer haber tenido la suerte de disfrutar de tu profesionalidad. Gracias por todos los nuevos conocimientos en Ciencia de Polímeros, me siento muy afortunada de haber podido conocer tan de cerca el trabajo al más alto nivel que lleváis a cabo. The scientific and personal support provided by the involved institutions is also highly acknowledged. Asimismo, gracias a la *Dr. Nidia Estrada,* y al *Dr. Roberto Yañez-Macías,* grandísimos compañeros de aventuras en Jena. Gracias también a *Anne*. Fue maravilloso compartir momentos con todos. Asimismo, no puedo olvidarme de *Isaac Álvarez Moises*. Tenerte como estudiante Erasmus ha sido un auténtico lujo Isaac, sigue así y llegarás donde te propongas. *VIELEN DANK!*

Gracias a la obtención de una de las "*Becas Santander Iberoamérica para Jóvenes Profesores e Investigadores*" tuve la grandísima suerte de poder llevar a cabo una estancia de investigación durante 6 meses en dos instituciones en México: el *Laboratorio Nacional de Nano y Biomateriales* (LANNBIO) en el *Centro de Investigación y de Estudios Avanzados del Instituto Politécnico Nacional* (CINVESTAV), en Mérida (Yucatán) y el *Laboratorio de Microbiología Aplicada* de la *Universidad Juárez Autónoma de Tabasco* (UJAT). En estas páginas quiero agradecer profundamente todo lo aprendido durante estos intensos meses. Aprendizaje que va más allá de la Ciencia.

Primeramente, desde el CINVESTAV-LANNBIO (Mérida, Yucatán), quisiera agradecer a la *Dr. Patricia Quintana Owen*. Dr. Paty, gracias infinitas por todo lo aprendido durante este tiempo en el CINVES. Por su característica energía. Su vasto conocimiento en Ciencia e Ingeniería de Materiales ha sido una gran fuente de inspiración para mi. Asimismo, gracias por su hospitalidad y ayuda siempre que lo he necesitado haciéndome sentir como en casa. Por su lección de vida, con la guitarra y voz del *Dr. Juan Ku* de fondo (ahora es cuando podré empezar a aprender todas las canciones). Traslado mi agradecimiento a todos los miembros integrantes del LANNBIO, que siempre se preocuparon de mi bienestar con la mejor de las sonrisas.

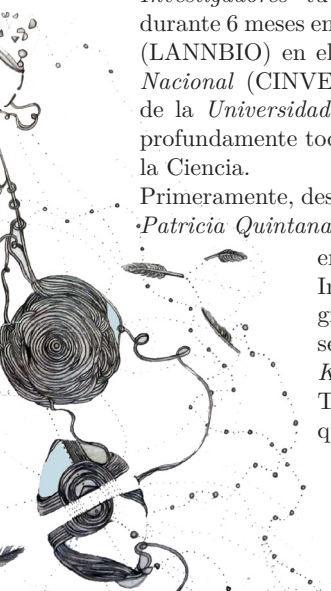

Agradecimientos/Acknowledgements

Especialmente, al *Dr. Santiago González*, por toda la ayuda ofrecida explicándome el funcionamiento del laboratorio así como sus lecciones sobre jade, con la ilusión y los ojos de un niño. Por supuesto, también por proveerme de mi "extra-dosis" de azúcar diaria :). A *Montserrat Soria Castro*, por toda su ayuda en el laboratorio así como por ser una perfecta guía de Yucatán, gracias comadre. Mención especial a los técnicos de laboratorio, que con su profesionalidad y dedicación han colaborado enormemente durante la caracterización de las muestras que conforman parte de esta tesis doctoral. Gracias a *Ana R. Cristóbal Ramos* (Anita), por alternar maravillosas imágenes de SEM con las mejores recetas de mole, a *Dora A. Huerta* por su profesionalidad microscopista y su dulzura, a *Daniel Aguilar* por su siempre disposición, ayuda en XRD y por todo. Ha sido un lujo, Gracias mil veces.
Durante mi estancia en Mérida, he tenido además el privilegio de convivir con grandes personas pertenecientes a otros departamentos de investigación que me han ayudado siempre que lo he requerido. *Dr. Geonel Rodríguez*, *Dr. Gerko Oskam*, *Dr. Juan José Alvarado Gil*, *M.C. José Bante Guerra, Dr. José Antonio Azamar Barrios*. Desde estas páginas mi más sincero agradecimiento a todos ellos. Asimismo, también he tenido el inmenso privilegio de convivir con grandes investigadores y amigos. Mención especial a las "*nanocholas*", chicas... vuestra grandeza va más allá de la escala nanométrica. Me declaro *nanochola* de por vida. Gracias a *mi Wen*, por espantarme cuando ya era tarde y aún seguía en el laboratorio, por introducirme en la cultura mexicana, desde sus recetas (prometo aplicarme ahora un poco más en la cocina), su música, su forma de ver la vida. Nuestras aventuras... jamás olvidaré lo que sentí cuando mis ojos vieron *Palenque*. Y tampoco a Pakal :). Cuando mis pies pisaron *Chichen-Itzá*, *Uxmal*, *Tulum*. Asimismo, convivir con los huicholes fue una experiencia vital difícil de olvidar. Gracias también a *Frank*, *Dena*, *Gabi* y por supuesto a *Matsua*. Asimismo, gracias a *Ram (*junto a *Gunter)*, por tu música, por ser un gran ñoño :), por tu amistad. Gracias también a *Santy*. Sois los mejores *roomies* que pude tener. Gracias a *Andrea*, *Juan*, *Gabi* (gracias también a tu maravillosa familia), *Betza*, *Willi*, a las comadres *Monse*, *Gloria*, *Melissa, Carlita, Laura,* jamás olvidaré nuestra *"tormenta tropical"* en alta mar, sois gigantes. Gracias a todos por su valiosa amistad. Ahora sí, vestida de rosa mexicano (*¡qué vergüenza!*): ¡Viva México!. Que la vida nos regale cientos de reencuentros. Por vuestra forma de cantarle a la vida.

Desde la *Universidad Juárez Autónoma de Tabasco* (UJAT) hay también mucho que agradecer. Primeramente Gracias a la *Dr. Susana Del Carmen De La Rosa García*. Dr. Susy, gracias por toda su ayuda siempre desde el cariño y profesionalidad. Sus enseñanzas en la microbiología aplicada a la conservación del parimonio, han supuesto un hermoso punto de inflexión en mi carrera investigadora. Gracias por sus triplicados, tetraplicados... su profesionalidad y rigurosidad científica. Todo un ejemplo. Extiendo mi agradecimiento al *Dr. Sergio Gómez Cornelio*. Gracias Sergio por compartir tus amplios conocimientos sobre hongos desde la absoluta humildad. Me siento inmensamente afortunada de haber tenido el privilegio de vivir su saber hacer de primera mano. Agradezco enormemente la ayuda recibida por parte del grandísimo equipo que componen el grupo del laboratorio de *Microbiología Aplicada*: *Brenda del Rosario Camacho Marín*, mi Bren, *Evvy Gerardo Rico*, *Viviana Marcela Gutierrez*, *Gibran Darvey González*, *Carlos Leyva*, *Y. Sánchez Román*. Gracias infinitas por toda su ayuda durante mi estancia en la UJAT. Chicos, son increíbles, sigan pedaleando con esa intensidad. Pronto el mundo les va a quedar pequeño. Un abrazo gigante.
Gracias también a la *Dr. Silvia Cappello*, por su energía e ilusión explicándome distintas especies micológicas. Nunca olvidaré nuestra salida de campo a Teapa. Qué belleza nos brinda la naturaleza, gracias por mostrarme su mundo con total generosidad, por esa noche estrellada. GRACIAS. Asimismo, Gracias *Santa*, por las lecciones de cocina (con Chicoché), por toda tu

ayuda. Gracias también a *Mario*.
También, agradezco al *Mtro. Ricardo Gamboa*, por enseñarme el México DF de Luis Buñuel, a ver la ciudad desde el punto de mira de "Las batallas en el desierto", junto a cientos de recomendaciones literarias y cinematográficas. Gracias por su generosidad Ricardo, es inmensa.

Agradezco la colaboración del Centro Nacional de Microscopía Electrónica de la Universidad Complutense de Madrid, por facilitar toda la infraestructura de equipos para la caracterización de las muestras de esta tesis doctoral, así como la asistencia técnica, en especial al *Dr. Juan Luis Baldonedo* y al *Dr. Adrián Gómez Herrero*. Gracias por vuestra profesionalidad y disponibilidad siempre que lo he necesitado.

Asimismo, agradezco al *Dr. Francisco Javier Alonso Rodríguez*, de la Facultad de Geología, de la Universidad de Oviedo, quien me aportó todo el material de dolomía de Laspra de esta tesis. Gracias por su sonrisa, ayuda y disponibilidad siempre que lo he necesitado.

Este trabajo no habría sido posible sin la financiación recibida por la Comunidad de Madrid y el Fondo Social Europeo a través de los programas GEOMATERIALES (2009/MAT-1585), GEOMATERIALES II (S2013/MIT-2914), CLIMORTEC (BIA2014-53911-R), ESTRUMAT (S2009/MAT-1585), MULTIMAT CHALLENGE (S2013/MIT-2862), así como al Grupo de Investigación de la Universidad Complutense de Madrid (UCM) Alteración y conservación de materiales pétreos del patrimonio (921349). Gracias.

Gracias eternas a mis *amigos*, los de siempre y los que habéis llegado en esta maravillosa etapa. Por entender mis ausencias, los "ahora no puedo, pero al rato si termino me uno", y luego el rato no llegaba. Por vuestro apoyo y comprensión. ¿Cuándo es el próximo concierto? ¿cañas-tapas? ¿cuándo volvemos a nuestro intento surfero?:)... Os quiero a todos. Gracias también a *Luis*, que vivió de primera mano parte importante de esta tesis. Gracias por tu siempre comprensión. Esta tesis es también tuya. Te mereces lo mejor de esta vida.

Gracias infinitas a mi familia, de la que me siento más que orgullosa. A mis hermanos: *Miguel* por tu fuerza, por ser un cabezota adorable, por preocuparte siempre y ser un ejemplo. A mi hermano *Pablo*, por tu valentía, por ser para mi una constante inspiración, tu siempre ayuda, por ser un ángel. A mi hermana *Nuria*, mi gemela. No puedo estar más orgullosa de ti, eres gigante mi Nuri. Aún no me queda claro que David Guetta sea *follower* tuyo pero vaya... aquí tienes la mayor de las *followers* para toda la vida y más allá :). Por haber "volado" juntas el 14 de junio y por los vuelos que aún nos quedan por vivir. A mis sobrinitos: *Paula*, qué rápido estás creciendo. Pronto celebramos todas las cosas pendientes, mi niña. Y a *Samuel*, cuánto tengo que aprender de ti pequeño gran hombrecito. Eres increible. A mi padre *Maximino*, ejemplo de trabajo incansable. Estoy segura que desde arriba estarás orgulloso de todos nosotros y del maravilloso trabajo que ha hecho mamá. A mi madre *Olga*, a quién dedico especialmente esta tesis. Por sacrificar tu vida por tus hijos siempre desde tu amor y apoyo incondicional. Por enseñarnos que desde el trabajo, la constancia y el amor no hay sueño inalcanzable y aquí estamos, cumpliendo uno de ellos. Mi estrella. Espero y deseo llegar a ser una mínima parte de la mujer que eres. Eso ya es gigante. *Os quiero.*

Gracias también a los kilómetros recorridos a golpe de zapatilla durante estos maravillosos años. Parte de esta tesis fue gestada en esos momentos. A la música (modo bucle), que tanto me ha regalado y acompañado en horas de laboratorio y ordenador. Gracias a *Billie Holiday*, *Nina Simone*, *Louis Armstrong*, *Duke Ellington* (debo tanto a "*The Great Summit*"...), *Miles Davis*.

Agradecimientos/Acknowledgements

Al gran *Bob*, *Bach*, *Max Richter*, *Explosions in the Sky*, *Coldplay*, y un largo etcétera.

Gracias también a mi primera y valiosa formación como conservadora-restauradora del patrimonio cultural. A todos los profesionales, compañeros, amigos con los que tuve el gusto de aprender, de compartir horas de laboratorio y de andamio. Aunque mi piel ahora sea otra, me siento muy orgullosa de toda la formación que he recibido. Formación que por supuesto, también ha guiado esta tesis. Gracias a todos.

Finalmente, GRACIAS al motor de todo. A la mano de los grandes maestros que han hecho posible que hoy seamos lo que somos. Gracias por vuestra herencia, legado. Por el patrimonio. Por largas colas en los museos, los monumentos. Por hacer que sienta lo que siento delante del gesto escultórico de *Rodin*, *Miguel Ángel*... la pincelada de *Velázquez*, *Goya*, *Caravaggio*, *Rembrandt*... Por hacerme pensar cada vez que piso el laboratorio que tengo el mejor trabajo posible. Por mi amor a ello. Por muchos años más. Aún queda mucho por hacer. Sigamos.

Thank you very much to all of you, Muchas gracias a todos,

• Aránzazu Sierra Fernández •

Contents

Abstract

The degradation of the stone cultural heritage represents an irreversible loss; an issue that has become urgent since the increase of natural decay caused by climate change, the impact of atmospheric pollution and/or the current use of inappropriate treatments against stone weathering. Among different degradation processes, the loss of stone cohesion and the biodeterioration produced due to the biological colonization of stone heritage, are two of the most common issues that affect stone substrates.

The present research work uses the application of nanotechnology to develop innovative strategies for improving these specific issues of crucial importance for the stone preservation. In this way, the research work consists of three main contributions:

Firstly, the design, optimization and development of new nanomaterials based on brucite ($Mg(OH)_2$) and portlandite ($Ca(OH)_2$) nanoparticles (NPs) for the consolidation of carbonatic stones were treated. Pure $Mg(OH)_2$, $Ca(OH)_2$, and mixed formulations of $Mg(OH)_2$ and $Ca(OH)_2$ NPs were synthesized by hydrothermal method and sol-gel method. The changes in experimental parameters such as synthesis temperature, time reaction and/or precursor reactivity can determine the viability of a particular synthesis design. This is why firstly; studies of the optimal synthesis method and the influence of experimental parameters on the physico-chemical properties of the nanomaterials were carried out. After this, the application of these nanoparticles on carbonatic stones (dolostone, a sedimentary rock that contains high percentage of calcium and magnesium carbonate), widely used in the cultural heritage of Spain, was investigated. The selection of the type of nanoparticles according to the petrophysical properties and chemical composition of the stone substrate was achieved. In this sense, the designed inorganic nanomaterials based on brucite and portlandite NPs constituted stable products with enhanced chemical-physical affinities f or n atural s tone.

In the second part, the combination of the strong antimicrobial activity of ZnO, with the safe-to-use antimicrobial effectiveness and good compatibility of MgO with dolostone was taken as the starting point to develop new antifungal coatings highly compatible with the built-stone heritage. Thus, the photocatalytic and antifungal properties of Zn-doped MgO ($Mg_{1-x}Zn_xO$) NPs obtained by sol-gel method, and their application as antifungal coatings for stone cultural heritage have been explored. The photocatalytic activity of the Zn-doped MgO NPs was comparatively studied with pure MgO and ZnO NPs. The antifungal activity was assessed against representative fungal species (*Aspergillus niger*, *Penicillium oxalicum*, *Paraconiothyrium* sp., and *Pestalotiopsis maculans*), which are especially active in the deterioration of stone heritage. The results showed that the

development of a high surface defects content detected in the Zn-doped MgO nanoparticles changed its surface morphology, structural properties and defect density producing thus increased photocatalytic and antifungal effectiveness in comparison with pristine MgO and ZnO nanoparticles. The development of Zn-doped MgO nanoparticles by sol-gel synthesis method, with promising multifunctional photocatalytic and antifungal properties for carbonatic stone heritage was achieved.

Finally, an additional research field was explored in the present research work with the use of different strategies to modify the cellulose surfaces and improve the interaction of adjacent fibers. The main results showed that $Mg(OH)_2$ nanoparticles synthesized via hydrothermal method were successfully deposited onto pine cellulose fibers with different refining degrees and chemical compositions. These findings also showed for the first time that the physical and mechanical properties of the pine pulp fibers can be modified by the joint action of the presence of residual lignin and heteropolysaccharides in the pulp, the low consistency refining process and the application of brucite nanoparticles.

Resumen

La degradación del patrimonio cultural construido representa una pérdida irreversible. Este riesgo se ha convertido en un problema urgente gracias al incremento del propio deterioro natural de sus materiales constituyentes, causado por el cambio climático, el impacto de la contaminación atmosférica y/o el uso de tratamientos de conservación-restauración inadecuados. Entre los diferentes procesos de degradación, la pérdida de cohesión interna y el biodeterioro producido en el patrimonio cultural por su colonización por microorganismos, constituyen dos de los problemas más comunes que afectan a los sustratos pétreos.

El presente trabajo de investigación lleva a cabo la aplicación de la nanotecnología para desarrollar estrategias innovadoras con el fin de aportar soluciones a estos problemas de importancia en la preservación del patrimonio cultural. De esta forma, la investigación ha dado lugar a tres principales contribuciones:

Primeramente, el diseño, la optimización y el desarrollo de nuevos nanomateriales basados en nanopartículas de brucita ($Mg(OH)_2$) y portlandita ($Ca(OH)_2$) para la consolidación de rocas carbonatadas fue llevada a cabo. Así, nanopartículas de $Mg(OH)_2$, $Ca(OH)_2$ y formulaciones mixtas de $Mg(OH)_2$ y $Ca(OH)_2$ fueron sintetizadas mediante método hidrotermal y sol-gel. Los cambios en los parámetros experimentales tales como temperatura de síntesis, tiempo de reacción y/o reactividad de los materiales precursores representan un papel determinante en la viabilidad de un determinado diseño de síntesis. Por este motivo, el estudio del método de síntesis más óptimo, así como la influencia de los parámetros experimentales en las propiedades físico-químicas de los nanomateriales diseñados fue llevado a cabo. Posteriormente, se estudió la aplicación de estas nanopartículas como producto consolidante en dolomía. Esta roca sedimentaria, que contiene un alto porcentaje de carbonatos de calcio y magnesio, es de sumo interés dado que ha sido ampliamente utilizado en el patrimonio cultural de España. La selección del tipo de nanomaterial de acuerdo a las propiedades petrofísicas y la composición físico-química del sustrato pétreo fue alcanzado. De este modo, los nanomateriales inorgánicos diseñados basados en nanopartículas de brucita y portlandita constituyeron productos estables con mejorada afinidad físico-química con la piedra natural.

La segunda parte de la presente investigación tomó como objetivo diseñar y desarrollar nuevos nanomateriales protectores antifúngicos altamente compatibles con el patrimonio pétreo. Para ello, se tomó como punto de partida la combinación de la actividad antimicrobiana del ZnO con la efectividad, baja toxicidad y buena compatibilidad del MgO con la dolomía. De esta forma, el estudio de las propiedades antifúngicas y fotocatalíticas de nanopartículas de MgO dopadas con Zn ($Mg_{1-x}Zn_xO$) obtenidas mediante método sol-gel, además de su aplicación como capas protectoras antifúngicas para el patrimonio pétreo construido

ha sido llevado a cabo. La actividad antifúngica ha sido estudiada frente a especies fúngicas representativas y especialmente activas en el deterioro del patrimonio pétreo (*Aspergillus niger*, *Penicillium oxalicum*, *Paraconiothyrium* sp., y *Pestalotiopsis maculans*). Los principales resultados mostraron que el desarrollo de un alto contenido de defectos detectado en las nanopartículas de $Mg_{1-x}Zn_xO$ cambió su morfología superficial, propiedades estructurales y densidad de defectos produciendo así una incrementada actividad fotocatalítica y antifúngica, en comparación con las nanopartículas de MgO y ZnO. Así, el desarrollo de nanopartículas de $Mg_{1-x}Zn_xO$ mediante método sol-gel, con propiedades multifuncionales, tanto fotocatalíticas como antifúngicas, prometedoras para la preservación del patrimonio pétreo construido fue llevado a cabo.

Finalmente, el presente trabajo exploró un campo adicional de investigación mediante el empleo de diferentes estrategias para modificar la superficie de celulosa y mejorar así, la interacción entre fibras adyacentes. Los principales resultados mostraron que las nanopartículas de $Mg(OH)_2$ sintetizadas mediante método hidrotermal fueron satisfactoriamente depositadas en fibras de celulosa de pino con diferentes grados de refinamiento y composición química. Asimismo, estos resultados mostraron que las propiedades físico químicas y las propiedades mecánicas de las fibras de pulpa de pino pueden ser modificadas por la acción conjunta de la presencia de lignina residual y heteropolisacáridos, el proceso de refinamiento a baja consistencia y la aplicación de nanopartículas de brucita.

Preface

This dissertation is submitted for the degree of Doctor of Philosophy in the Carlos III University of Madrid. The research described in this thesis has been carried out at the Department of Materials Science and Engineering and Chemical Engineering of the **Carlos III University of Madrid** and at the **Geosciences Institute IGEO (CSIC, UCM)** during the period from November 2013 to March 2017.

This research work has been developed in the frame of the projects awarded by the Community of Madrid GEOMATERIALES Programme (2009/MAT-1585), GEOMATERIALES II Project (S2013/MIT-2914), CLIMORTEC Project (BIA2014-53911-R), ESTRUMAT Programme (S2009/MAT-1585), and MULTIMAT CHALLENGE Programme (S2013/MIT-2862) and has been recognized with the mention of *International PhD*. Part of the design and development of new antimicrobial coatings has been carried out at the **Friedrich Schiller University** in **Germany** during a 30 day period and at the Center for Research and Advanced Studies of the **National Polytechnic Institute (CINVESTAV)-Unidad Mérida** and the Applied Microbiology Laboratory of the **Universidad Juárez Autónoma of Tabasco**, both in **México** during six months. In addition, the application of nanostructured metal particle adsorption to aged and fresh cellulose fibers has been researched in order to develop a protective coating thus slowing down the ageing on cultural heritage documents. This work was developed at the **University of West Hungary** and the **Institute of Wood based Products and Technologies** during a 30 day period. Moreover, four international experts in the field of Nanotechnology and Materials Science have reviewed the present manuscript.

The results obtained during the course of this thesis have been published in peer-reviewed international journals in the field of Materials Science and Chemistry, and Conservation of Cultural Heritage, such as *ACS Applied Materials & Interfaces*, *Ceramics International*, *Advanced Powder Technology*, or *RSC Advances*. Furthermore, this work has been well received at international conferences and workshops in the field of Materials Science and Chemistry. It has been mentioned in fifteen oral communications, in which four of them were as keynote/invited speaker. As well as eight contributions as poster presentations, two of which won the first place poster and excellence awards.

The research work performed and the results obtained are described in this thesis. First, the background of the scientific topic is provided and the work is placed in context in *Chapter 1*. *Chapter 2* describes the main objectives and motivation of the present Ph.D Thesis. *Chapter 3* describes the main materials and experimental techniques used. *Chapter 4* presents a summary of the key results which are reported in detail in the appended papers. These results are divided into three parts.

Part 1 (*Section 4.1.*) is related to the design and development of consolidating products, based on $Mg(OH)_2$ and $Ca(OH)_2$ nanoparticles for stone heritage.

Part 2 (*Section 4.2.*) is centered on the design and optimization of antifungal coatings. These are composed of MgO and ZnO ($Mg_{1-x}Zn_xO$, x=0.096) nanoparticles used for the antifungal protection of calcareous stone heritage.

Part 3 (*Section 4.3.*) explores other applications of the $Mg(OH)_2$ nanoparticles in the cultural heritage field such as, their application for the protection of fresh and aged cellulose fibers.

Moreover, the conclusions include an outlook and recommendations for future research and are provided in *Chapter 5.*

• *Aránzazu Sierra Fernández* •
Madrid
September 2017

List of publications

This thesis is based on the following manuscripts, which will be referred to in the text by Roman numerals:

I. New nanomaterials for applications in conservation and restoration of stony materials: A review.

Sierra-Fernandez, A.; Gomez-Villalba, L.S.; Rabanal, M.E.; Fort, R.

Materiales de Construcción. 2017, doi: 10.3989/mc.2017.070616

II. Synthesis and morpho-structural characterization of nanostructured magnesiumhydroxide obtained by a hydrothermal method.

Sierra-Fernandez, A.; Gomez-Villalba, L.S.; Milosevic, O.; Fort, R.; Rabanal,M.E. Ceramics International 40 (8), 2014, doi: 10.1016/j.ceramint.2014.04.073

URI: http://hdl.handle.net/10016/26936

III. Effect of temperature and reaction time of the synthesis of nanocrystalline brucite.

Sierra-Fernandez, A.; Gomez-Villalba, L.S.; Muñoz, L.; Flores, G.; Fort, R.; Rabanal, M.E. International Journal of Modern Manufacturing Technologies 6, 2014.ISSN 2067-3604

IV. Atomic scale study of the dehydration/structural transformation in micro andnanostructured brucite Mg(OH)2 particles: Influence of the hydrothermal synthesisconditions.

Gomez-Villalba, L.S.; **Sierra-Fernandez, A**.; Milosevic, O.; Fort, R.; Rabanal,M.E. Advanced Powder Technology, 2017, doi: 10.1016/j.apt.2016.08.014

URI: http://hdl.handle.net/10016/26938

V. Effect of morpho-structural properties on the intrinsic cathodoluminiscence emission from synthetic nanocrystalline brucite (Mg(OH)2) obtained by different synthesis processes. Gomez-Villalba, L.S.; **Sierra-Fernandez, A**.; Quintana, P.; Rabanal,M.E.; Fort, R. Submitted

VI. TEM-HRTEM study on the dehydration process of nanostructured Mg-Ca hydroxide into Mg-Ca oxide.

Gomez-Villalba, L.S.; **Sierra-Fernandez, A**.; Rabanal, M.E.; Fort, R.

Ceramics International 42 (8), 2016. doi: 10.1016/j.ceramint.2016.03.007

URI: http://hdl.handle.net/10016/26949

VII. New consolidant product based on nanoparticles to preserve the dolomiticstone heritage.

Sierra-Fernandez, A.; Gomez-Villalba, L.S; Rabanal, M.E.; Fort. R.

M.A. Rogerio Candelera (Ed.), Proceedings of the 2nd International Congress onScience and Technology for the Conservation of Cultural Heritage, Sevilla, 24-27Jun. 2014. ISBN 9781315712420.

VIII. Nuevos avances en el diseño de nanomateriales para la consolidación del patrimonio pétreo.

Sierra-Fernandez, A.; Gomez-Villalba, L.S.; Muñoz, L.; Rabanal, M.E.; Fort. R

M. Moreno Oliva, M.A. Rogerio-Candelera, J.T. López-Navarrete, V. Hernández-Jolín (Ed.). *Proceedings of the National Congress Estudio y Conservación del Patrimonio Cultural*, Málaga, 16-19 Nov., 2015. ISBN 9788460824527

URI: http://hdl.handle.net/10016/26958

IX. Consolidation of calcareous stones by Mg-Ca hydroxide nanoparticles: Treatment-Stone Interactions during Drying Revealed by Neutron Radiography

Sierra-Fernandez, A.; Gomez-Villalba, L.S.; Rabanal, M.E.; Quintana, P.; Fort, R. *Manuscript*

X. Synthesis, photocatalytic, and antifungal properties of MgO, ZnO and Zn/Mg oxide nanoparticles for the protection of calcareous stone heritage

Sierra-Fernandez, A.; De la Rosa-García, S.C.; Gomez-Villalba, L.S.; Gómez-Cornelio, S.; Rabanal, M.E.; Fort, R.; Quintana, P.

ACS Applied Materials & Interfaces, 2017, doi: 10.1021/acsami.7b06130.

XI. Application of magnesium hydroxide nanocoatings on cellulose fibers with different refining degrees

Sierra-Fernandez, A.; Gomez-Villalba, L.S.; Rabanal, M.E.; Fort, R.; Csóka, L.

RSC Advances 6, 2016, doi: 10.1039/C6RA10336G.

URI: http://hdl.handle.net/10016/26726

Additional publications not included in this PhD Thesis are:

xii. Book Chapter:

A. Sierra-Fernandez, L.S. Gomez-Villalba, S.C. De la Rosa-García, S. Gómez-Cornelio, P. Quintana, M.E. Rabanal, R. Fort. 2017. (*In press*, 2017) "Inorganic nanomaterials for the consolidation and antifungal protection of Stone heritage". In Majid Hosseini and Ioannis Karapanagiotis (Eds): *"Advanced Materials for the Conservation of Stone"*. Volume 1, *Springer International Publishing*.

xiii. Solvothermal synthesis of Ag/ZnO micro/nanostructures with different precursors for advanced photocatalytic applications

Muñoz, L.; **Sierra-Fernandez, A.**; Flores-Carrasco, G.; Milosevic, O.; Rabanal, M.E.

Advanced Powder Technology, 28 (1), 2017, doi: 10.1016/j.apt.2016.09.033

xiv. Solvothermal synthesis of Ag/ZnO and Pt/ZnO nanocomposites and comparison of their photocatalytic behaviors on dyes degradation

Muñoz, L.; **Sierra-Fernandez, A.**; Milosevic, O.; Rabanal, M.E.

Advanced Powder Technology, 27 (3), 2016, doi: 10.1016/j.apt.2016.03.021.

xv. Synthesis, characterization and photocatalytic properties of nanostructured ZnO particles obtained by low temperature air-assisted-USP

Flores, G.; Carillo, J.; Luna, J.A.; Martínez, R.; **Sierra-Fernandez, A.**; Milosevic, O.; Rabanal, M.E.

Advanced Powder Technology, 25 (5), 2014, doi: 10.1016/j.apt.2014.02.004.

List of Figures

List of Abbreviations

Abbreviation	Description
A. niger	*Aspergillus niger*
BSE	Back-scattered Electron Detector
CL	Cathodoluminescence
CLSI	Clinical and Laboratory Standards Institute
CrI	Crystallinity Index
CTMP	Chemi-Thermo Mechanical Pulp
DSC	Differential Scanning Calorimetry
EDX	Energy Dispersive X-ray Spectroscopy
EELS	Electron Energy Loss Spectroscopy
ESEM	Environmental Scanning Electron Microscopy
FESEM	Field Emission Scanning Electron Microscopy
FFT	Fast Fourier Transformation
FWHM	Full width at half maximum
HRTEM	High Resolution Transmission Electron Microscopy
JCPDS	Joint Committee on Powder Diffraction Standars
MIC	Minimum Inhibitory Concentration
MIP	Mercury Intrusion Porosimetry
NPs	Nanoparticles
NR	Neutron Radiography
PDA	Potato Dextrose Agar
PL	Photoluminescence
PLOM	Polarized Light Optical Microscopy
P. maculans	*Pestalotiopsis maculans*
P. oxalicum	*Penicillium oxalicum*
RH	Relative Humidity
SAED	Selected Area Electron Diffraction
SE	Secondary Electrons
SEM	Scanning Electron Microscopy
T	Temperature
TEM	Transmission Electron Microscopy
TGA	Thermogravimetric Analysis
UV	Ultraviolet
wt	Weight Percent
XRD	X-Ray Diffraction

CHAPTER 1

Paper I:

New nanomaterials for applications in conservation and restoration of stony materials: *A review*
Sierra-Fernandez, A.; Gomez-Villalba, L.S.; Rabanal, M.E.; Fort, R.
Materiales de Construcción. **2017**, doi: 10.3989/mc.2017.070616

Introduction and State of Art

Chapter 1

Introduction and State of Art

While the development in material science has generated important nanostructured materials long time ago, conservation of cultural heritage was, until recently, mainly based on the traditional conservation and restoration treatments. These traditional methods often lack the vital compatibility with the original substrate and a durable performance. More recently, nanomaterials have been proposed for the improvement of conservation strategies of the built and sculptural heritage with the aim to improve the consolidation and protection treatments of damaged building materials (*Figure 1.1.*). The use of nanotechnology also creates possibilities to produce construction materials with enhancing material properties and novel functionalities. Thereby, nanotechnology has an important impact in the cultural heritage conservation science and the construction sector, improving the safety of the buildings, the durability and the consequently enhanced performance of construction materials and the energy efficiency.

This chapter presents a comprehensive study of the state of art on the application of nanotechnology to the conservation and restoration of the stony cultural heritage. Thereby, the different types of nanomaterials currently used to produce conservation treatments for consolidation, water repellent, as well as for protection with self-cleaning and antimicrobial properties are reviewed in detail below in *Paper I.*

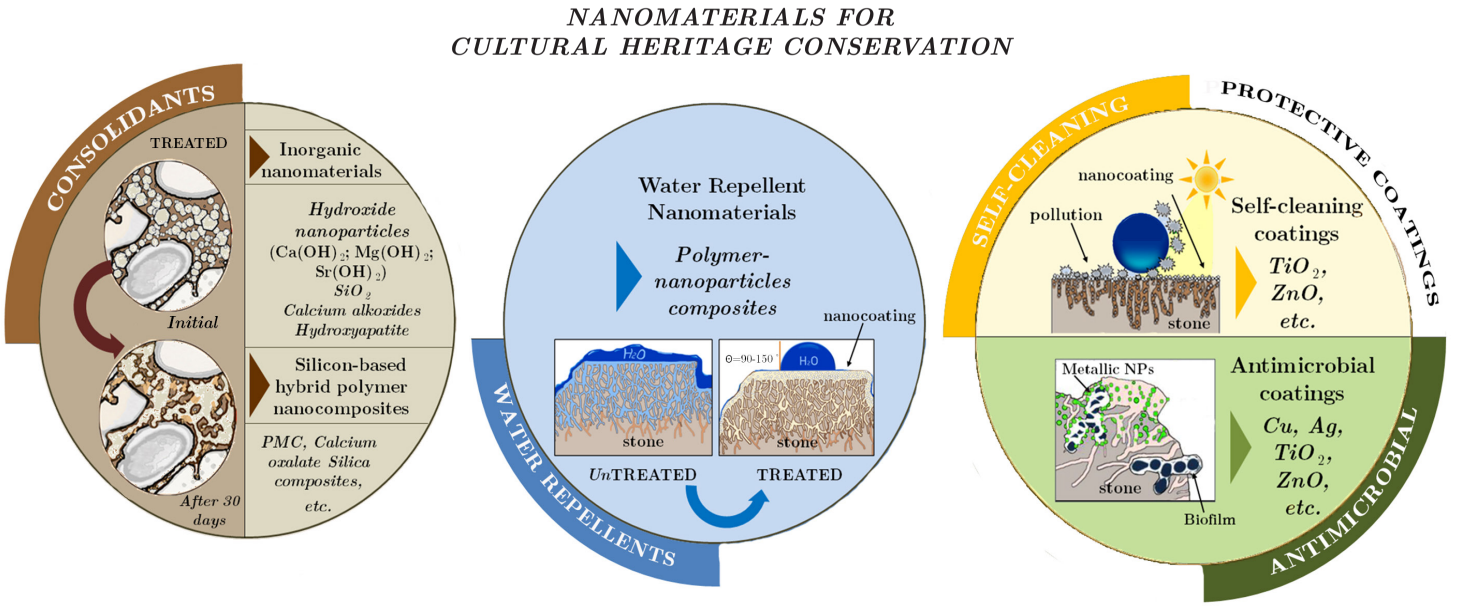

Figure 1.1.: *Schematic illustration of the current nanomaterials specifically designed for consolidation, water repellence, as well as for self-cleaning and antimicrobial treatments for the cultural heritage conservation.*

Paper I

New nanomaterials for applications in conservation and restoration of stony materials: *A review*
Sierra-Fernandez, A.; Gomez-Villalba, L.S.; Rabanal, M.E; Fort, R.

Reprinted with permission from
Materiales de Construcción, **2017,** doi: 10.3989/mc.2017.070616

CHAPTER 2

Motivation and Objectives

Chapter 2

Motivation and Objectives

The aim of this Ph.D. dissertation was the design, the optimization and the development of **new inorganic nanomaterials** for the **conservation of cultural heritage objects**. The present Ph.D. dissertation constitutes thus an example of synergy and integration between research and conservation science, which is necessary to ensure a future for our rich past. Thus, the research work is divided into three parts, with each one focused on providing solutions to a single specific issue of paramount importance in the field of cultural heritage conservation. The specific objectives to reach are described below (grouped by their corresponding part), and are schematically represented in *Figure 2.1.*

2.1. PART I. Consolidating products, based on magnesium hydroxide ($Mg(OH)_2$) and calcium hydroxide ($Ca(OH)_2$) nanoparticles

2.1.1. Motivation

Carbonate stones have been widely used since ancient times in architecture and sculpture and are subject to several physical and chemical weathering mechanisms (for more details see *Chapter 1*). Mostly due to the susceptibility of dolomite and calcite, which are their main constituents. Both types of minerals have a relatively high solubility, which makes them prone to dissolution with the acidic rain, causes anisotropic deformation due to thermal cycles, and are also pronely vulnerable to the formation of black crusts. Moreover, carbonate stones may be especially porous, thus susceptible to other phenomena, such as freeze-thaw cycles or salt crystallization. In this way, the damage experienced by these materials generates a significant loss of internal cohesion that makes the application of consolidant products necessary.

As mentioned in previous *Chapter 1*, consolidant products based on calcium hydroxide nanoparticles are one of the most commonly used nanomaterials for stone consolidation. Significant progress has been achieved using this type of nanoparticles as consolidating products in dolostone and calcitic dolostones, getting an improvement in their physical properties and increasing the resistance of stone to aging [1-3]. However, it is important to notice certain points according to their compatibility with the stone substrate to treat because the proportions of magnesium and calcium in dolostones and limestones often differ widely both within a single rock formation and between formations. It is of great significance to assess whether their characteristics are compatible or not with petrological and/or mineralogical aspects, diagenetic and geochemical conditions, or mineralogical, or local environmental factors they are exposed and amend the process and therefore its effectiveness [4]. Thereby, variables

such as the possible Mg^{2+} / Ca^{2+} ion exchange in the stone-consolidant system, the influence of particle size on carbonation kinetics or the surface tension differences in the medium, have to be taken into account [5]. Thus, the application of calcium hydroxide nanoparticles in dolostone could generate recrystallized nano-calcite, leading the dolomite dissolution due to the calcium ion enrichment [6]. The incorporation of the $Ca(OH)_2$ nanoparticles and their subsequent carbonation on $CaCO_3$, entails a change in the dolomite crystals of dolostones. Any modification in the nucleation and growth of crystals may produce aesthetic modifications, such as changes in color or brightness [7]. In this way, the dedolomitization is an important risk arising as a result of the use of $Ca(OH)_2$ nanoparticles for the dolostone consolidation. In alkaline conditions, the dolomite can react with these alkali hydroxides causing a fine intergrowth of brucite, calcite and alkali carbonates. This process would regenerate alkalis and thus allows a continued reaction with the dolomite [8]. Therefore, the effectiveness of the use of calcium hydroxide nanoparticles is severely reduced in dolostone substrates.
In order to solve this demanding task and to develop appropriate consolidant treatments with increased compatibility with the stone substrate to treat, further research is needed, becoming in a crucial challenge to be overcome. So to assure an optimal consolidant result, the chemical composition of the nanoparticles-based consolidant products should mirror as much as possible that of the stone substrate to treat. Having this premise in mind, the use of mixed $Ca(OH)_2$ and $Mg(OH)_2$ nanoparticles for the consolidation of dolostone was proposed in this thesis work. The application of these types of hydroxides as consolidating product represents an example of adapting the consolidant composition to that of the substrate in search of better compatibility, effectiveness and durability of the treatment, and was the main aim of the First Part of this Ph.D dissertation.

2.1.2. Objectives

The main objective of the **First Part** of the present Ph.D dissertation was **the design, the optimization and the development of controlled consolidating products based on $Mg(OH)_2$ and $Ca(OH)_2$ nanoparticles,** highly **compatible** with a large part of the **built and sculptural heritage.** The following partial objectives derive from the previous general one:

- The synthesis and the morpho-structural characterization of functional $Mg(OH)_2$ nanoparticles obtained by hydrothermal method.
    - Developing and optimization of the synthesis parameters in order to obtain pure $Mg(OH)_2$ nanoparticles.
    - Assessing of the influence of the synthesis parameters (effect of synthesis temperature, reaction time and reactant concentrations) in the physico-chemical properties of the different nanoparticles of brucite obtained.

- Synthesis and physico-chemical characterization of functional $Mg(OH)_2$ nanoparticles obtained by sol-gel method.
    - Optimization of the synthesis parameters in order to obtain $Mg(OH)_2$ nanoparticles with suitable and potential physico-chemical properties.
    - Carrying out the comparative study of the sol-gel synthesis method and the

hydrothermal route in order to determine the most suitable synthesis method to obtain nanoparticles with high potential for the cultural heritage preservation.

- To select the optimal synthesis method to obtain hydroxide nanoparticles with high compatibility with the stone materials.
- The synthesis and the morpho-structural characterization of functional $Mg(OH)_2$ and $Ca(OH)_2$ nanoparticles with different % weight ratio, specifically selected according to the chemical composition of the stone substrates to treat.
    - Developing and optimization of the synthesis parameters in order to obtain pure $Mg(OH)_2$ and $Ca(OH)_2$ nanoparticles in a 10:90%, 90:10% and 50:50% weight ratio.
- Investigation of the influence of particle size, particle orientation and morphological characteristics on the carbonation kinetic.
- Study of the stability of the selected synthesized hydroxide nanoparticles at atomic scale level through their dehydration reaction.
- Selection of the most optimal nanoparticles to be used as consolidating product for dolostone and limestone lithotypes.
- Determination of the most effective procedure for consolidant application on porous dolostones and limestones.
- Evaluation of the effectiveness and compatibility of the most promising hydroxide nanoparticles as consolidating nanomaterials in carbonatic stone.
- Investigation of the use of Neutron Radiography as a new non-destructive technique for the study of stone treatments.

2.2. PART II. New antifungal protective coatings for the protection of carbonatic stone heritage

2.2.1. Motivation

Unfortunately, no work of art is immune to microbial colonization. Archaeological historic stone monuments and artworks are exposed to the effects of biological deterioration factors. Thereby, microorganisms are a threat to monuments worldwide, as they are always present in the environment, and waiting for the optimal conditions to occur in order to flourish. This is particularly alarming in tropical regions or areas with high levels of humidity [9]. Therefore, biodeterioration is considered one of the main degradation processes of outdoor stone heritage. These microbial agents can deteriorate stone because they secrete enzymes and organic acids during their metabolic processes, highly harmful for monumental stones. These organic acids can cause solubilization or chelation of different minerals present in the stone composition. In addition, the generation of biological patinas on stone surfaces can change the diffusion of water vapor into the material and in

the capillary water uptake, alongside the chromatic changes caused by a series of biogenic pigments [10, 11]. Among all microorganisms, fungi are considered the most active microorganisms in the biodeterioration of stone substrates [12].

To address this important problem, conservation strategies usually aim to reduce the bioreceptivity characteristics, for example by applying water repellent coatings with antifungal properties. However, these current chemical treatments used to avoid biodeterioration are unfortunately not capable of inhibiting biological recolonization for long periods of time. Besides, well-known problems of these biocides are their high toxicity or the risk of producing harmful subproducts, which can cause chromatic alterations, dissolution of calcite or oxidation of minerals [13].

In order to solve this demanding task, the Second Part of the present Ph.D. dissertation aims to engineer novel antifungal protective coatings, following the idea of combining the strong antimicrobial activity of ZnO with the safe-to-use antimicrobial effectiveness and high compatibility of MgO with the dolomite stones to prevent the colonization of lithic microorganisms on stone-built heritage.

2.2.2. Objectives

The main objective of the **Second Part** of the present thesis was **to engineer new nanomaterials with enhanced antifungal properties** that will act as protective coatings to help prevent biodeterioration in the cultural stone heritage. The following are the partial objectives to be achieved for the fulfillment of the main objective of this research work.

- The synthesis and the morphological microstructural and chemical analysis of multifunctional MgO, ZnO and Zn-doped MgO ($Mg_{1-x}Zn_xO$) nanoparticles obtained by sol-gel method.
- Investigation of changes in the photocatalytic and antifungal capacities of MgO nanoparticles with Zn doping.
- Study of the photocatalytic efficiency of the different types of nanoparticles in order to determine multifunctional properties of the nanoparticles studied.
- Investigation of the photoluminescence properties of the synthesized systems.
- To determine the antifungal activity of the different synthesized nanoparticles against different fungal species isolated from stones with a biogenic surface, and potentially active in the biodeterioration of stone heritage.
    - Study of the antifungal activity for each type of synthesized nanoparticles against *Aspergillus niger*, *Penicillium oxalicum*, *Paraconiothyrium* sp. and *Pestalotiopsis maculans,* using the agar well diffusion assay, and also to establish their minimum inhibitory concentrations (MICs) by microdilution method in culture broth.

- Selecting the most effective type of nanoparticles for the antifungal protection of stone substrates (dolostone and limestone).
- Study of the bioreceptivity to fungal colonization of the different lithotypes, with a particular focus in to determine the influence of the petrophysical properties of the stone substrates over their susceptibility for fungal colonization.
- Investigation of the antifungal effectiveness of the nanoparticles as protective coatings.
    - To establish a methodology for studying the efficiency of the nanoparticles as antifungal coatings for stone heritage.
    - Determining of their antifungal properties as coatings using different substrates: glass microscope slides and stone substrates: dolostone (Laspra dolostone, Spain) and limestone (Conchuela limestone, México).
    - Determining and characterization of the induced damage by the biological activity in the different stone substrates with a particular focus on the spread and the depth of the hyphal penetration component according to the influence of the type of nanoparticles-based treatment and the petrophysical properties of the stone.

2.3. PART III. Application of $Mg(OH)_2$ nanoparticles on cellulose fibers

2.3.1. Motivation

Cellulose is one of the most abundant natural carbohydrate resources on Earth and an important raw material. In order to preserve the paper materials, the use of alkaline earth hydroxide or carbonate nanoparticles has been proposed to stably neutralize pH [14]. This part of the present Ph.D. thesis explores additional applications of the brucite nanoparticles over the cultural heritage conservation field. In this way, $Mg(OH)_2$ nanoparticles synthesized by hydrothermal method have been studied for the modification of cellulose sheets prepared with different methods in order to improve their final physico-chemical properties, creating highly aging-resistant cellulose fiber sheets.

2.3.2. Objectives

The main objective of the **Third Part** was to explore how **highly aging-resistant cellulose fiber sheets** can be obtained by the **refining** of their chemical pulp and their **modification with magnesium hydroxide nanoparticles**. The aim of the study is accomplished through the following steps:

- Preparation and characterization of cellulose fiber sheets with different refining degrees and chemical compositions (bleached and unbleached pine cellulose fibers and their 50% / 50% mixture).
- Treatment of cellulose fiber sheets with magnesium hydroxide nanoparticles obtained by hydrothermal method. Focusing in:

  - Investigation of the influence of the refining degree of the different cellulose composites in their treatment with the brucite nanoparticles.
  - Determination of the influence of the chemical composition of the different types of cellulose composites in their modification with the nanoparticles.
  - Establishing of the influence of the methodological application (spraying and immersion) of the $Mg(OH)_2$ nanoparticles on the treatment of the cellulose sheets.

- Exploration of the possible changes induced by the magnesium hydroxide nanoparticles on the morphological, smoothness, mechanical properties and pH variation of the different types of treated cellulose sheets.

- To study the ageing resistance of the different untreated and $Mg(OH)_2$ treated cellulose fiber sheets.

Figure 2.1.: *Representative scheme of the specific objectives of the present PhD Thesis.*

2.4. References

[1] Chelazzi, D.; Poggi, G.; Jaidar, Y.; Toccafondi, N.; Giorgi, R.; Baglioni, P. (2013) Hydroxide nanoparticles for cultural heritage: consolidation and protection of wall paintings and carbonate materials. *J. Colloid Interface Sci.*, [392], 42-49.

[2] Ziegenbalds, G. (2008) Colloidal calcium hydroxide: a new material for consolidation and conservation of carbonate stone, En: *11th International Congress on deterioration and conservation of stone III*, 1109.

[3]López-Arce, P.; Zornoza-Indart, A.; Gomez-Villalba, L.S.; Fort. R. (2012) Short-and Longer-Term Consolidation Effects of Portlandite ($Ca(OH)_2$) Nanoparticles in Carbonate Stones. *J. Mater. Civil Eng.*, 25 (11), 1655-1665.

[4] Gomez-Villalba, L. S., López-Arce, P., de Buergo, M. A., Zornoza-Indart, A., & Fort, R. (2013). Mineralogical and textural considerations in the assessment of aesthetic changes in dolostones by effect of treatments with $Ca(OH)_2$ nanoparticles. *Science and Technology for the Conservation of Cultural Heritage,* 235-329.

[5] Gomez-Villalba, L. S., López-Arce, P., Alvarez de Buergo, M., & Fort, R. (2011). Structural stability of a colloidal solution of $Ca(OH)_2$ nanocrystals exposed to high relative humidity conditions. *Applied Physics A: Materials Science & Processing*, 104 (4), 1249-1254.

[6] Gomez-Villalba, L. S., López-Arce, P., de Buergo, M. A., Zornoza-Indart, A., & Fort, R. (2013). Mineralogical and textural considerations in the assessment of aesthetic changes in dolostones by effect of treatments with $Ca(OH)_2$ nanoparticles. *Science and Technology for the Conservation of Cultural Heritage*, 235-329.

[7] López-Arce, P.; Gomez-Villalba, L.S.; Pinho, L.; Fernández-Valle, M.E.; Álvarez de Buergo, M.; Fort, R. (2010) Influence of porosity and relative humidity on consolidation of dolostone with calcium hydroxide nanoparticles: effectiveness assessment with non-destructive techniques. *Mater.Charact.,* 61, 168-184.

[8] Deng, M.; Mingshu, T. (1993) Measures to inhibit alkali-dolomite reaction. *Cement Concrete Res.* 23 (5), 1115-1120.

[9]Gómez-Ortiz, N.M.; González-Gómez, W.S.; De la Rosa-García, S.C.; Oskam, G.; Quintana, P.; Soria-Castro, M.; Gómez-Cornelio, S.; Ortega-Morales, B.O. (2014) Antifungal activity of $Ca[Zn(OH)_3]_2] \bullet 2H_2O$ coatings preservation of limestone monuments: An in vitro study. *Int.Biodeterior. Biodegradation*, 91, 1-8.

[10] Gaylarde, C.; Ribas Silva, M.; Warscheid, TH. (2003) Microbial impact on building materials: an overview". *Mater. Struct.* 36, 342-352.

[11] De los Ríos, A; Pérez-Ortega, S; Wierzchos, J; Ascaso, C (2012) Differential effects of biocide treatments on saxicolous communities: Case study of the Segovia cathedral cloister (Spain). *Int. Biodeterior. Biodegradredation*, 67, 64-72.

[12] Gadd, G.M. (2017) Geomicrobiology of the built environment. *Nat. Microbiol.*, 2, 16275.

[13] Nugari, M.P.; Salvadori, O (2002) Biocides and treatment of stone: Limitations and future prospects. En: *Art, Biology and Conservation. Biodeterioration of works of art. The Metropolitan Museum*, 518-535.

[14] Giorgi, R.; Bozzi, C.; Dei, L.; Gabbiani, C.; Ninham, B.W.; Baglioni, P. (2005) Nanoparticles of $Mg(OH)_2$: synthesis and application to paper conservation. *Langmuir*, 21, 8495-8501.

CHAPTER 3

Materials and Methods

Chapter 3

Materials and Methods

3.1. Stone substrates

Petrographic studies were carried out on representative samples of the Laspra and Conchuela stones using the Polarized Light Optical Microscopy (PLOM) with transmitted light under parallel and crossed nicols. Representative thin sections having a surface of 3 cm x 2 cm and a thickness of 30 micrometers were prepared and observed in an OLYMPUS BX51 petrographic optical microscope equipped with digital camera.

3.1.1. Laspra dolostone (Asturias, Spain)

The petrographic studies allowed classifying the Laspra dolostone as a fossiliferous dolomicrite. The microcrystalline matrix consists of predominant dolomitic mud and anhedral calcitic mosaics (~4.25 µm) developing the typical micritic texture (*Figure 3.1*).

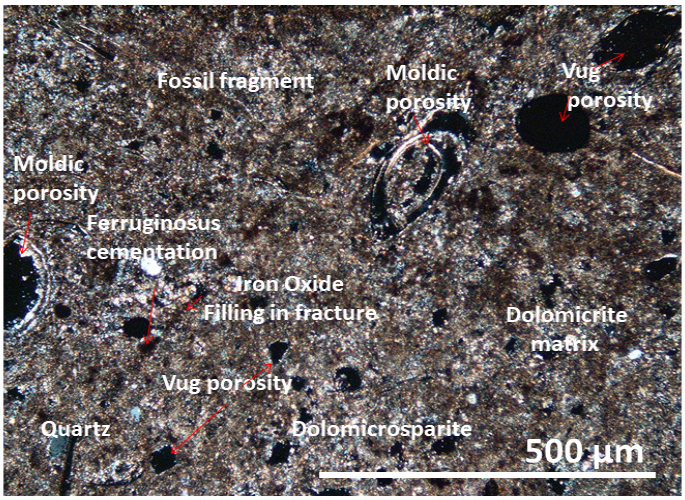

Figure 3.1. *Fossiliferous dolomicrite from Laspra stone showing bioclasts of molluscs in the dolomicritic matrix. Moldic and vug porosities are observed. Polarized light optical microscope image (crossed nicols).*

Some of the calcitic mosaics are recrystallized developing microsparite (~10 µm). Well preserved bioclasts (8%) corresponding to fragments of mollusc

shells and foraminifera are frequently present in the very fine-grained dolomitic mud (*Figure 3.2.*). Occasionally, detrital minerals mixed with the carbonate matrix are observed, especially quartz (~59 µm) randomly distributed (~5%) and clay minerals. Iron oxides are present filling fissures or as cementing material around the calcareous microcrystals. Fragments of foraminifera are well preserved developing rounded clasts (38-40 µm). Sometimes, the skeletal grains have been cemented by iron oxides films as overgrowth around the chambers.

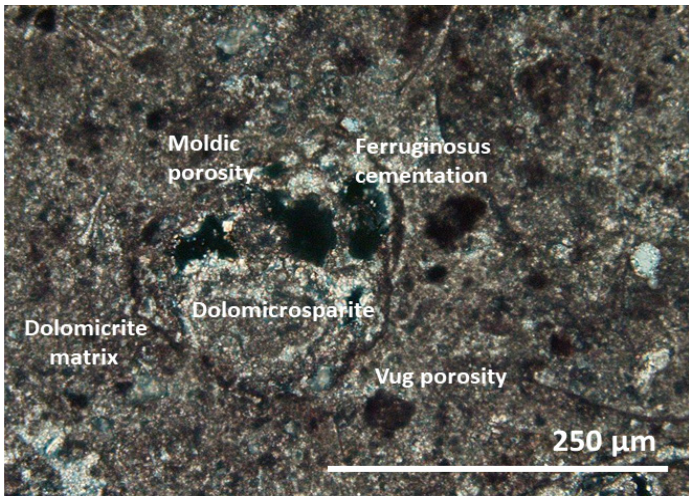

Figure 3.2. *Detail of the fossiliferous dolomicrite from Laspra stone showing a moldic porosity outlined by dolomicrosparite. The overgrowth indicates a cementation with clay minerals and iron oxides. Internal pores (45-55 µm) in the mold of mollusc shell are present. The shell filling with iron oxides varies between 7.5 and 9 µm. Besides vug porosity is observed as scattered pores (17-44 µm) affecting the dolomicritic matrix. Polarized light optic microscope image (crossed nicols).*

The mollusc molds raise diameters ~227 µm to 260 µm, with frequent cementation of microsparitic calcite (7.7 µm). The porosity reaches the order of 15% to 20% being able to group mainly in two general categories, moldic and secondary vugs. The moldic porosity is observed in the inner part of the fossil chambers, which is produced by dissolution of the sparitic cement. Moldic secondary voids, easily recognizable in the mollusc molds, are developed in the interstitial crusts preserving sometimes the earlier cementation of sparitic growth. The secondary vug porosity is observed as rounded or sub-rounded pores in two types of sizes, as small pores with diameters around 34 to 52 µm or bigger sizes reaching 175 µm. Furthermore, some vugs appear as scattered rhombs or sub-angular shapes (~55 µm to 64 µm), whose pore walls are partially cemented by microsparite(~5.5 µm). Besides, inter-crystalline porosity is preserved or appears partially filled with fine particulate carbonate mud.

3.1.2. Conchuela limestone (Yucatán, México)

The petrographic characteristics of the Conchuela stone under polarized light optical microscopy indicated its classification as biomicritic limestone with a high content of fossil fragments (*Figure 3.3.*). The bioclasts/matrix relationship becomes of the order of 80%/20%. The predominant porosity is inter-particular, which has been partially cemented by microsparite, giving place to internal porosity with irregular morphologies and sizes around 0.6 mm to 1 mm. This porosity reaches values of 10%. Besides, moldic and fissural porosities are also common. Cracks affecting the fossil fragments and part of the matrix are visible (*Figure 3.4.*). Internally the cracks are filled by phyllosilicates or cemented by thin veins of iron oxides (3-4.5 µm). In some cases, the cracks produce transversal fracturing of the bigger bioclasts.

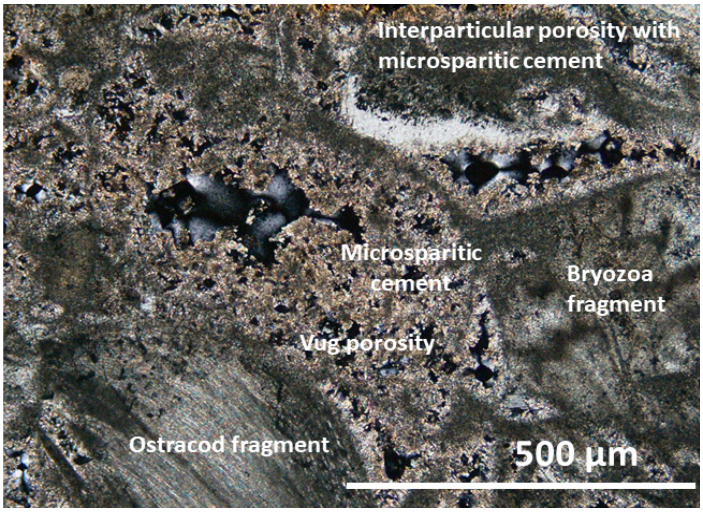

Figure 3.3. *Biomicritic limestone from Conchuela stone showing high content of fossiliferous fragments. The bioclasts (ostracods and bryozoans) are floating in the calcitic mud (micrite) partially recrystallized in microsparite. The stone is affected by Inter-particular and vug porosities with local cementation of microsparite. Polarized light optic microscope image (crossed nicols).*

Fossil fragments of ostracods, bryozoans and bivalves are observed. There is a predominance of fragments of ostracods (7-9 mm) whose shells are recrystallized by fine grained mosaics of calcite (microsparite) and occasionally sparite. Details of the shell fragments indicate that consists of micro fibrous calcite. In less content, bryozoan (~4-10 mm) and bivalve fragments (3-5 mm) appear scattered in the very fine grained calcite matrix. Particularly, bryozoans are well preserved (4-10 mm). Eventually, it is possible to identify original skeletal pores (diameters ~0.4 mm to 0.5 mm), whose walls are cemented with microsparite. Besides, the presence of well-preserved lithic fragments (500 µm) is frequent. Rounded fragments coming from ancient biomicritic limestones are identify. Internally, these fragments are composed by bioclasts of small size (~56 µm-60 µm). Foraminifera and mollusc fragments recrystallized by microsparite cement or locally filled with clay minerals can be identified. Inside, pores with very small diameters (6-11 µm) are developed. Texturally, in most of the cases, the shells are filled mainly by micrite or cemented by microsparite. However, sometimes these shells appear

recrystallized by sparite.

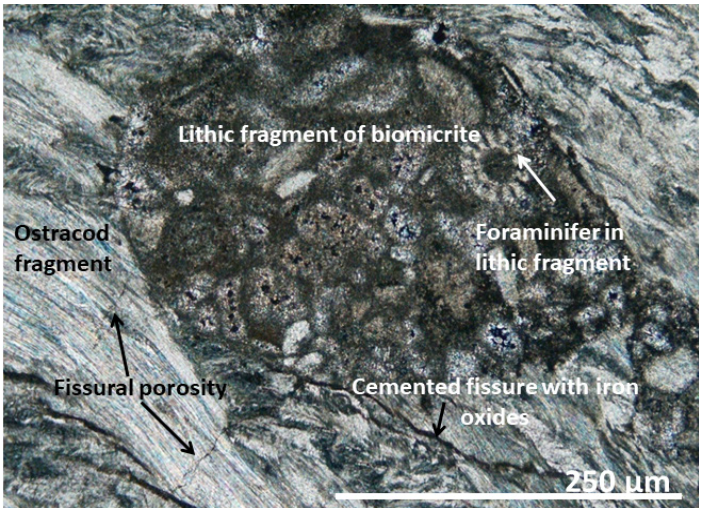

Figure 3.4. *Detail of the biomicritic limestone from Conchuela stone showing a lithic fragment of biomicritic limestone and a fragment of ostracod. Note the fissural porosity affecting the bioclast and fissures filled by iron oxides. Polarized light optic microscope image (crossed nicols).*

3.2. Cellulose samples

Two types of pine cellulose fibers were used in this research work: i) bleached (Buckeye Technologies Inc.) with low ligning content (<0.5%), and unbleached chemi-thermomechanical pulp (CTMP, from Dunapack Ltd, Hungary) with high lignin content (22.5%). Homogeneous hand sheets with a basic weight of 95 g m^{-2} were prepared from each pulp sample in laboratory procedure. In this way, three types of cellulose sheets composed by unbleached fibers, bleached fibers, and 50%/50% mixture of unbleached and bleached fibers were prepared (*Figure 3.5.*).

Before making the hand sheets, cellulose fibers were disintegrated in a laboratory pulp disintegrator machine. Initial test in the laboratory showed how more compact cellulose sheets are obtained if the bleached fibers are refined before mixing with unbleached fibers. This is why the low lignin content samples were disintegrated and subsequently beaten up to 35 Schopper-Riegler degrees (SR°) by using a commercial laboratory valley-beater (*Figure 3.6.a*). HAAGE D-4330 laboratory sheet former (*Figure 3.6.b and c*) was used for the fabrication of the different hand sheets according to standard DIN EN ISO 5269-2. After filtration and drying and prior the characterization, all the samples were conditioned at a temperature of 23ºC and 50% relative humidity (RH) for 48 hours.

This research was carried out in collaboration with the laboratory facilities of the University of West Hungary and the Institute of Wood Based Products and

Technologies, in Sopron (Hungary).

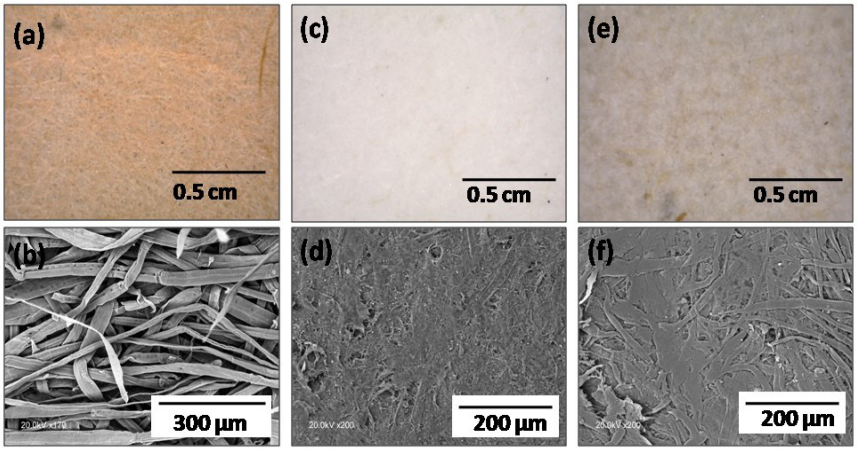

Figure 3.5. *Optical (Binocular Stereo Zoom) micrographs of cellulose sheets made of (a) unbleached and unrefined fibers; (b) bleached and refined fibers; and (c) the 50%/50% mixture of fibers. BSE-SEM micrographs of non-bleached and unrefined, bleached and refined, and a 50%/50% mixture of fibers (b, d, and f, respectively).*

Figure 3.6. (a) *Valley Laboratory Beater used in the present research work. (b and c)HAAGE D-4330 laboratory sheet former, and image detail of HAAGE Vacuum Dryer, respectively.*

3.3. Synthesis procedures

The inorganic NPs synthesized in this research work have been obtained by using two synthesis methods: hydrothermal and sol-gel, which are described in detail in the corresponding papers.

3.3.1. $Mg(OH)_2$ NPs synthesized by hydrothermal method

$Mg(OH)_2$ NPs were prepared by using the hydrothermal method in an autoclave at different reaction times, synthesis temperatures, and reactant concentrations. The hexahydrated magnesium nitrate ($Mg(NO_3)_2 \bullet 6H_2O$) and hydrazine hydrate

(N_2H_4 x H_2O) were used as starting materials. In a typical procedure, low and high concentrations of $Mg(NO_3)_2 \bullet 6H_2O$ (0.12 g and 0.24 g) and aqueous solutions of N_2H_4 x H_2O (0.08 mL of 0.0002M; and 2 mL of 0.14M) were mixed and dissolved ultrasonically in 25 mL of high-purity water. Hydrazine hydrate was added in all cases dropwise to the magnesium nitrate solutions. The mixtures were vigorous magnetic stirring at room temperature, and placed in a Teflon-lined stainless-steel autoclave which was sealed and hydrothermally treated in an oven at a constant temperature of 150 °C, 180 °C, and 200 °C, for 4, 6, 12, 24, 48 and 72 h. An aging process of suspension for 1 h was followed after the hydrothermal treatment. After cooling down to room temperature naturally, $Mg(OH)_2$ samples were centrifuged and washed several timed with distilled water and ethanol, and dried again in oven at the constant temperature of 60 °C with an inert gas atmosphere.

3.3.2. $Mg(OH)_2$ and $Ca(OH)_2$ NPs obtained by sol-gel method

The $Mg(OH)_2$ samples were synthesized dissolving 22.02 g of magnesium methoxide ($Mg(OCH_3)_2$, Aldrich, 98%) in 85.2 mL of denaturalized ethanol at 60 °C. Subsequently, 25.2 mL of deionized water was added into the solution dropwise and allow to reflux at 60 ° C for 24 h. The sample was cooled at room temperature and then the solution was centrifuged and washed with ethanol: distilled water with a volume ratio of 7:3, 6:4, and 1:1. Finally, the obtained sample was dried in an inert gas atmosphere at 100 °C for 4 h.

In a typical procedure, $Ca(OH)_2$ nanoparticles were obtained dissolving 32.19 g of $Ca(NO_3)_2$ $4H_2O$ (Aldrich, 99%) in 21.3 mL of water, and 11.13 g of NaOH (Aldrich, 97%) in 42.6 mL of deionized water. Both solutions were separately heated at 60 °C, and then were mixed under stirring. The reaction solution was cooled under nitrogen atmosphere, and the resulting suspension was centrifuged and washed five times with deionized water and ethanol with different volume ratios: 7:3, 6:4, and 1:1. Finally, the obtained sample was dried in an inert gas atmosphere at 100 °C for 4 h.

Different mixed formulations of $Ca(OH)_2$ and $Mg(OH)_2$ nanoparticles were prepared by sol-gel method in order to obtain suspensions of $Mg(OH)_2$:$Ca(OH)_2$ at 10:90 wt%, 50:50 wt%, and 90:10%wt. In a typical reaction, to prepare $Mg(OH)_2$:$Ca(OH)_2$ nanoparticles in a weight percentage of 90:10 wt%, 19.82 g of $Mg(OCH_3)_2$ were dissolved with stirring in 76.6 mL of ethanol, and 1.11 g of NaOH (Aldrich, 97%) in 6.3 mL of water. Both solutions were mixed under stirring for 10 minutes. Then, a solution of $Ca(NO_3)_2 \bullet 4H_2O$ (3.21g) in 22.7mL of water was added drop by drop and allow to reflux at 60 ° C for 24 h. The sample was cooled at room temperature and then the solution was centrifuged and washed as in the previous cases. Finally, the obtained sample was dried in an inert gas atmosphere at 100 °C for 4 h. The same procedure was followed to prepare the rest of samples in the respective $Mg(OH)_2$/$Ca(OH)_2$ weight percentage (50:50 wt% and 10:90 wt%).

3.3.3. MgO, ZnO and Zn-doped MgO ($Mg_{1-x}Zn_xO$) NPs obtained by sol-gel method

All the chemical reagents used in this research work, magnesium ethoxide ($Mg(OC_2H_5)_2$) as a magnesium precursor, zinc acetate dihydrate ($Zn(CH_3COO)_2 \bullet 2H_2O$) as zinc precursor, and sodium hydroxide (NaOH), were purchased from Sigma-Aldrich and used as received, without further purification. For a typical preparation process, MgO nanopowders were synthesized from denatured ethanol mixing $Mg(OC_2H_5)_2$ (0.5 M) with aqueous solution of NaOH (0.2 M). ZnO was obtained by adding zinc acetate dihydrate ($Zn(CH_3COO)_2 \bullet 2H_2O$) at a concentration of 0.62 M into denatured ethanol. Then, sodium hydroxide (NaOH) at a concentration of 0.3 M was gradually added. In both synthesis procedures, the two solutions were vigorously stirred at room temperature for 24 h. Moreover, $Mg_{1-x}Zn_xO$ NPs were synthesized from denatured ethanol using $Mg(OC_2H_5)_2$ (0.5M) and $Zn(CH_3COO)_2 \bullet 2H_2O$ (0.62 M). The two solutions were mixed and kept at room temperature with vigorous stirring. Subsequently, aqueous solution of NaOH (2M) was prepared and added to the solution with continuous stirring with magnetic stirrer for 24 h at room temperature (25 °C ±4). Then, the obtained samples were centrifuged and washing using distilled water and ethanol and then, were dried at 70 °C, in an inert gas atmosphere till the solution dried. Finally, the samples were annealed in a programmable muffle furnace at 650 °C at a rate of 2 °C/min for 3 h.

3.4. General characterization techniques

The morpho-structural characterization of the different inorganic nanoparticles has been carried out by different analytical techniques on the micro and nanometric scale, which are described in this section.

3.4.1. Powder X-Ray diffraction (XRD)

The phase purity and crystallographic structures of the obtained inorganic nanoparticles have been studied by XRD. Measurements were carried out on a Philips X´Pert, operating at 40 kV and 40 mA and employing Cu Kλ radiation=1.5418 Å. Moreover, Rietveld refinements were determined for unit cell parameters calculation and phase quantification using the Fullprof program [1]. The average crystallite size (CS) of the inorganic nanoparticles were determined by the Scherrer formula $D=k\lambda/\beta\cos\theta$) where λ is the wavelength of the X-ray radiation (in Å), K is a constant taken as 0.9, β the full width at half maximum height (FWHM) and θ is the diffraction angle (in rad) used in calculus [2].

The samples for XRD analysis were ultrosonically dispersed in ethanol and then deposited onto silicon wafer.

3.4.2. Scanning Electron Microscopy (SEM)

The morphological microstructural and chemical analysis of the different as-prepared samples were conducted by Scanning Electron Microscopy (SEM). A Philips XL 30 with tungsten filament, operating at 15 kV, and 20 kV and equipped with a detector of secondary (SE) and back-scattering electron (BSE) detectors was employed. In this way, different types of signals were obtained due to the interaction between the electron beam and the specimen structure.

Both types of interactions revealed important information about the samples to determine the surface properties and the chemical nature of the specimens. In addition, the semi-quantitative analysis of the different samples was studied by a Philips EDAX DX4 energy dispersive spectroscopy (EDS) detector. The SEM images were obtained with the surface of the samples coated with a thin gold layer in order to avoid charging accumulation during SEM analysis.

Moreover, a Field-emission scanning electron microscopy (FESEM, JEOL JSM-7600F) was used in order to obtain improved spatial resolution and minimized sample charging and damage.

3.4.3. Cathodoluminescence (CL)

The CL is a non-destructive analytical technique based on the emission of photons of characteristics wavelengths from a material that is stimulated by high-energy electron bombardment of an electron microscope. The CL signal is produced in the visible light range and can be detected spectroscopically. Any variation in the material to analyze as a result of the high-energy electrons can indicate the existence of structural defects, phase transformations, and/or the presence of impurities, among others. Therefore, this analytical technique is unique to characterize the composition and optical and electronic properties of the sample, obtaining information that often cannot be obtained by other analytical techniques and methods at the micro and sub-nanoscale [3]. In this thesis, the intrinsic cathodoluminescence emission in the region between ~300 to ~660 nm from pure nanocrystalline brucite was studied using an environmental scanning electron microscope (ESEM). Specifically, an ESEM-FEI INSPECT in low vacuum mode was used, which was equipped with a cathodoluminescence detector (Gatan MONO CL3) and a PA-3 photomultiplier tube attached to the microscope. The CL measurements were analyzed applying 10, 15, and 20 kV with 4mA as excitation source in the sensitive range (280-670 nm). The beam was scanned with a pixel size of 2nm and a dwell time of 1.5 s. The luminescence database (CSIRO) was employed for the CL study [4].

3.4.4. Photoluminescence (PL)

The PL measurements allow the non-destructive characterization of semiconductor materials. This technique was employed to investigate the electronic structure, both intrinsic and extrinsic, of the metal oxide nanoparticles synthesized. Specially, the PL spectroscopy was mainly employed to identify possible defect complexes in the samples. Thus, room temperature photoluminescence (PL) spectra were recorded by fluorescence photoluminescence spectrophotometry using an Edinburg Instruments Co., 235 nm xenon lamp. For sample preparation, the obtained samples were made as thin layer on an ultrasonically cleaned glass slides and loaded in the equipment sample holder.

3.4.5. UV-vis absorption spectroscopy

In this Ph.D thesis, the UV-vis absorption spectroscopy was used to test the

adsorption performance of the metal oxide nanoparticles synthesized. Thus, the photocatalytic efficiency of the synthesized nanoparticles was studied by degradation of methylene blue (MB) solution under UV-light irradiation with time. Typically, 0.003 g of synthesized nanoparticles were dispersed in 50 mL (1.88 x 10^{-5} M) MB aqueous solution. Prior to irradiation, the suspensions were magnetically stirred in dark for 2 h to reach the adsorption-desorption equilibrium. After this, the suspensions were exposed to light from a 20W halogen lamp with UV emission. During UV irradiation process, MB solution was continuously stirred in the dark. The solutions, collected at definite intervals, were centrifuged in order to remove the catalysts and their absorbance was analyzed using a UV-visible absorption spectrophotometer (Agilent, 8453 diode array).

3.4.6. Transmission Electron Microscopy (TEM)

The TEM was used to analyze the morphological and chemical composition of the synthesized NPs. In addition, this microscopy technique was also used to study the changes produced in morphology, porosity, phase transformation and structural defects of the synthesized nanoparticles as a result of the exposition to the electron beam. The following microscopes were used in this thesis:

A JEOL JEM 2100 TEM, operating at 200 kV (0.25 nm point to point resolution) equipped with selected area electron diffraction (SAED) and energy dispersive X ray detector (EDS-OXFORD INCA) with a goniometer of 45° angle. The distribution and average size of the nanostructures synthesized were also obtained from TEM images using the Digital Micrograph™ (DM, Gatan Inc.) software.

A JEOL JEM 3000F TEM, operating at 300 kV, with a point to point and lattice resolution of 0.17 nm (in TEM mode) and 0.14 nm (in STEM mode), equipped with a goniometer of 25° angle, was used to the High Resolution TEM study. The chemical analysis of the synthesized nanoparticles was carried out using Energy Dispersive X-ray Spectroscopy (EDS) and Electron Energy Loss Spectroscopy (EELS). A Gatan Enfina filter provided in the TEM was used to detect electron energy loss spectra. The analyzed surface with the EELS detector was 2-3nm, with an energy dispersion of 1.0 eV/channel, a collection angle of 8 mrad and a convergence angle of 9 mrad. The obtained results were compared using the EELS database [4]. Furthermore, Gatan digital Micrograph software was used to process the High Resolution Transmission Electron Microscopy (HRTEM), EELS, and SAED patterns.

The samples for TEM analysis were ultrasonically dispersed in acetone and deposited over the carbon coated Cu-grids. Both transmission electron microscopes are located in the National Center for Electron Microscopy (CNME, Madrid, Spain).

3.4.7. Thermogravimetrical and calorimetric analysis (TGA-DSC)

The Simultaneous thermal analysis method was employed for the thermal stability

study of the hydroxide nanoparticles synthesized. A Perkin Elmer STA 6000 simultaneous thermal analyzer was employed for the simultaneous evaluation of losses and gains of mass (Thermo gravimetrical analysis, TGA) and the specific interchange of heat (Differential scanning calorimetry, DSC). These processes are associated to decomposition, desorption and absorption, oxidation, among other chemical reaction. The measurements were made under nitrogen atmosphere (flow rate 20 mL/min) from 25 to 600 °C with a continuous heating rate of 10 °C min^{1-}.

3.5. Effectiveness evaluation of the hydroxide NPs as consolidating agents for carbonate stone

3.5.1. Consolidation treatments

Dolostone samples (4 x 4 x 4 cm) were freshly cut with a diamond disk saw in perpendicular orientation to the stone bedding in order to avoid the influence of microstructural anisotropy in the results. The selected dolostone substrate was Laspra dolostone, which have been widely used in the spanish cultural heritage.

The selection of the nanoparticles as consolidating product in stone substrates were carried out according to the chemical composition and the petrophysical properties of the different lithotypes. So, to assure an optimal consolidation results in terms of compatibility, among all developed nanoparticles, the Laspra dolostone was treated with a solution of $Mg(OH)_2$, and $Mg(OH)_2/Ca(OH)_2$ 50%/50 wt%. All stone samples were assayed in triplicate.

The selected hydroxide dispersions were applied in a concentration of 2.5 g/L in ethanol by brushing (one of the most commonly used method in stone treatments) in one of the dry and clean surfaces of each stone (six specimens of each composition), until refusal. Moreover, the application by capillary absorption was carried out in each lithotype (six specimens of each stone material). The bottom surface of the dolostone samples were immersed in the nanoparticle dispersions, until the full saturation.

Previous research works have proved the important influence of relative humidity on the effectiveness of hydroxide nanoparticles, employed as consolidating agent in stone heritage, achieving the best results of consolidation treatment at high relative humidity (75% RH) [6, 7]. This is the reason why, all stone samples were treated in a climatic chamber at 20 °C ± 5 °C and 75% RH ±5%.

3.5.2. Characterization techniques

The following characterization techniques were carried out before and after the consolidant treatments by nanoparticles:

3.5.2.1. Environmental Scanning Electron Microscopy (ESEM)

The consolidating effectiveness of the different treatments on the stone surfaces

were inspected by Environmental Scanning Electron Microscopy (ESEM) using a Quanta 200 FEI microscope with Energy Dispersive X-ray Spectroscopy (EDS, model 7509 Oxford Instrument Analytical, UK).

3.5.2.2. Spectrophotometry

Spectrophotometry was performed to study the possible color changes induced by the treatments. The measurements were evaluated by means a portable spectrophotometer (MINOLTA CM-700d), equipped with a CM-S100W DATA Software COLOR SpectraMagic NX, before and after the treatments. Conditions used were Standard illuminant D65 and observer angle 10 ˚. The CieLab Color Space (L*, a* and b*) were chosen for the study, i.e., lightness (L*), which ranges from 0 for black to 100 for white, and the chromatic coordinates a* and b*. Coordinate a* ranges in value from +60 (magenta) to −60 (green) and b* from +60 (yellow) to −60 (blue). The global color change in the different stone samples was determined according to the formula $\Delta E = (\Delta L^{*2} + \Delta a^{*2} + \Delta b^{*2})^{1/2}$. These measurements were made according to the UNE-EN 15886 (2011).

3.5.2.3. Surface hardness

Surface hardness measurements were made by an Equotip3 (proceq) portable testing device with an impact device D, and an impact energy of 11N/mm. This testing instrument operates with the dynamic rebound method. Five measurements were performed on each face of sample. The instrument was held vertically downwards and also perpendicular to the stone surfaces within 5 mm of the stone edges. A total of 30 measurements per stone samples were taken and an average was calculated for each type of stone and treatment. The value of hardness is expressed how the number of Leeb (L value), which corresponds to the ratio of the rebound velocity impact multiplied by 1000. These valued are considered equivalent to stone strength [8].

3.5.2.4. Measurements of ultrasonic pulse velocity (Vp or P-wave velocity)

The P-wave propagation was measured to a precision of 0.1 µs with a PUNDIT CNS Electronic instrument. Standard recommendations were followed according to the Spanish and European standard (UNE-EN 14579,2007 and Spanish Association for Standardization and Certification (AENOR) 2005). The frequency of the transducers (11.82 mm of diameter) used was 1 MHz. Measurements were taken in direct transmission/reception mode, across opposite parallel sides of the stone specimens in the three spatial directions, using the mean of four measurements of each stone face as the accepted value.

3.5.2.5. Mercury Instrusion Porosimetry (MIP)

Mercury Intrusion Porosimetry (MIP) was carried out to assess sample pore structure, including total porosity (P), macro- and micro-porosity, which have a pore diameter of > 5µm and < 5 µm, respectively [9] and Pore Size Distribution (PSD), before and after the treatments. Readings were taken at pore diameter range of 0.005<d<400 µm, under measuring conditions ranging from atmospheric pressure to 60.000 psia (414 MPa) using a Micromeritics Autopore IV 9500 porosimeter (maximum pressure, 414 MPa (60000 psi).

3.5.2.6. Neutron Radiography (NR)

Typically, the main parameters to evaluate the effectiveness treatment are: i) the consolidant penetration depth and, ii) its distribution into the stone matrix. Most of the techniques used for evaluating the penetration of consolidant products are destructive in nature, such as staining techniques or micro-drilling. The analyses of art works that constitute our cultural heritage require non-destructive and non-invasive approaches and analytical tools due to the high cultural values. Therefore, during last years, the possibility of monitoring the consolidant action in natural stone by means of neutron and X-rays radiography has been introduced by E.H. Lehmann et al. [10]. Due to its high sensitive toward hydrogen the advantage of neutron radiography provides the possibility to visualize materials which can be hardly distinguished with other non-destructive techniques such as X-rays, nuclear magnetic resonance and/or ultrasound. Thus, the application of neutron radiography is particularly favorable in cases in which hydrogen and carbon need to be recognized, as in the case of the carbonation of hydroxide nanoparticles into the stone. Furthermore, researches carried out by R. Hassanein et al. [11] have shown the neutron radiography as an excellent tool to imaging water content in treated porous stones. This is why, the main aim was to evaluate the penetration depth of the developed nanomaterials and its distribution into the stone substrates, according to the methodological application (by brushing, and capillary absorption).

This study was carried out in a neutron transparent sample climatic chamber (*Figure 3.7.*) at 25°C, and 75 %RH at the NEUTRA facility at Paul Scherrer Institute (PSI, Villigen, Switzerland) [12]. The treatment was monitoring in situ in twelve cubic dolostone (Laspra dolostone) specimens of 4 x 4 x 4 cm side. The samples were treated by brushing until refusal, on the dry and clean dolostone and limestone surfaces and by capillary absorption. The neutron beam had a flux $9.8 \bullet 106$ cm^{-2} s^{-1} and the detector was a 100 µm thick 6LiF/ZnS-scintillator with a Andor Neo 5.5 Scmos 2560 X 2160 px camera. The collimation ratio (L/D) was equal to 350. The field of view (FOV) was 98x116 mm and the nominal pixel size was 90µm. The distance between the sample and the detector screen was 80 mm. Their radiograms were measured during the consolidation treatments at different times.

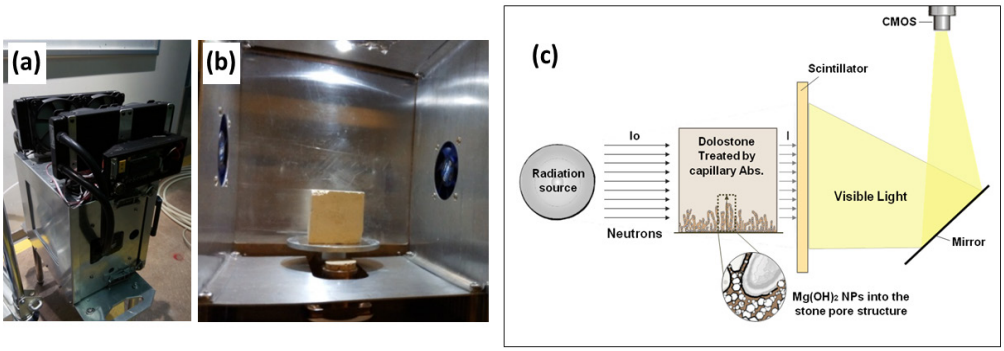

Figure 3.7. *Neutron transparent climatic sample chamber used in this Ph.D thesis, (a) outside view, (b) inside view with the location of stone sample, and (c) Experimental set-up for neutron radiography.*

3.6. Determination of the antifungal activity of the metal oxide NPs

This research was carried out in the Applied Microbiology laboratory at the Juárez Autónoma University of Tabasco (México) and the Center for Research and Advanced Studies of the National Polytechnic Institute (CINVESTAV) in Mérida (Yucatán, México).

3.6.1. Fungal strains and culture conditions

The fungal activity of the metal oxide NPs was studied against four fungal species: *Aspergillus niger* (R3T2M774), *Penicillium oxalicum* (R3T3M877), *Paraconiothyrium* sp. (R1T2C113), and *Pestalotiopsis maculans* (R3T2C756) (*Figure 3.8.*). All these fungi were obtained from biofilm samples on limestone walls with different exposure times [1 year (young biofilm), 5 years (middle-aged biofilm), and 10 years (old biofilm)] to a subtropical climate at 81% HR, in Mexico Gómez-Cornelio et al. 2016 [13]. These fungi were isolated by washing and the particle filtration technique, and were substantial concern because they have shown to be potentially active in solubilizing $CaCO_3$ plates and limestone through the production of oxalic acids during their metabolic processes [13]. The objective was to study the antifungal effectiveness of the different types of NPs in fungal species from different biofilms. Thus,

- *P. oxalicum* and *A. niger* were isolated from a black biogenic adhered to stone surfaces for 10 years of environmental exposure.
- *Paraconiothyrium* sp. was isolated from biofilms with an environmental exposure period between 1 to 5 years.
- *P. maculans* was found in biofilm biomass with different time periods (1, 5, and 10 years).

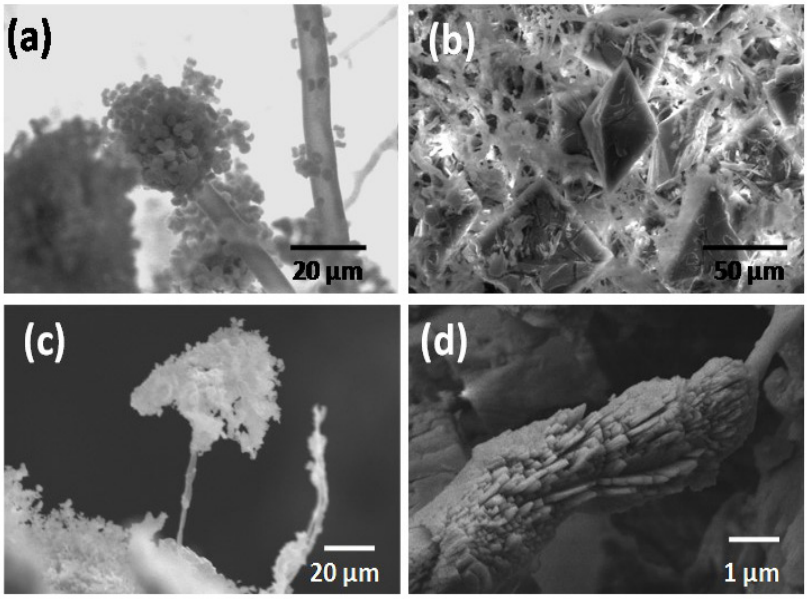

Figure 3.8. *ESEM micrographs of (a) A. niger growing over stone substrate [14], (b) presence of fungal hyphae of P. oxalicum and precipitation of crystal oxalates over stone, (c) Presence of fungal hyphae of Paraconiothyrium sp. on the edge of the stone [15], and d) Pestalotiopsis maculans hyphae and the precipitation of crystal oxalates growing in the stone substrate.*

The four fungal species were cultivated in Petri dishes with the appropriate medium, Potato Dextrose Agar (PDA, Difco), and incubated at 28 °C for 3-5 days. Once fungal growth was detected covering the totality of the petri dishes, fungal growth from plates was flooded using a sterile saline solution (0.85%) with 0.025% of Tween 20 (Sigma, Aldrich), and stirred gently with a sterile swab (*Figure 3.9 a.*). The spore concentrations in the stock suspensions were determined using a Nebauer chamber and adjusted to $1x10^6$ conidia /mL (*Figure 3.9 b and c*).

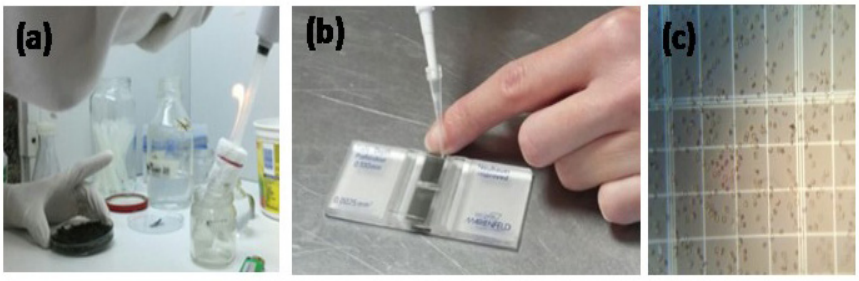

Figure 3.9. *(a) Preparation of fungal inoculum, (b and c) Determination of spore concentrations using a Nebauer chamber.*

3.6.2. *In vitro* determination of antifungal activity of metal oxide NPs

The antifungal activity of the different synthesized NPs was studied using the agar well diffusion method, a standard method carried out according to the Clinical and Laboratory Standards Institute (CLSI) [16]. The antifungal activity was measured as the diameter (in mm) of clear zone for growth inhibition. Thereby, this method allow to determine quantitatively and qualitatively the antifungal activity of the different systems by measure of diameter of the zone of inhibition.

Briefly, 3.5 mL of each fungal suspensions were mixed with 31.5 mL molten PDA (Difco) and poured slowly on the Petri dish with 12 stainless steel cylinders (*Figure 3.10 a*). When the agar layer solidified, the cylinders were retired. Then, each well was filled with 100 µL of the metal oxide NPs dissolved in dimethyl sulfoxide (DMSO) to get different concentrations: 10, 5, and 2.5 mg/mL. Besides, 100 µL of DMSO was used as negative control. The different square Petri dishes (*Figure 3.10 b*) were incubated at 5 °C for 4 hours to allow a good diffusion and then were incubated at 28 °C for 48-72 hours. These essays were carried out in triplicate and the mean diameter of the zone of inhibition ±SD were determined for each fungal species.

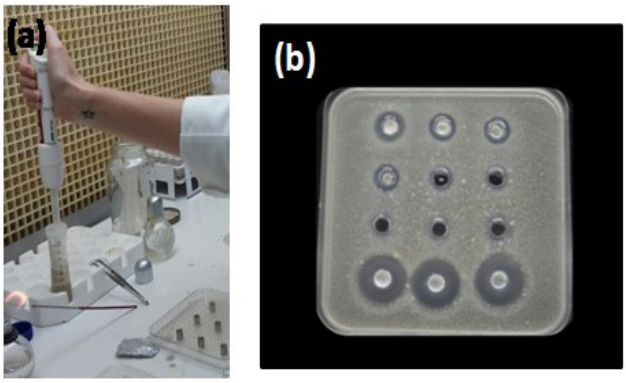

Figure 3.10. *(a) Preparation phase of agar difussion method, (b) Image of the square Petri dish used in this research. Note the inhibition halos.*

In addition, the minimum inhibitory concentrations (MICs) were determined by microdilution method in culture broth (*Figure 3.11*), according to the Clinical Laboratory Standard recommendations (CLSI) [17], using 96-well microtiter plates. Thus, the inoculums of each fungus (*A. niger*, *P. oxalicum*, *Paraconiothyrium* sp., and *P. maculans*) were prepared, as was described in the previous subsection 3.6.1, and the suspensions were adjusted to 5 x 10^5 conidia/mL.

All metal oxide NPs were dissolved in DMSO and diluted in microtiter plates by cultural medium (Potato Dextrose Broth, Difco) in a progression from 2 to 2048 times. Therefore, the obtained concentrations of NPs were from 5 to 0.003 mg/mL. (5, 2.5, 1.25, 0.625, 0.31, 0.15, 0.07, 0.03, 0.015, 0.007, and 0.003 mg/mL). After this, the NPs were diluted, and a standard amount of the test fungal was inoculated onto

microtiter plate so that the inoculums density in the well was equal 2.5 x 10^5 conidia/ mL. The microtiter plates were incubated at 28 °C for 48 h. DMSO was used as negative control. The MIC values were determined visually and by optical microscopy (OM) as the lowest NPs concentrations that resulted in a 100% reduction in the visible growth compared with that of NPs free growth control well after 24 h of incubation.

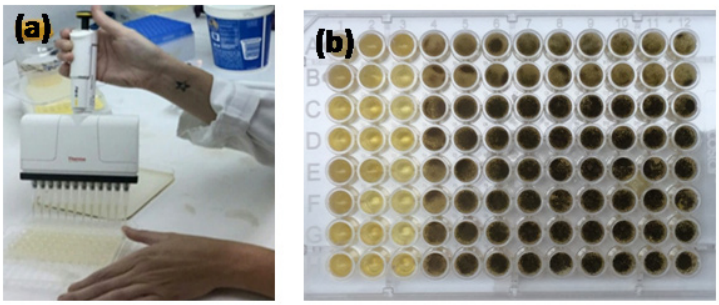

Figure 3.11. *(a) Microdilution method in culture broth, (b) 96-well microtiter plate used in the research.*

3.6.3. *In vitro* Determination of antifungal activity of the NPs as coatings

The antifungal activity of the MgO and $Mg_{1-x}Zn_xO$ NPs was studied using glass microscope slides, Laspra dolostone (Asturias, Spain) and Conchuela limestone (Yucatán, México) coupons of 2 cm x 2 cm x 1 mm size as substrates. These stone substrastes were described in detail in the previous 3.1. subsection. The different stone samples were completely dried in an oven at 60 ° C, until the dry weight was achieved.

Firstly the antifungal activity of the metal oxide NPs was studied on grease free glass slides. Glass slides were cleaned with ethanol and coated on one side using drop-wise addition of 1 mL of nanoparticle suspensions and allowed to dry overnight at room temperature (23 ± 5 ° C). After allowing the covered slides to dry completely, 20 µL of fungal inoculum (1 x 10^5 conidia/mL) was applied to an area of 1 cm^2. All the slides were prepared in triplicate and fungal growth was compared with control glass slides without coatings. Fungal growth was inspected daily by visual counting of colonies using a stereoscopic and optic microscope (Carl Zeiss).

Dolostone and limestone samples were freshly cut with a diamond disk saw, without polishing the obtained stone faces. Subsequently, the samples were treated drop-by-drop with 2 mL of ethanol dispersions of MgO and $Mg_{1-x}Zn_xO$ nanoparticles (2.5 gL-1) on the dry and clean top surfaces of each stone. After that, the specimens were left to dry in air at 23 ± 5 ° C and 55 ± 5% RH for 2 days. Then, a sufficient volume to homogeneously cover the stone surface of 1 mL of the fungal conidia suspension was applied using a micropipette. Control samples were not subjected to any treatment. All stone samples were assayed in tetraplicate.

The antifungal activity of the treatments on the stone surfaces and the cross sections were inspected by a stereoscopic microscope (Nikon), and an Environmental

Backscattered Electron Scanning Microscopy (ESEM-BSE) (JEOL JSM 6400).

3.7. Analytical methods used for the effectiveness evaluation of the refining and the modification of cellulose samples with $Mg(OH)_2$ nanoparticles

3.7.1. Application of magnesium hydroxide nanoparticles on cellulose fiber sheets

The modification of the sheets with $Mg(OH)_2$ nanoparticles was carried out by using two methods: spraying and immersion. Part of the cellulose sheets were sprayed with 2.5 ml of the $Mg(OH)_2$ nanoparticles dispersion (only one side). Another part of paper sheets was immersed in the dispersion for 40 minutes. After that, the cellulose samples were first dried between blotting paper in order to eliminate the excess solvent and then left to dry in air at 23 °C and 50% RH for 10 days. Control samples were not subjected to any treatment. All cellulose samples were studied in triplicate.

3.7.2. Characterization techniques of cellulose samples

3.7.2.1. X-Ray diffraction (XRD)

XRD was used to study the crystallographic structures and crystallinity of the cellulose samples. This technique was also performed in order to determine the influence of the application of the brucite nanoparticles on the cellulose samples. The XRD measurements were carried by using a X-ray diffractometer (Philips X-Pert´), operating with Cu Kλ radiation (λ=1.54 Å), a voltage of 40 kV, and a current of 40 mA. The crystallinity index (CrI) was calculated from XRD data using the Segal method [18] $CrI=[(I002-Iam)/I002] \times 100$. In this formula, I002 is the maximum intensity of the (002) lattice diffraction peak (positioned at $2\theta= 22.5°$), and Iam is the minimum in peak intensity between the main and secondary peaks (between the 101/10-1 and 002 lattice planes).

3.7.2.2. Scanning electron Microscopy (SEM)

The morphological and chemical analyses of untreated and treated fibers were carried out by Scanning Electron Microscopy (SEM) using a HITACHI S-3400 138 N instrument with an operating voltage of 17kV.

3.7.2.3. Smoothness

The smoothness measurements of the untreated and treated cellulose fiber sheets were carried out on a Smoothness tester (Bendtsen 143). The smoothness was determined by measuring the air flow between the cellulose samples (backed by flat glass on the bottom side) and two pressurized, concentric lands that are impressed into the sample from the top side. The rate of air flow (mL/min) is related to the smoothness of the paper.

The mechanical properties of the untreated, treated, unaged, and aged cellulose samples were measured in accordance with the EN ISO 1924-2 standard. The tensile tests were carried out on a universal testing machine (INSTRON 3345, USA Tensile Tester). The cross-head speed was 50 mm min^{-1} and the distance between the clamps was 180mm. The cellulose samples were rectangular in shape with a size width of 15mm. At least three test strips of each cellulose sample were evaluated, and all the presented data were the average of these tests.

3.7.2.5. pH measurements

Prior to pH measurements, 120 mg of the samples were preconditioned at 23 °C and 50 %RH for two days. Then, the samples were weighed, cut in pieces and placed inside screw top vials. 10ml of ultrapure water (with a resistivity of 18 $M\Omega \bullet cm^{-1}$) were added and vial was sealed. The vials were kept in ultrasound bath for 1 hour and the pH measurements of the cold-water extracts were carried out with a digital pH meter 165 (LovibondSensoDirect pH 110 model).

3.8. References

[1] Khorsand, Zang, A., Abd Majid, W.H., Ebrahimizadeh Abrishami, Ramin Yousefi, Parvizi, R. (2012) Synthesis, magnetic properties and X-ray analysis of Zn0.97x0.03O nanoparticles (X=Mn, Ni, and Co) using Scherrer and size-strain plots methods. *Solid State Sci.* 14, 488-494.

[2]Rodríguez-Carvanal, J.J. (1993) Recent advances in Magnetic structure Determination by *Neutron Powder Diffraction. Phys.* B. 192, 55-69.

[3] Götze, J. (2002) Potential of cathodoluminescence (CL) microscopy and spectroscopy for the analysis of minerals and materials. *Analytical and Bionalytical Chemistry*, 374 (4), 703-708.

[4] Mcrae, C.M., Wilson, N.C. (2008). Luminescence database I-minerals and materials. *Microscopy and Microanalysis.* 14 (02), 184-204.

[5] EELS Database, EMES and IMN laboratories, the European microscopy network ESTEEM 2, The French microscopy network METSA and by the French microscopy Societ SFμ <<https://eelsdb.eu/>>.

[6] López-Arce, P.; Gomez-Villalba, L.S.; Pinho, L.; Fernández-Valle, M.E.; Álvarez de Buergo, M.; Fort, R. (2010) Influence of porosity and relative humidity on consolidation of dolostone with calcium hydroxide nanoparticles: effectiveness assessment with non-destructive techniques. *Mater.Charact.* 61, 168-184.

[7] Gomez-Villalba, L. S., López-Arce, P., Alvarez de Buergo, M., & Fort, R. (2011). Structural stability of a colloidal solution of $Ca(OH)_2$ nanocrystals exposed to high relative humidity conditions. *Applied Physics A: Materials Science & Processing.* 104 (4), 1249-1254.

[8] Viles, H., Goudie, A., Grab, S. and Lalley, J., (2011). The use of the Schmidt Hammer and Equotip for rock hardness assessment in geomorphology and heritage science: a comparative analysis. *Earth Surface Processes and Landforms.* 36, 320–333.

[9] Russel, S.A. (1927). *Stone preservation Committee Report (Appendix I)*; H.M. Stationary Office; London.

[10] Lehmann, E.H., Vontobel, P., Wiezel, L. (2001) Properties of the radiography facility Neutra at SINQ and its potential for use as european reference facility, *Nondestructive Testing and Evaluation.* 16: 2-6: 191-202.

[11] Hassanein, R., Meyer, H.O., Carminati, A., Estermann, M., Lehmann, E., Vontobel, P. (2006). Investigation of water imbibition in porous stone by thermal neutron radiography, *Journal of Physics D: Applies Physics*, 39: 4284-4291.

[12] Mannes, D., Schmid, F., Wehmann, T., Lehmann, E. (2017). Design and applications

of a climatic chamber for in-situ neutron imaging experiments. *Physics Procedia*. 88: 200-207.

[13] Gómez-Cornelio, S., Ortega-Morales, O., Morón-Ríos, A., Reyes-Estebanez, M., De la Rosa-García, S. (2016). Changes in fungal community composition of biofilms on limestone across a chronosequence in Campeche, Mexico. *Act. Bot. Mex*. 117: 56-69.

[14] González-Gómez WS. 2011. Análisis de la superficie de sustratos pétreos naturales y recubiertos bajo la influencia de la colonización fúngica de Penicillium sp. y Aspergillus sp. Tesis de Maestría en Ciencias con especialidad en Fisicoquímica. Centro de Investigación y de Estudios Avanzados del Instituto Politécnico Nacional. 65 pp.

[15] Gómez-Cornelio SA. 2016. Interacciones interespecíficas en la estructuración de las comunidades de hongos sobre roca calcárea. Tesis de Doctorado en Ciencias en Ecología y Desarrollo Sustentable. El colegio de la Frontera Sur. 105 pp.

[16] Clinical and Laboratory standards Institute (CLSI) (2004). Method for antifungal well diffusion susceptibility Testing of Yeast M-44A.

[17] NCLI (2012). Reference method for broth dilution antifungal susceptibility testing of filamentous fungi. Approved standard M3.

[18] Segal, L., Creely, J.J., Martin, A.E., Conrad, C.M. (1959). An Empirical Method for Estimating the Degree of Crystallinity of Native Cellulose Using the X-Ray Diffractometer. *Text. Res. J.,* 29: 786-794.

CHAPTER 4

4.1. **PART I. Consolidating products, based on magnesium hydroxide ($Mg(OH)_2$) and calcium hydroxide ($Ca(OH)_2$) nanoparticles**

- *Papers II - IX*

4.2. **PART II. New antifungal protective coatings for the protection of calcareous stone heritage**

- *Paper X*

4.3. **PART III. Application of $Mg(OH)_2$ nanoparticles on cellulose fibers**

- *Paper XI*

Summary of Key Results

Chapter 4

Summary of Key Results

Introduction to the experimental results

This chapter presents a summary of the key results of the current research (see list of publications on page *xxxiii*), which are reported on detail in the appended papers. These research findings are divided into three parts.

In the **first part** (**Section 4.1**), the results regarding the design, the optimization and the development of consolidating products, based on magnesium hydroxide ($Mg(OH)_2$) and calcium hydroxide ($Ca(OH)_2$) NPs synthesized by hydrothermal and sol-gel methods and specifically designed for calcareous stone heritage are presented. Particular attention was paid to the study of the changes in experimental parameters such as reaction time, synthesis temperature and/or surfactant/precursor concentrations due to the fact that these parameters can determine the viability of a particular synthesis design. Their applicability as consolidant products have been studied on dolostone substrates (Laspra dolostone).

The **second part** of this research (**Section 4.2**), includes the design and optimization of protective coatings composed of MgO and ZnO ($Mg_{1-x}Zn_xO$) nanoparticles with multifunctional photocatalytic and antifungal properties for the protection of historic monuments and stone works. The application of these nanoparticles was carried out on two types of calcareous stones, widely used in the cultural heritage of Spain and México, the Laspra dolostone (Asturias, Spain) and the Conchuela limestone (Yucatán, México) because of their different compositions and microstructural features.

Finally, an additional application of the $Mg(OH)_2$ nanoparticles is presented in the **third part** (**Section 4.3**). Fresh and aged cellulose fibers with different refining degrees and chemical compositions have been treated by $Mg(OH)_2$ NPs, thereby showing that these types of nanoparticles have a broad range of applications in the field of heritage conservation.

PART I

Design, optimization and development:

Consolidating Products $Mg(OH)_2$ & $Ca(OH)_2$ nanoparticles

4.1. Design, optimization and development of consolidating products for the conservation of stone heritage: $Mg(OH)_2$ and $Ca(OH)_2$ nanoparticles

The design and the development of consolidating products, based on $Mg(OH)_2$ and $Ca(OH)_2$ nanoparticles and specifically designed for calcareous stone heritage, is presented in *Papers II-IX*. Changes in experimental parameters such as synthesis temperature, time reaction and/or precursor´s reactivity can determine the viability of a particular synthesis design. This is why firstly; the optimal synthesis method and the changes in experimental parameters were studied (*Figure 4.1.1*). Thus, *Papers II, III, IV, V* and *VI* are centered on the design and the stability study of the different $Mg(OH)_2$ and $Ca(OH)_2$ NPs synthesized by hydrothermal and sol-gel methods, in order to obtain nanocrystals with certain morphologies, particle sizes, agglomeration levels and crystallographic structures.

After this, the application of these nanoparticles on calcareous stones, widely used in the cultural heritage of Spain, was investigated. The consolidant treatments were evaluated in dolostone (Laspra dolostone, Spain). Its petrographic features make this type of stones prone to different weathering phenomena and lead to different consolidant uptake and consolidant distribution. All the aspects concerning treatments efficacy and compatibility studied for the different stone substrates are tried in *Papers VII, VIII*, and *IX*.

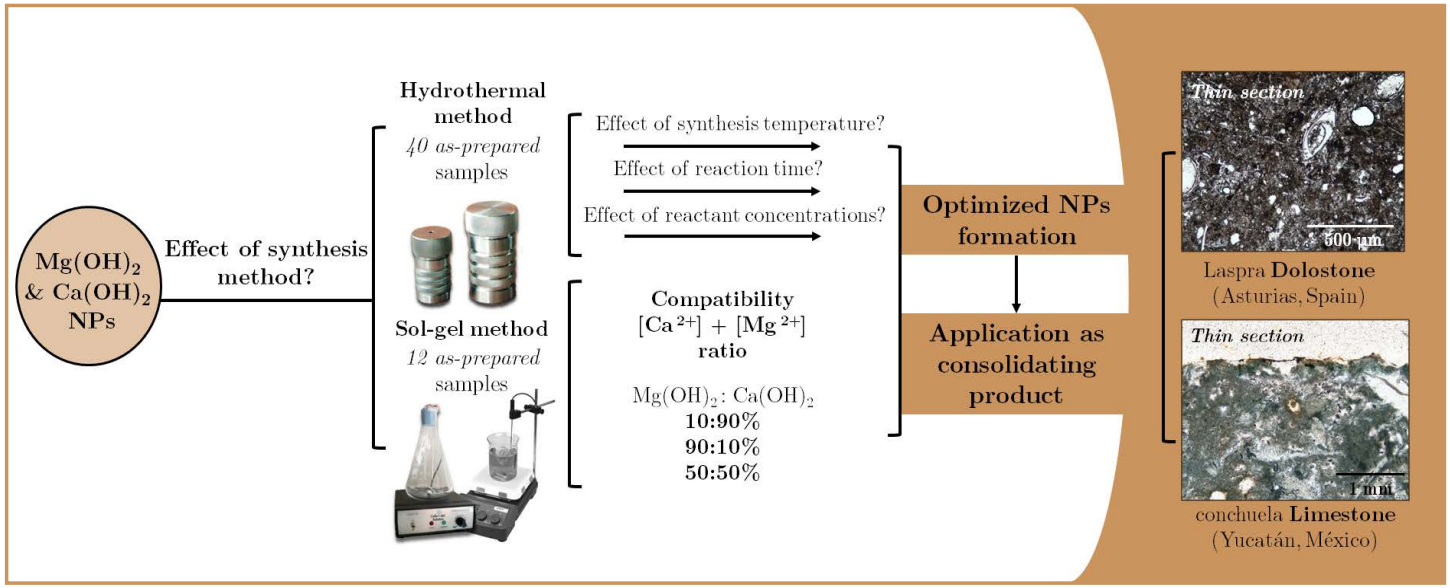

Figure 4.1.1: *Scheme of the experimental set-up followed to study and optimize the different types of nanoparticles, specifically designed for the consolidation of stone heritage.*

4.1.1. *Paper II.* Synthesis and morpho-structural characterization of nanostructured magnesium hydroxide obtained by a hydrothermal method.
Sierra-Fernandez, A.; Gomez-Villalba, L.S.; Milosevic, O.; Fort, R.; Rabanal, M.E
Ceramics International 40 (8), **2014,** doi: 10.1016/j.ceramint.2014.04.073

One of the most important challenges in any synthesis approach is to identify the role of each reaction parameter in controlling the morphology and crystal structure of the final nanomaterials obtained. This understanding is essential to distinguishing and establishing the reaction mechanism for the targeted compound formation. Among synthesis methods, the hydrothermal route has been known as a powerful method for the preparation of high purity, highly crystalline and homogeneous nanoparticles. An important advantage of this route is that the synthesis of magnesium hydroxide nanoparticles can be performed under moderate temperatures and reaction times. However, many factors such as synthesis temperature, reaction time and medium may influence the crystallization process. This is why the conditions of the synthesis method need to be controlled to obtain nanocrystals with certain physico-chemical properties according to the petrographic features of the stone substrate to treat (for further information see *Chapter 1*). Thus, the synthesis and the characterization of controlled magnesium hydroxide ($Mg(OH)_2$) nanostructures with different morphologies, particle sizes, high purity and preferred orientation have been carried out. The main focus of this research work was to study the influence of reaction time and synthesis temperature on the different types of $Mg(OH)_2$ obtained by using the hydrothermal method, employing magnesium nitrate hexahydrate as reagent and hydrazine hydrate as surfactant in the precursor solution.

The presented results highlighted the importance of the synthesis method. All brucite samples obtained by using the hydrothermal route showed an inversion in the intensities of (001) and (100) diffraction maxima confirming a preferred growth orientation of the brucite crystals affecting the (001) plane. In addition, the findings obtained have shown that the synthesis temperature and reaction time have a strong influence on the morphology, the particle size, the agglomeration level and the crystallographic structures of the different nanocrystallines $Mg(OH)_2$ synthesized. Thus, the prolongation of reaction time (from 6 to 24 hours) increases the crystalline degree of magnesium hydroxide particles. A prolonged hydrothermal treatment time would imply a relatively adequate dissolution-recrystallization process in the hydrothermal method. In addition, the crystallinity and the particle size of brucite nanoparticles increase at higher synthesis temperature (180 ˚ C), indicating that the synthesis temperature also plays an important role in restricting the crystal growth and the aggregation of $Mg(OH)_2$ nanoparticles. In this way, the increase of temperature from 150 ˚ C to 180 ˚ C led to the formation of well-defined hexagonal nanoparticles of brucite, with a bigger uniform size of ~ 160 nm. In addition, these samples exhibited better thermal stability, due to this increase of the crystallinity degree. It was also possible to determine that the synthesis carried out at a lower synthesis temperature (150 ˚ C) requires longer hydrothermal reaction times to obtain nanoparticles suited for applications in stone heritage. Therefore, defined hexagonal nanoparticles of magnesium hydroxide with average particles sizes around 120 nm were detected in the samples obtained at the synthesis temperature of

150 ˚C for 24 h. Conversely, irregular flakes of $Mg(OH)_2$ with hexagonal habit and a high level of agglomeration were detected in the brucite samples obtained at 150 ˚C for 12 h. Moreover, the HR-TEM study showed that the $Mg(OH)_2$ nanoparticles are not stable under the exposition to the high energy electron beam of the TEM. This degradation of brucite nanoparticles under electron beam irradiation in the transmission electron microscope was studied in the next research works (*Papers IV and V*) in order to study the stability of the nanoparticles from their dehydration at atomic level.

So from these results, it was possible to determine that controlling the reaction conditions (reaction time and synthesis temperature) during the hydrothermal synthesis can result in pure and high crystalline magnesium hydroxide nanoparticles. The conditions of hydrothermal treatment significantly affected the crystallinity, the morphology and the particle size of the brucite nanocrystals prepared at the synthesis temperatures of 150 ˚C and 180 ˚C.

Paper II

Synthesis and morpho-structural characterization of nanostructured magnesium hydroxide obtained by a hydrothermal method.
Sierra-Fernandez, A.; Gomez-Villalba, L.S.; Milosevic, O.; Fort, R.; Rabanal, M.E

Reprinted with permission from
Ceramics International, **2014,** doi: 10.1016/j.ceramint.2014.04.073

4.1.2. *Paper III.* Effect of temperature and reaction time of the synthesis of nanocrystalline brucite.
Sierra-Fernandez, A.; Gomez-Villalba, L.S.; Muñoz, L.; Flores, G.; Fort, R.; Rabanal, M.E
International Journal of Modern Manufacturing Technologies 6, **2014**. ISSN 2067-3604

It has previously been identified that the variation of the synthesis temperature and the reaction time is crucial in directing the morphology, the particle size and the final crystal structure of the product. In this sense, additional research was required to evaluate the influence of synthesis parameters on the properties of the nanoparticles. Thus, the present investigation aimed at comparatively exploring the impact of the influence of synthesis temperature (from 180 ˚C to 200 ˚C) and reaction time (from 4 hours to 12 hours) on the solid properties of the $Mg(OH)_2$ samples obtained under the synthesis conditions previously established in *Paper II*.

In the assessment of the results achieved, it should mention the establishment of better conditions for continuing to improve the performance of the nanomaterials and make them more effective. In this way, the synthesis parameters exercise a strong influence on the morphology and the particle size of the different magnesium hydroxide particles obtained by using the hydrothermal method. Thus, the comparison between samples synthesized at 180 ˚C during different reaction times (4 and 12 hours) shows the tendency to develop particles with larger particle size with the increase of the time reaction (from ~ 60 ± 20 nm to ~ 170 ± 30 nm). In addition, the physico-chemical characterization of the synthesized magnesium hydroxide nanoparticles has shown how an increase in temperature from 180 ˚C to 200 ˚C promoted the formation of particles with a higher particle size from around 200 ± 20 nm to around 270 ± 40 nm. As the hydrothermal synthesis temperature rises, particle size also increases. These research findings were correlated with the previous work, where the tendency of growing the particle sizes with the increase in temperature was detected at temperatures up to 180 ˚C. Moreover, the rising of the synthesis temperature and reaction time increased the crystallite size from ~ 28 ± 4 nm to ~ 48 ± 5 nm. It is also worth nothing that all samples obtained at these synthesis conditions showed also a preferential orientation, which is in good agreement with the previous research work. The study of the thermal decomposition and the stability study of the magnesium hydroxide nanoparticles obtained at these synthesis conditions showed their interesting properties for its use as a flame retardant due to their high thermal stability marked by a $Mg(OH)_2$ to MgO phase transformation at 375 ˚C.

To sum up, magnesium hydroxide nanoparticles with flake-shaped morphologies were successfully synthesized via hydrothermal method, by controlling the synthesis conditions and using hydrate hydrazine as a surfactant. These results showed a significant correlation with the previous research work. In this way, it could be confirmed that an increase of synthesis temperature from 180 ˚C to 200 ˚C improved the crystallinity degree of $Mg(OH)_2$ nanostructures and also, promoted the formation of plates with bigger and uniform size. As well, it was demonstrated that the increase in the reaction time induced the formation of bigger size brucite plates, which was in agreement with our previous findings.

Paper III

Effect of temperature and reaction time on the synthesis of nanocrystalline brucite.
Sierra-Fernandez, A.; Gomez-Villalba, L.S.; Muñoz, L.; Flores, G.; Fort, R.; Rabanal, M.E

Reprinted with permission from
International Journal of Modern Manufacturing Technologies, **2014.** ISSN 2067-3604

4.1.3. *Paper IV.* Atomic scale study of the dehydrated / structural transformation in micro and nanostructured brucite ($Mg(OH)_2$) particles: Influence of the hydrothermal synthesis conditions
Gomez-Villalba, L.S.; **Sierra-Fernandez, A.**; Milosevic, O.; Fort, R.; Rabanal, M.E *Advanced Powder Technology,* 28**, 2017**. doi: 10.1016/j.apt.2016.08.014

Once the important influence of reaction time and hydrothermal temperature on the physicochemical properties of the $Mg(OH)_2$ nanoparticles was known (*Papers II and III*), the need to determine the effect of reactant concentrations on their hydrothermal synthesis was also stated. Hence, the main objective was to study in depth the role of the hydrazine/nitrate concentration on the morphological variations, the crystal growth and the behavior at an atomic level of the different magnesium hydroxide samples prepared. Therefore, $Mg(OH)_2$ particles synthesized from solutions with high content of hydrazine (0.14 M) and nitrate (0.24 g) were compared with samples obtained from low hydrazine content (0.0002 M) and nitrate (0.12 g) synthesized at the synthesis temperature of 180 ˚C for 4 h, 6 h and 12 h. In addition, the understanding of several processes during the *in situ* observation in a Transmission Electron Microscope (TEM) can shed light on the control of crystal growth and the particles morphology during the preparation of brucite samples. This is why the use of electron radiation in a TEM was used to monitor the transformation process from brucite to periclase for the different synthesized samples during the irradiation at 300 kV.

The research findings reveal how micro and nanostructured $Mg(OH)_2$ crystals showed important differences in particle size, morphology, crystallinity and kinetic of reaction, according to the hydrazine/nitrate content used during the synthesis reaction by hydrothermal method. Thus, the tendency to form bigger hexagonal flakes with higher crystallinity degrees and a strong preferential orientation was observed in samples prepared with high hydrazine and nitrate content. Regarding the morphology of the $Mg(OH)_2$ nanoparticles obtained, it is worth noting that although the samples obtained with low doses of synthesis reagents showed typical hexagonal shapes. Besides, amorphized edges were frequently developed in these samples in comparison with the $Mg(OH)_2$ samples prepared with higher reagents concentrations. In agreement with the previous studies the particle size of the nanoparticles was also highly increased by the prolonged reaction time. Therefore, the largest particles correspond to the samples subjected to prolonged heating treatment (180 ˚C for 12 h) using a high dose of hydrazine/nitrate (986 nm ± 372 nm) and a low dose of hydrazine / nitrate (672 nm ± 216 nm). Furthermore, Rietveld refinements carried out in the different $Mg(OH)_2$ samples showed that the unit cell parameters are bigger in the samples obtained with higher hydrazine/nitrate contents in comparison with those obtained with lower concentrations of the reactants, being the smaller unit cell parameters detected in the samples obtained at short reaction time (180 ˚C for 4 h). These differences in the lattice parameters of the brucite samples showed how the dose of hydrazine/nitrate and the reaction time can modify the dimensions of the unit cell and thereby could cause a change in the specific properties of the synthesized materials. Moreover, while the samples prepared with higher hydrazine/nitrate content developed strong preferential orientations, the samples prepared with a fewer dose presented a lower defect density with an aleatory

distribution. These significant differences were key factors in the reaction kinetic detected during the dehydration process in the different micro and nanostructured $Mg(OH)_2$ particles. In this way, the rapid formation of a porous surface, the amorphised cortex or the presence of highly oriented strains were detected in samples prepared from higher hydrazine / nitrate content during the electron beam irradiation. The presence of preferential orientations observed in these $Mg(OH)_2$ samples increased the kinetic of reaction producing a faster dehydration process in these brucite samples.

This research highlighted the importance of a careful monitoring of the concentration of hydrazine and nitrate during synthesis of $Mg(OH)_2$ in order to determine the appropriate hydrothermal synthesis conditions to the design of nanoparticles with specific particle size, shape, chemistry or textural properties according to their application for the conservation of stone heritage.

Paper IV

Atomic scale study of the dehydration/structural transformation in micro and nanostructured brucite $Mg(OH)_2$ particles: Influence of the hydrothermal synthesis conditions

Gomez-Villalba, L.S.; Sierra-Fernandez, A.; Milosevic, O.; Fort, R.; Rabanal, M.E.

Reprinted with permission from
Advanced Powder Technology, **2017**, doi: 10.1016/j.apt.2016.08.014

4.1.4. *Paper V.* Effect of morpho-structural properties on the intrinsic cathodoluminescence emission from synthetic nanocrystalline brucite ($Mg(OH)_2$) obtained by different synthesis processes.
Gomez-Villalba, L.S.; **Sierra-Fernandez, A.**; Quintana, P.; Rabanal, M.E.; Fort, R. **2017**. *Submitted*

The determination of the synthesis method is fundamental for the design of nanomaterials with defined morphologies, besides allowing a control of the mineral phases, its stability, the phase transformation mechanism, its particle size, its agglomeration degree or the defects associated with the synthesis process. It is also crucial when in addition to getting a single mineralogical phase, it is intended to synthesize a mixture of several phases which will make the nanomaterials more suitable and adaptable to the needs of the material to be treated. As was detected in the previous studies (*Papers II, III and IV*), the hydrothermal method employed for the synthesis of the different magnesium hydroxide nanoparticles could have led the generation of a strong preferential orientation in the samples due to the use of hydrazine hydrated as reducing agent, and/or the high pressure and temperature used during the reaction. Therefore, in order to study different synthesis methods to obtain magnesium hydroxide nanoparticles and to explore the obtaining of unoriented nanostructures $Mg(OH)_2$, distinct synthesis methods were carried out and types of brucite nanoparticles were synthesized. Apart from the hydrothermal synthesis route, the sol-gel method was chosen because of its many advantages, including the obtaining of particles of a smaller size, highly homogeneous and without the risk of developing preferential orientations.

Hence, the present research work aims to compare the physical and chemical properties of nanostructured $Mg(OH)_2$ prepared by using the hydrothermal method, the sol-gel synthesis method and a commercial product based on $Mg(OH)_2$ nanoparticles. To do this, the intrinsic cathodoluminescence (CL) emission in the region between ~ 300 to 660 nm from different nanocrystalline $Mg(OH)_2$ samples was performed. When a sample in this region is analyzed, it is possible to obtain information about the degree of disorder of the material, which gives rise to luminescence signals, which are typical for a specific mineralogical phase. The combination of several techniques, including TEM-SEM and cathodoluminescence spectroscopy usefully provides a simultaneous information about morpho-structural properties, and the possible presence of lattice defects in a selected area of the nanomaterial. In addition, XRD and TEM-ED results obtained for the different samples were correlated with their cathodoluminescence spectra for a better understanding of the origin of the luminescence. The integration of this information contributes to a better understanding not only of the origin of the intrinsic cathodoluminescence, but it can also be taken into account to evaluate its response to strains, including weakness or fracturing risks in certain crystallographic orientations of the different synthesized materials.

The results obtained led to evidence of important differences on the crystallographic structures, the particle orientation, the particle sizes, and the morphologies of all magnesium hydroxide samples according to the synthesis method. In this way, a preferential

growth orientation affecting the (0001) plane was detected in the magnesium hydroxide samples obtained by using the hydrothermal method and the commercial $Mg(OH)_2$. Whereas, the different XRD patterns obtained from the sol-gel samples showed the presence of brucite with a similar order in the intensities, respect to the JCPDS card, revealing the formation of unoriented $Mg(OH)_2$ nanoparticles. Regarding the particle size of the samples according to the synthesis method, the brucite samples synthesized by the hydrothermal method presented the formation of plates with a bigger particle size in comparison with the $Mg(OH)_2$ samples obtained by the sol-gel method. In this way, the samples obtained by hydrothermal method exhibited variable particle sizes ranging from 350 nm to 1.8 μm in the largest length and the commercial samples showed particle sizes in the range between 250 nm and 430 nm in the largest length. In the case of the sol-gel samples, the nanoparticles exhibited smaller and more uniform size ranging between 40 to 80 nm. Furthermore, the synthesis method also played an important role in controlling the morphology of the nanocrystals. Thus, the formation of more uniform and defined hexagonal nanoflakes was detected in the $Mg(OH)_2$ nanoparticles obtained by the sol-gel method, in comparison with the samples obtained by hydrothermal synthesis and the commercial $Mg(OH)_2$, which exhibited more irregular shapes. This research highlighted the importance of a careful monitoring of the concentration of hydrazine and nitrate during synthesis of $Mg(OH)_2$ in order to determine the appropriate hydrothermal synthesis conditions to the design of nanoparticles with specific particle size, shape, chemistry or textural properties according to their application for the conservation of stone heritage.

The CL measurements carried out in the three samples allowed to establish that the CL emission showed a strong dependence according to the particle orientation. Therefore, it was possible to detect three peaks with different intensity order depending on the crystalline orientation. Three peaks at 381 nm, 419 nm and 466 nm were common for the three samples in oriented along (0001) with similar order in the intensity. Whereas, when the CL was registered in the $(11\bar{2}0)$ plane, the main peak appeared at 409 nm, preserving the 481 nm and 466 nm in all $Mg(OH)_2$ samples. Moreover, additional signals at ~425 nm, ~654 nm and ~488 nm were detected in the sol-gel sample confirming the presence of magnesite produced by carbonation reaction, in agreement with the XRD results. The high reactivity detected in this sample with a rapid carbonation process with regard to another one, constituted an important point to take into account for the use of these nanomaterials for the consolidation of stone heritage.

The CL analytical technique has resulted especially useful for the analysis of the magnesium hydroxide nanoparticles, which as it could be determined in the previous studies (*Papers II and IV*) are radiation-sensitive materials. The combination of this technique with the TEM results was useful and complementary, pointing to the sol-gel synthesis as a potential method to synthesize nanoparticles with important physical and chemical properties as a consolidant product.

Paper V

Effect of morpho-structural properties on the intrinsic cathodoluminescence emission from synthetic nanocrystalline brucite ($Mg(OH)_2$) obtained by different synthesis processes

Gomez-Villalba, L.S.; Sierra-Fernandez, A.; Quintana, P.; Rabanal, M.E.; Fort, R.

Manuscript, *Submitted* **2017**.

4.1.5. *Paper VI.* TEM-HRTEM study on the dehydration process of nanostructured Mg-Ca hydroxide into Mg-Ca oxide
Gomez-Villalba, L.S.; **Sierra-Fernandez, A.;** Rabanal, M.E; Fort, R.
Ceramics International, 42 (8), **2016**. doi: 10.1016/j.ceramint.2016.03.007

As was shown in the previous works (*Papers II* and *IV*), the study of the interaction of electron irradiation with matter and the response of the material to the passage of electrons shows a great variety of fundamental importance phenomena that may be studied by in-situ electron microscopy. This study is essential to improve the nanocrystals shape-control mechanisms as well as the design and the study of nanomaterials. Therefore, the present research study aimed to explore the transformation kinetics of Mg-Ca hydroxide ($Mg_{0.97}Ca_{0.03}(OH)_2$, brucite hexagonal type structure) to Mg-Ca oxide ($Mg_{0.97}Ca_{0.03}O$, periclase type cubic structure) as a result of the exposition to the electron beam by combining TEM, HRTEM, EELS and image analysis. Particular emphasis was placed on the exploration of the influence of the presence of calcium on the stability of $Mg(OH)_2$ nanoparticles within the electron beam. In this way, the transformation process was monitored in function of reaction time applying 200 kV to study the porosity evolution with the irradiation time and for to analyze the chemical composition. Moreover, the chemical behavior of the samples during the exposition to the electron beam energy was carried out operating at 300 kV, because it is possible to get more suitable and valuable information due to its higher resolution power. An important point of this research work is that the observed effects are completely free of some factor commonly present in liquid cell TEM, such as additional agents, which can interfere in the process.

So, the main results showed that it was possible to detect different reaction times during the transformation in function to the beam accelerating voltage applied. The dehydration process of Mg-Ca hydroxide to produce the corresponding Mg-Ca oxide modified the porosity because of the water release. These changes in the particle´s porosity were monitored during the exposure to the electron beam at 200 kV. The dynamic of porosity generated during the irradiation starts at the particle's edge, gradually increasing from the outside to the inside of the particle depending on the irradiation time. However the dehydration process happens simultaneously everywhere, especially at the electron-exit surface. Consecutively, the pore size is increased to finally collapse the structure with a decrease in porosity and pore size. When samples were exposed to 300 kV, the dehydration process was much faster, and the pores structure was destroyed in a shorter time (after 120 s) in comparison with lower doses of radiation, where the structure was destroyed after 700 s. These changes in the porosity of the samples during the dehydration with the electron beam were also observed in the previous studies carried out in the $Mg(OH)_2$ synthesized by hydrothermal method (*Papers II* and *IV*).

On the other hand, the chemical behavior during the exposition to the electron beam energy, which resulted in the dehydration of $Mg_{0.97}Ca_{0.03}(OH)_2$, was followed by using TEM-HRTEM and spectroscopy measurements (EELS-EDS), operating at 300 kV. It was determined that, although the $Mg_{0.97}Ca_{0.03}(OH)_2$ nanoparticles had a similar

behavior that $Mg(OH)_2$ nanoparticles during the dehydration process, the presence of calcium could affect the transformation kinetic, and at the same time, cell parameters and hence its specific properties could also be affected finally. In this way, the replacement of Mg ions by Ca ions affects the local properties of the nanomaterial. Moreover, differences in the ionic radius, Ca= 0.99Å > Mg =0.72Å, could be responsible for the generation of atomic defects, which affect the kinetic of reaction modifying the hydroxide into oxide reaction time. Hence, the study of the structural changes during the exposition at 300 kV allowed to identify different stages of transformation, showing the progressive changes from brucite to periclase, including the formation of an intermediate dehydrated brucite phase. Furthermore, the EELS results allowed calculating a local thickness reduction of 34% in one representative particle, due to mass loss during the dehydration.

These findings brought new insight into the effects of the electron beam in crystal growth studies, contributing to the better understanding of the transformation kinetics from Mg-Ca hydroxide to Mg-Ca oxide. Interestingly, the comparison of these results with the previous results reported to pure $Mg(OH)_2$ (*Papers II* and *IV*) allowed determining an increase in the stability of the $Mg_{0.97}Ca_{0.03}(OH)_2$ under electron beam irradiation with slower decomposition reactions. Thus, the application of Mg-Ca hydroxide nanoparticles for the consolidation of stone heritage not only can result in a nanomaterial highly compatible with the calcareous stone but also the Ca ions could also modify different properties of the $Mg(OH)_2$, such as its catalytic performance among many more things. Besides, the presence of Ca ions could induce the generation of atomic defects, which affecting the kinetic of decomposition reaction, as was previously determined.

Paper VI

TEM-HRTEM study on the dehydration process of nanostructured Mg-Ca hydroxide into Mg-Ca oxide

Gomez-Villalba, L.S.; Sierra-Fernandez, A.; Rabanal, M.E.; Fort, R.

Reprinted with permission from
Ceramics International 42 (8), **2016**. doi: 10.1016/j.ceramint.2016.03.007

4.1.6. *Paper VII.* New consolidant product based on nanoparticles to preserve the dolomitic stone heritage
Sierra-Fernandez, A.; Gomez-Villalba, L.S; Rabanal, M.E.; Fort. R
M.A. Rogerio Candelera (Ed.), Proceedings of the 2nd International Congress on Science and Technology for the Conservation of Cultural Heritage, Sevilla, 24-27 Jun. **2014**. ISBN 9781315712420

As shown throughout the present Ph.D dissertation, the properties of the nanomaterials have significant advantages that could solve many problems found in traditional interventions of stone consolidation. Among all requirements that a product must have to be used for safeguarding the stonework of buildings and historic monuments, its physical and chemical compatibility with the stone substrate is one of the most important (for further information see *Chapters 1* and *2*). Due to that the action of these nanomaterials in the stone heritage is based on their own carbonation reaction, to our knowledge it is essential to evaluate the behavior of these types of nanomaterials when they are being exposed to factors such as relative humidity, exposition time and carbon dioxide concentration before being applied to the stone substrates. Hence, the main objective of this research was the study of the behavior and the carbonation process of the nanoparticles when they are exhibited exposed under controlled conditions to a high relative humidity (RH) of 75%. Thus, this research work shows the stability study of the magnesium hydroxide nanoflakes, specifically designed in order to obtain a consolidant product with increased compatibility with the calcium-magnesium carbonate substrates. Specifically, this research work is centered on the effectiveness and compatibility study of the nanoparticles according to the stone substrate to be treated (Laspra dolostone).

The selection of the nanoparticles in this study was made according to the careful monitoring carried out to obtain the most optimal nanoparticles for the stone consolidation, which was widely explained in the previous *Papers II, III* and *IV*. From these results it could be determined that: i) the particle size of magnesium hydroxide is reduced at lower synthesis temperatures (150 ˚C), ii) a prolonged reaction time of 24 hours would imply a relatively adequate dissolution-recrystallization process in the hydrothermal method, and iii) the tendency to form the smallest crystals was observed in the samples obtained with low hydrazine / nitrate content. This is why among all the types of nanoparticles studied in our previous works, the selected $Mg(OH)_2$ nanoparticles were obtained at 150 ˚C for 24 h and with a low dose of hydrazine/nitrate content. The processing and the physico chemical characterization of these nanoparticles have previously been described in *Paper II*.

The main results revealed that the nanoparticles showed a particle size of around 160 ± 40 nm and around 240 ± 30 nm before and after their exposition to 75% for 31 days, respectively. These particle sizes were determined as suitable for their application as consolidating product in the Laspra dolostone, according to its small sizes of pores (0.2 µm of radius). Moreover, the study of the crystalline structure and

the identification of the mineral phases carried out by XRD showed the high reactivity of the as-prepared magnesium hydroxide nanoparticles with a rapid carbonation process under the studied conditions. Therefore, after 31 days of exposure, the XRD analysis showed the identification of different magnesium carbonates polymorphs [hydromagnesite, $Mg_5(CO_3)4(OH)_2 \cdot 4(H_2O)$, and magnesite ($MgCO_3$)].

These experimental findings showed the promising properties of this type of brucite nanoparticles to be used as consolidating products for the stone built-heritage. In addition, this research highlighted the importance of determining the stability of the synthesized inorganic nanomaterials under different environmental conditions, prior to their application in stone substrates.

Paper VII

New consolidant product based on nanoparticles to preserve the dolomitic stone heritage

Sierra-Fernandez, A.; Gomez-Villalba, L.S; Rabanal, M.E.; Fort. R.

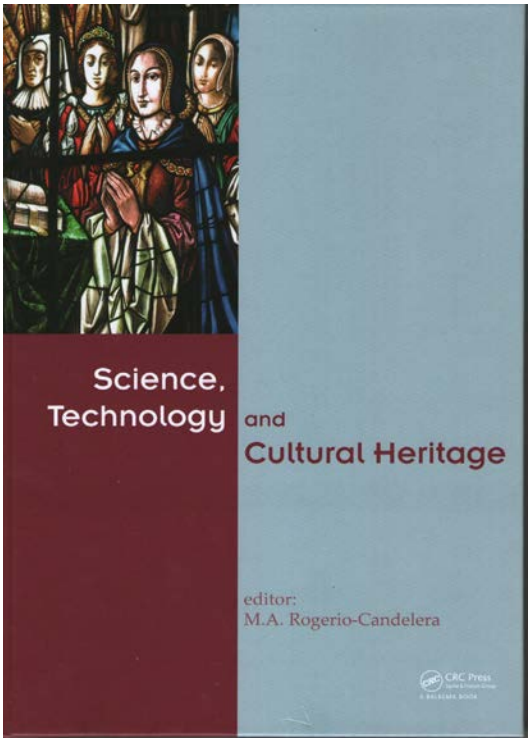

M.A. Rogerio Candelera (Ed.), *Proceedings of the 2nd International Congress on Science and Technology for the Conservation of Cultural Heritage*, Sevilla, 24-27 Jun. 2014. ISBN 9781315712420.

4.1.7 *Paper VIII.* Nuevos avances en el diseño de nanomateriales para la consolidación del patrimonio pétreo: Evaluación de su efectividad en la dolomía de Laspra.
New developments in the design of nanomaterials for the consolidation of stone heritage: Effectiveness evaluation in Laspra dolostone.
Sierra-Fernandez, A.; Gomez-Villalba, L.S.; Muñoz, L.; Rabanal, M.E.; Fort. R M. Moreno Oliva, M.A. Rogerio-Candelera, J.T. López-Navarrete, V. Hernández-Jolín (Ed.). Proceedings of the National Congress Estudio y Conservación del Patrimonio Cultural, Málaga, 16-19 Nov., **2015**. ISBN 9788460824527

Dolostone represents one of the most used materials in the history of construction in the world. The damage experienced by these stone materials generates a significant loss of internal cohesion that makes the application of consolidant products necessary. Up to know, as was discussed in *Chapter 2,* the calcium hydroxide nanoparticles are one of the most commonly used consolidant products of stone heritage. However, it is important to emphasize that variables such as the possible Mg^{2+}/Ca^{2+} ion exchange in the stone-consolidant system, the influence of particle size on carbonation kinetics or the possible surface tension differences in the medium, have to be taken into account. The dedolomitization is another important risk arising as a result of the use of calcium hydroxide nanoparticles for the dolostone consolidation, due to the calcium ion enrichment. Thus, this research work aims the effectiveness evaluation of a developed consolidating product based on $Mg(OH)_2$ nanoparticles obtained by the hydrothermal method, with morphologies, particle sizes, crystalline structures, and compatibility suitable for application in the dolostone, as it was shown in the previous research work (*Paper VII*).

In this way, the nanoparticles were applied in Laspra dolostone (Asturias, Spain), which is mainly composed of dolomite ($MgCa(CO_3)_2$, 90 %wt), and the consolidation process was monitored before and after 31 days of the treatment under a controlled environmental atmosphere of 75% Relative Humidity. For the application of the nanoparticles dispersions, six cubic samples (5 cm side) were treated by brushing until apparent refusal. The concentration of the nanoparticles in the ethanol dispersion was 5.0 gL^{-1}. Moreover, the carbonation reaction of the $Mg(OH)_2$ nanoparticles synthesized by hydrothermal method, were comparatively evaluated with a commercial sample of $Mg(OH)_2$, whose physical and chemical properties haves been previously determined in *Paper IV*.

The results showed important differences in the physico-chemical properties of both $Mg(OH)_2$ samples after 31 days of the treatment to 75 %RH. Therefore, while the brucite nanoparticles obtained by the hydrothermal method showed the formation of elongated particles with a particle size of around 240 ± 30 nm and a thickness of ~ 20 nm, the commercial product showed larger particles (340 ± 30 nm) with a preferential crystal growth and irregular shapes, after 31 days of treatment. The comparative study carried out in both types of $Mg(OH)_2$ samples confirmed the optimal suitability of the nanoparticles obtained by the hydrothermal method according to the petrophysical properties of the Laspra dolostone. After the consolidant treatment with magnesium hydroxide

nanoparticles, the surface appearance of the Laspra dolostone changed slightly due to the formation of a uniform layer over the surface. Besides, it was possible to see how the pores were partially filled by the nanomaterial. In this form, these findings indicated that the consolidant product did not modify the stone microstructure, maintaining the general pore space. The designed inorganic nanomaterial constitutes thus a stable product with enhanced chemical-physical affinities for natural stone.

Paper VIII

Nuevos avances en el diño de nanomateriales para la consolidación del patrimonio pétreo: Evaluación de su efectividad en la dolomía de Laspra.
New developments in the design of nanomaterials for the consolidation of stone heritage: Effectiveness evaluation in Laspra dolostone.
Sierra-Fernandez, A.; Gomez-Villalba, L.S.; Muñoz, L.; Rabanal, M.E.; Fort. R

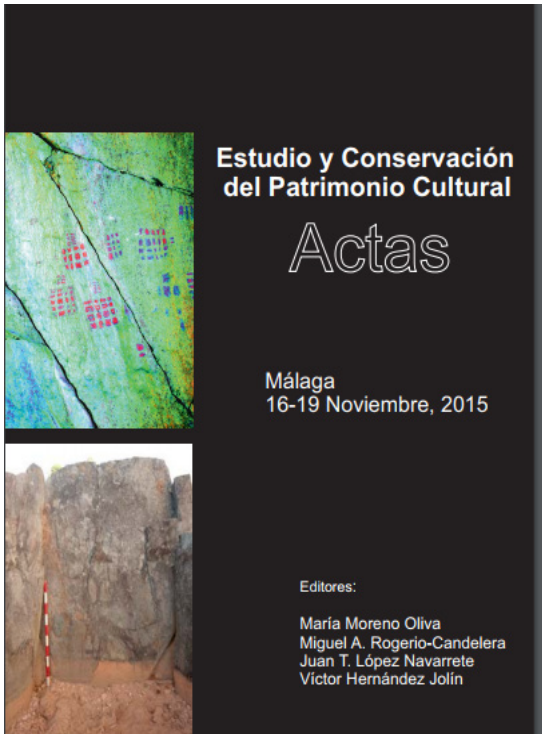

M. Moreno Oliva, M.A. Rogerio-Candelera, J.T. López-Navarrete, V. Hernández-Jolín (Ed.). *Proceedings of the National Congress Estudio y Conservación del Patrimonio Cultural*, Málaga, 16-19 Nov. 2015. ISBN 9788460824527

4.1.8 *Paper IX.* Consolidation of calcareous stones by Mg-Ca hydroxide nanoparticles: Treatment-Stone Interactions during Drying Revealed by Neutron Radiography. **Sierra-Fernandez, A.**; Gomez-Villalba, L.S.; Rabanal, M.E.; P. Quintana; Fort. R **2017**, *Manuscript*

The effectiveness of consolidant products applied in the stone heritage is often doubtful due to the lack of effective and compatible of the own consolidating materials. Dispersions of magnesium hydroxide nanoparticles in alcohol could offer an important solution for the consolidation of dolostone substrates, as it was shown in *Paper VIII*. When these hydroxide nanoparticles are exposed to atmospheric CO_2 in wet conditions, the layered network of their hexagonal packing structure favors the incorporation of such CO_2 to the structure producing the carbonation process, which consists of reacting and transforming into magnesium carbonate, resulting in a structural consolidation of treated stone. However, to our knowledge it is important to take into account that according to the compatibility, the proportions of magnesium and calcium in limestones and dolostones often differ widely both within a single rock formation and between formations. In this sense, in order to improve the compatibility, effectiveness, and durability of these nanomaterials applied to calcareous substrates, magnesium and calcium hydroxide nanoparticles with different weight ratios (10:90 %wt; 90:10 %wt; and 50:50 %wt) were synthesized by sol-gel method, being specifically designed in function of the chemical composition of the stone to treat. In addition, the idea to explore these types of systems was motivated by the fact that the replacement of Mg ions by Ca ions could affect the local properties of the Mg-Ca hydroxide nanoparticles, as it was shown in *Paper VI* where an increase in the stability of the nanoparticles based on magnesium and calcium hydroxides was detected under electron beam irradiation.

Hence, this research work aimed to conduct the morpho-structural characterization of the different nanostructured magnesium and calcium hydroxide NPs obtained via sol-gel method by using XRD, SEM and TEM. The selection of the nanomaterials as consolidating product in dolostone substrates was carried out according to the chemical composition and the petrophysical properties of the lithotypes. So, to assure an optimal consolidation result, the Laspra dolostone was treated with a solution of $Mg(OH)_2$/$Ca(OH)_2$ 50:50 %weight NPs dispersed in ethanol in a concentration of 2.5 g/L. The Laspra dolostone is a calcareous stone widely used in the cultural heritage of Spain. Moreover, the knowledge of the penetration depth of the consolidant and its distribution into the stone matrix determines the treatment effectiveness. From the literature, it is not clear the absorption and drying kinetics of the materials based on hydroxide NPs applied to stone substrates. This consolidant penetration inside the stone substrate is dependent on multiple parameters, such as the competition between capillary absorption and solvent evaporation, the pore system of the stone or the properties of the consolidating product, among others parameters. Thus, in order to monitor the consolidant action in the dolostone samples, neutron radiography (NR) was used to evaluate the effectiveness of the magnesium and calcium hydroxides and its spatial distribution into the lithotypes. The hydroxide dispersions were applied in a concentration of 2.5 g/L in ethanol by

brushing and capillary absorption. The penetration depth and its distribution into the stone samples were monitored by NR. This study represents the first in going deeper into the application of this method in direct monitoring of the stone treatments based on hydroxide nanoparticles for cultural heritage conservation.

The ESEM-EDS technique was used in order to evaluate the morphological variations deriving from the consolidation treatment. Furthermore, the consolidant effectiveness of the different nanomaterials applied in dolostone substrates was evaluated by ultrasonic velocity, mercury intrusion porosimetry (MIP), and micro-hardness tests.

Different Mg-Ca hydroxide nanoparticles with distinct weight ratios (10:90 wt%; 90:10 wt% and 50:50 wt%) were successfully synthesized via the sol-gel method. The majority of the nanoparticles presented average sizes from ~30 to ~150 nm with well-defined hexagonal shapes and high crystallinity. Interestingly, meanwhile the sample based on $Ca(OH)_2$ showed hexagonal shape particles with a bigger uniform particle size of from around 62 nm to 450 nm, the results obtained for the Mg-Ca hydroxide nanoparticles with the different weight ratios of 10-90 wt%, 90:10 wt% and 50:50 wt% showed a uniform particle size of around 64.7 nm ± 34 nm, 31.4 nm ± 4.7 nm, and 30.13 nm ±10 nm, respectively. These findings suggested that $Mg(OH)_2$ could slow down the $Ca(OH)_2$ crystal growth diminishing its particle size up to 78%.

Related to the efficacy as consolidating products, the neutron radiography has shown that the effectiveness of the nanoparticles as a consolidant product in stones is strongly affected by the methodological application. Thus, the application of NR for the study of the nanoparticles consolidant action has defined the absorption and drying kinetics of the alcohol dispersions of magnesium and calcium hydroxide NPs followed as a function of time. Therefore, the dispersion of magnesium hydroxide and calcium hydroxide NPs in ethanol can easily penetrate in the Laspra dolostone substrates treated by capillary absorption, reaching a maximum particles penetration of 1.52 cm, after 100 minutes of the treatment. Moreover, the study revealed a maximum particle penetration of 0.55 cm after 100 minutes of treatment into the Laspra with a solution of $Mg(OH)_2/Ca(OH)_2$ NPs 50:50 wt% 2.5 g/L in ethanol by brushing. However, at the drying phase the radiographs show the accumulation of nanomaterial just underneath the surface, limiting the penetration depth of the NPs into the dolostone treated by brushing.

Moreover, the ESEM analysis carried out in the treated lithotypes showed the Mg-Ca hydroxides (50:50 wt%) NPs filling the pores and inter-crystalline dolomite grain contacts in the Laspra dolostone. A decrease in total porosity was detected by MIP in all stones after the consolidant treatment due to the filling of pores by the consolidating product. In addition, an increase in ultrasonic velocity was produced after treatment in all dolostone samples. Thus, the treatment of dolostone by $Mg(OH)_2/Ca(OH)_2$ in a % weight ratio of 50:50 NPs by brushing and capillary absorption generated a 1.96% and a 3.08% increase, respectively. This increase in the ultrasonic velocity values was related to the decrease in total porosity in both types of stones. According to the surface hardness results obtained for the different treated lithotypes,

the highest increase was observed in the samples treated with the nanoparticle systems.

As general conclusions, it is important to point out how the different systems of magnesium and calcium hydroxide nanoparticles were successfully synthesized by sol-gel method with important physical and chemical properties for its use as novel materials for the consolidation of carbonatic stones in cultural heritage. These nanomaterials could solve many problems found in the traditional interventions, shown a successful effectiveness as a consolidant product with high compatibility with the stone to treat. In addition, the results show that the neutron radiography has proven to be an excellent tool to monitor clearly the nanoparticles diffusion in porous carbonate stone non-destructively.

Paper IX

Consolidation of calcareous stones by Mg-Ca hydroxide nanoparticles: Treatment-Stone Interactions during Drying Revealed by Neutron Radiography.

Sierra-Fernandez, A.; Gomez-Villalba, L.S.; Rabanal, M.E.; P. Quintana; Fort. R

Manuscript, 2017.

PART II

Designing:

New antifungal protective coatings: Zn-doped MgO **($Mg_{1-x}Zn_xO$) nanoparticles**

4.2. Designing new antifungal protective coatings for the stone heritage: $Mg_{1-x}Zn_xO$ nanoparticles

Biodeterioration is considered one of the main degradation processes of outdoor stone heritage. The microbial agents can deteriorate stone because they secrete enzymes and organic acids during their metabolic processes, highly harmful for monumental stones. This is particularly alarming in tropical regions or areas with high levels of humidity. Thus, part of this research has been carried out in the Yucatán Peninsula, in southeastern Mexico, which corresponds in average to a humid tropical region. Yucatán has Mayan archaeological sites of immense cultural significance, such as *Tulum*, *Chichén Itzá*, *Uxmal* or *Ek´Balam*. However, the biodeterioration is one of the most important degradation factors in these iconic sites, due to the special environmental factors in these regions, such as heavy rainfall, high temperatures or high relative humidity levels, which make it particularly favorable for the sustenance of most organisms. These special conditions make this region an important operational area for the present investigation.

Recurrent treatments are based on the application of chemical products that present, among other important inconveniences, their high toxicity or the risk of generating harmful subproducts. In this context, the importance of carrying out remediation actions for microbiologically contaminated historic materials is of crucial importance and is considered to be one of the priorities for the conservation of artworks. This chapter presents the results directed to offer a solution producing potential antifungal agents based on Zn-doped MgO ($Mg_{1-x}Zn_xO$) nanoparticles, designed for the protection of calcareous stone heritage (*Figure 4.2.1*). The antifungal activity of the different types of nanoparticles was assessed using *Aspergillus niger*, *Penicillium oxalicum*, *Paraconiothyrium* sp., and *Pestalotipsis maculans* as representatives of fungal species, which are especially active in the deterioration of limestone. These research findings are summarized below and they are widely discussed in *Paper X*.

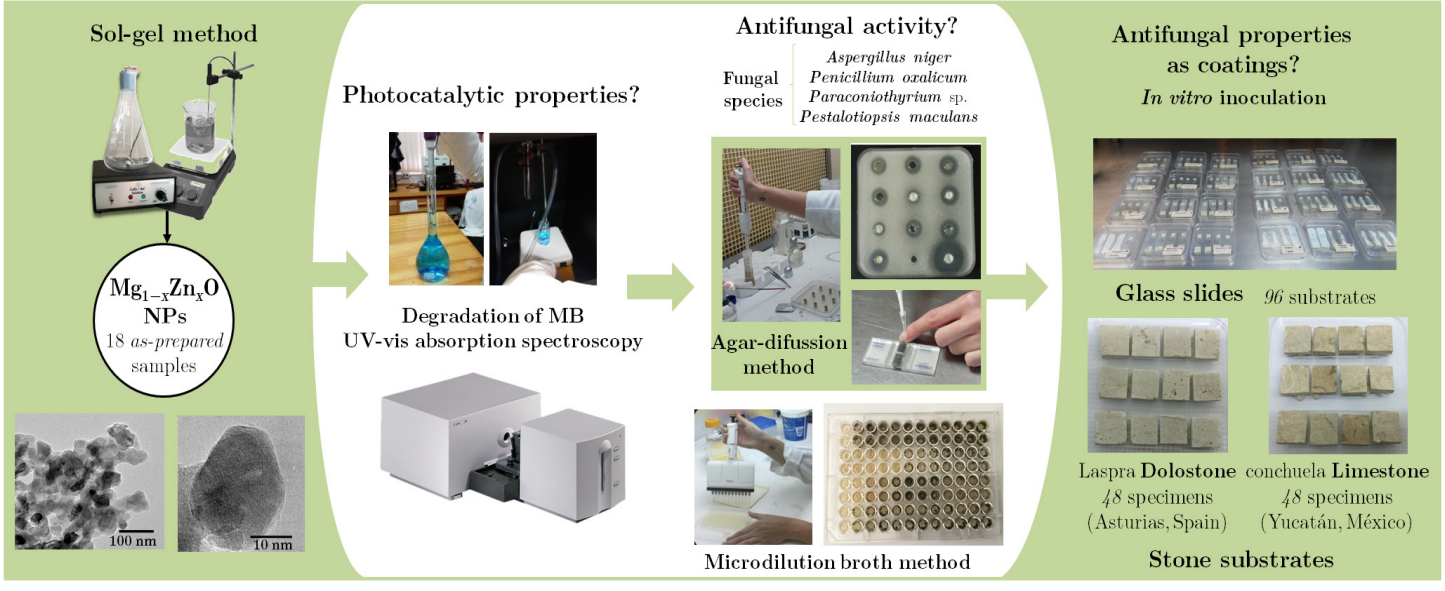

Figure 4.2.1: *A schematic illustration of the experimental set-up carried out for determination of the photocatalytic properties and the antifungal activity of the nanoparticles as coatings in different substrates (glass slides and calcareous stone substrates, dolostone and limestone).*

4.2.1. *Paper X.* Synthesis, photocatalytic, and antifungal properties of MgO, ZnO and Zn/Mg oxide nanoparticles for the protection of calcareous stone heritage.
Sierra-Fernandez, A.; De la Rosa-García, S.C.; Gomez-Villalba, L.S.; Gómez-Cornelio, S.; Rabanal, M.E.; Fort, R.; Quintana, P
ACS Applied Materials & Interfaces, **2017,** doi: 10.1021/acsami.7b06130

The present research work aims to combine the strong antimicrobial activity of ZnO with the safe-to use antimicrobial effectiveness and good compatibility of MgO with stony materials. This approach is intended to develope antifungal coatings with high effectiveness for stone preservation. In addition, the idea to combine both types of metal oxides was considered particularly interesting because the presence of both lattices could develop point defects into the nanocrystals, modifying their photocatalytic and antifungal properties. Therefore, in this investigation the processing via sol-gel method and the physico-chemical characterization of the different metal oxides, pure MgO, ZnO and Zn-doped MgO ($Mg_{1-x}Zn_xO$, x=0.096) nanoparticles, has been done aiming to derive an effective protective material with multifunctional photocatalytic and antifungal properties for calcareous stone heritage.

The morphological microstructural and chemical analysis carried out in the different types of metal oxides revealed that the MgO could slow down or inhibit the ZnO crystals growth and diminish its particle size. Hence, while the sample based on pure ZnO showed well-defined pseudo hexagonal nanoplates with an uniform particle size of around 130 ± 40 nm, the study of $Mg_{1-x}Zn_xO$ particles showed the formation of nanocrystals with an uniform average size of around 52 ± 13 nm. Moreover, the development of surface defects on Zn-doped MgO nanoparticles as a result of the presence of both lattices was confirmed by HR-TEM analysis and PL measurements. The findings obtained revealed how the MgO lattice is affected by the presence of ZnO particles, identifying the development of planar defects such as stacking faults, which originate small displacement in the (200) planes. Also, the presence of extra atoms of smaller diameter occupying spaces in the MgO lattice, contributed to the distortion and the development of dislocations.

The photocatalytic study revealed showed that the ZnO significantly improved the catalytic efficiency of MgO under UV light-irradiation, with a percentage of photodegraded methylene blue (MB) higher than 80%, after 60 minutes. At the same time, the study of the antifungal activity was carried out by the agar diffusion method in terms of zone of inhibition of fungal growth and also by establishing the Minimum Inhibitory Concentration (MIC). Based on this procedure was determined the lowest concentration of the nanoparticles that could completely inhibit the visible growth of fungal pathogens. Interestingly, in general the Zn-doped MgO nanoparticles showed growth inhibition efficiency against *A. niger*, *P. oxalicum*, *Paraconiothyrium* sp., and *P. maculans*. The enhanced photocatalytic and antifungal activity detected in the Zn-doped MgO nanoparticles was attributed to the formation of crystal defects by the incorporation of another element into the host phase, which changed its surface morphology and structural properties modifying their functional characteristics. Hence, this research work highlights the potential of surface defects in the design and the development of new nanomaterials for the preservation of stone heritage.

In terms of the antifungal properties of the nanoparticles as coatings, firstly the antifungal effectiveness of the nanoparticles against *A. niger* and *P. oxalicum* was evaluated using treated glass slides as model substrates. This study pointed out the antifungal effectiveness of the MgO and the Zn-doped MgO nanoparticles with the complete inhibition of both fungi. The application of these nanoparticles as antifungal coatings on stone substrates (Laspra dolostone and Conchuela limestone) showed that the fungi-stone interactions are potentially conditioned by the petrographic features (especially the type and extent of porosity) of the lithotypes. Thus, the higher porosity and the increased microporosity detected in Laspra dolostone by MIP, would allow a greater bioreceptivity to fungal growth in comparison with Conchuela limestone. Moreover, the BSE-ESEM results proved that the coatings substantially decreased substantially the epilithic and endolithic fungal colonization of the dolostone and limestone coupons, indicating a greater antifungal effectiveness on $Mg_{1-x}Zn_xO$ nanoparticles with a limited impact on their surface color. In addition, a higher loss of porosity was observed by MIP in the untreated stone specimens than the treated ones, which was attributed to the increased filling of pores by hyphae growth.

Summarizing the results, leads to the conclusion that the $Mg_{1-x}Zn_xO$ nanoparticles are new promising agents to prevent the fungal growth on stone-built heritage. These compounds can be used as additives for the production of novel biocides for conservation and restoration treatments, constituting an efficient and environmental safe solution for the biodeterioration of our precious world heritage.

Paper X

Synthesis, photocatalytic, and antifungal properties of MgO, ZnO and Zn/Mg oxide nanoparticles for the protection of calcareous stone heritage
Sierra-Fernandez, A.; De la Rosa-García, S.C.; Gomez-Villalba, L.S.; Gómez-Cornelio, S.; Rabanal, M.E.; Fort, R.; Quintana, P

Reprinted with permission from
ACS Applied Materials & Interfaces, **2017**, doi: 10.1021/acsami.7b06130

PART III

Further applications:

Treatment of paper: $Mg(OH)_2$ nanoparticles

4.3. Further applications: $Mg(OH)_2$ nanoparticles for the treatment of paper

The preservation of library collections, archives and cellulose-based works of art is of crucial interest. Specially, the cellulose-based materials which are usually affected by the action of hydrolysis and oxidation that leads to the loss of the mechanical resistance of the fibers and to discoloration phenomena of the substrate. To solve this problem, traditional deacidification methods are based on the use of highly alkaline aqueous solutions. The alkaline earth metal hydroxides are the ideal deacidifying agents because they are highly compatible with the substrate and at the same time are able to neutralize acidity. However, these methods present significant disadvantages such as the water-sensivity of several paper components, or the risk of producing alkaline depolimerization of cellulose due to the use of aqueous solutions with high alkalinity. To provide a solution to this important field, the next chapter shows the application of the $Mg(OH)_2$ nanoparticles synthesized by hydrothermal method and dispersed in alcohol on cellulose sheets in order to create protective coatings.

Moreover, another important point investigated in the present chapter was the use of different strategies to modify the fiber surfaces and improve the interaction of adjacent fibers. The refining has evolved into an important research area of papermaking science due to that the refining of chemical pulp can improve the bonding ability of fibers as well as to improve their strength properties and sheet formation. This is why, in order to obtain cellulose fibers highly age-resistant, the approach to study the modification of unrefined and refined pine cellulose fibers with different degrees of lignification through the application of brucite nanoparticles, was tried (*Figure 4.3.1*). Thereby, an important additional application of the magnesium hydroxide nanoparticles was revealed from these results and is shown in *Paper XI*.

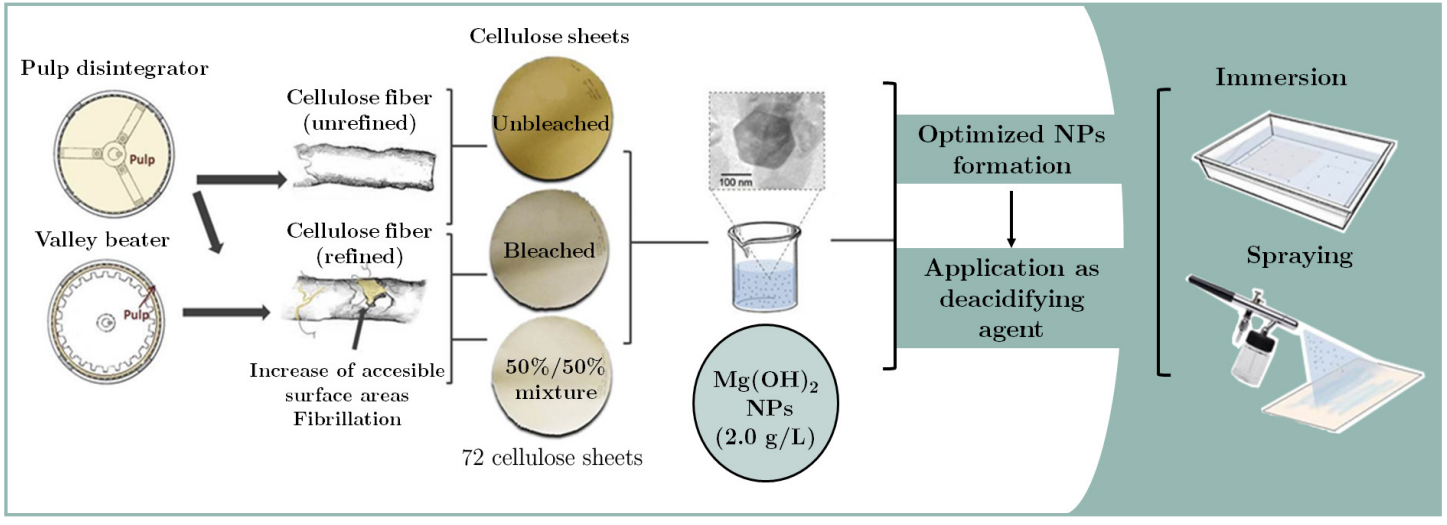

Figure 4.3.1: *Scheme of the experimental set-up of the application of the magnesium hydroxide nanoparticles on the surface of unbleached, bleached and 50%/50% mixture of unbleached and bleached fibers.*

4.3.1. *Paper XI.* Application of magnesium hydroxide nanocoatings on cellulose fibers with different refining degrees.
Sierra-Fernandez, A.; Gomez-Villalba, L.S.; Rabanal, M.E.; Fort, R.; Csóka, L.
RSC Advances 6, **2016,** doi: 10.1039/C6RA10336G

This research work explored how highly aging-resistant cellulose fiber sheets can be obtained by their modification with $Mg(OH)_2$ nanoparticles. This type of nanoparticles can inhibit or delay the cellulose degradation by acid hydrolysis, one of the more important open problems in the field of the preservation of the documentary heritage, producing a safe and stable deacidification. After their attachment to cellulose fibers, they provide an alkaline carbonate buffer reserve for deacidification and reduce the rate of degradation processes.

For this specific application, the deposition of the nanoparticles over the surface of the cellulose sheets was considered an important point to take into account in order to produce a protective coating from aging. As pointed out in our previous studies (*Papers II and IV)*, the increase of the synthesis temperature (180 °C) produced the generation of larger particle sizes and the prolonged reaction time (12 h) at this synthesis temperature improved the crystallinity degree of the $Mg(OH)_2$ particles. This is why in this study, the nanocrystalline $Mg(OH)_2$ particles obtained by hydrothermal synthesis method at a constant reaction temperature of 180 °C for 12 hours were selected for the treatment of the pine cellulose sheets. Their larger average particle size of 160 ± 40 nm with a thickness of ~18 nm, which allow their deposition over the surface of the cellulose sheets and their high chemical homogeneity and purity, were chemical properties considered suitable for paper conservation. Furthermore, this work also explored whether the refining degree and the chemical composition of the cellulose fibers influences the effect of applying $Mg(OH)_2$. Hence, two types of pine cellulose fibers were used in this study: i) bleached with low lignin content (<0.5%), and ii) non-bleached chemi-thermomechanical pulp with high lignin content (22.5%). The initial tests in our laboratory showed that more compact sheets were obtained if the bleached fibers were refined before mixing with unbleached fibers. For this reason, prior to sheet making the cellulose fibers were disintegrated in a laboratory pulp disintegrator machine up to 35 Schopper-Riegler degrees (SR °). Thus, cellulose fiber sheets bleached (B) and refined unbleached fibers (UB) as well as their 50%/50% mixture (M) were fabricated. Then, they were treated with $Mg(OH)_2$ nanoparticles by using two main methods used for the modification of the paper surface with inorganic dispersions: spraying and immersion. The main objective of this study was thus to investigate the influence of $Mg(OH)_2$ nanoparticles on the properties of the different types of cellulose sheets and to establish whether the observed effects depend on their initial morphology.

The main results showed that the $Mg(OH)_2$ nanoparticles synthesized via hydrothermal method were successfully deposited onto pine cellulose fibers with different refining degrees and chemical compositions. These findings also showed for the first time that the physical and mechanical properties of the pine pulp fibers can be modified by the joint action of the presence of residual lignin and heteropolysaccharides in the pulp, the low consistency refining process and the application of brucite nanoparticles. Particularly,

the refining degree of cellulose played an important role in the treatment of the cellulose composites with magnesium hydroxide nanoparticles. Therefore, the refined cellulose sheets experienced an increased fibrillation and fines generation together with the gel-like layer throughout the cellulose network, which improved their mechanical properties and the interaction and adsorption of magnesium hydroxide nanoparticles into them. The presence of microfibrillated residual cell wall polymers in bleached fibers resulted in obtaining cellulose samples with higher smoothness and a strong fibril-fibril interaction. Thus, the refined sheets made with the mixture of the fibers (M type) exhibited higher tensile indices (strengths), paper smoothness and aging resistance compared to the refined and full bleached cellulose samples (B type). Besides, the methodological application of the magnesium hydroxide nanoparticles had a crucial role in the modification of the cellulose composites. While in the case of cellulose treatment by the spray-deposition process, the nanoparticles are deposited mainly on the fiber surface, most of the nanoparticles are distributed through the interior of the refined fibers treated by immersion. The $Mg(OH)_2$ nanoparticles facilitated the inter-fiber bonding and, consequently improved the smoothness of the paper sheets. In addition, the brucite nanoparticles were shown to be potential deacidifying agents, increasing the pH of the sheets to values in the range from 8 to 8.5 which is a recommended value for the paper protection found in the literature. These changes were higher when the nanoparticles were applied by immersion of the sheet into the dispersion. Moreover, the application of brucite nanoparticles did not significantly affect the mechanical properties significantly but it did improve the smoothness of all three types of paper sheets studied here.

These results showed that the modification of cellulose fibers with brucite nanostructured may contribute greatly to paper permanence.

Paper XI

Application of magnesium hydroxide nanocoatings on cellulose fibers with different refining degrees.
Sierra-Fernandez, A.; Gomez-Villalba, L.S.; Rabanal, M.E.; Fort, R.; Csóka, L.

Reprinted with permission from
RSC Advances, **2016**, doi: 10.1039/C6RA10336G

CHAPTER 5

Conclusions and Future directions

Chapter 5

Conclusions and Future directions

The rich cultural heritage is being destroyed faster than ever. Thereby, the development of new strategies to assure their conservation is needed to avoid more irreversible damage.

The present Ph.D thesis has firmly contributed in this direction with the design, optimization, and development of highly compatible inorganic nanomaterials for the preservation of stone heritage. This goal has been accomplished through the use of a strong interdisciplinary research activity, combining materials science and engineering, geology, biology, and/or conservation science in cultural heritage. Therefore, in the present chapter, the main conclusions and outlook of the thesis is given, which is structured in **three parts**. The first, concerning the design, optimization and development of new products based on **$Mg(OH)_2$ and $Ca(OH)_2$ NPs** for the consolidation of carbonatic stones is given in **section 5.1**. The general remarks about the design of new antifungal nanomaterials based on **Zn-doped MgO ($Mg_{1-x}Zn_xO$) NPs** for the protection of stone heritage is presented in **section 5.2.** Subsequently, the exploration of new applications of the **$Mg(OH)_2$ NPs for the production of age-resistant paper** is presented in **section 5.3**. Finally, the chapter is concluded with a **specific outlook** regarding the presented results of this Ph.D thesis (see **section 5.4**).

5.1. Summary of new consolidating products, based on $Mg(OH)_2$ and $Ca(OH)_2$ NPs

The properties of the hydroxide NPs depend on the synthesis method selected and they are crucial for their application in stone heritage preservation. Thus, the $Mg(OH)_2$ NPs were synthesized by using two synthesis methods: the hydrothermal method and the sol-gel method, and the results were comparatively studied. In this direction, a careful analysis of the physic-chemical properties and the textural and structural behavior of the different types of NPs synthesized have led to the following conclusions:

5.1.1. Regarding $Mg(OH)_2$ NPs obtained by hydrothermal method

The control in obtaining the $Mg(OH)_2$ NPs by using the hydrothermal synthesis method with high potential for their application in cultural heritage conservation was achieved. Pure and controlled magnesium hydroxide NPs with different morphologies, particle sizes, and preferred orientation were successfully synthesized by hydrothermal method, using magnesium nitrate hexahydrate ($Mg(NO_3)_2 \cdot 6H_2O$) and hydrazine hydrate ($N_2H_4 \cdot H_2O$) as starting materials.

The conditions of hydrothermal treatment significantly affected the crystallinity, the morphology and the particle size of all brucite nanocrystals prepared under different synthesis temperatures (150 ˚C, 180 ˚C, and 200 ˚C), different reaction times (4 h, 6 h, 12 h, 24 h, and 72 h), and reactant concentrations (high hydrazine (0.14 M) and nitrate (0.24 g) content; and low hydrazine (0.0002M) and nitrate (0.12 g) content). Therefore, variations in the growth of brucite crystals have been observed as a function of the temperature, the duration of the hydrothermal reaction, and the initial reactant concentrations.

It was possible to determine that controlling the reaction conditions (reaction time, synthesis temperature and reactant concentrations) during the hydrothermal synthesis method can result in pure and high crystalline $Mg(OH)_2$ NPs with specific particle size, shape, chemistry and textural properties, as confirmed by XRD, SEM-EDS, TEM, HR-TEM, and SAED analysis. This approach makes it possible to influence the properties of the nanomaterial (e.g. a suitable particle size according to the petrophysical properties of stone material, optimal stability, high reactivity, among others) to satisfy the specific needs for its application to cultural heritage materials. Particularly:

- An increase in synthesis temperature improved the crystallinity degree of the different brucite NPs and also, promoted the formation of particles with bigger uniform size.
- Larger reaction times induced the growth of bigger and more uniform size $Mg(OH)_2$ crystals with brucite structure.
- The role of reactant concentrations in the synthesis of $Mg(OH)_2$ NPs by using the hydrothermal method was also stated. The findings showed that the dose of hydrazine/nitrate and the reaction time can modify the dimensions of unit cell and thereby cause a possible change in the specific properties of the synthesized materials. Thus, smaller unit cell parameters were typical of samples synthesized with short reaction time (180 ˚C for 4 hours). In addition, the largest particles were obtained with high dose of hydrazine/nitrate and prolonged heating treatment (180 ˚C for 12 hours), reaching a mean size from around 1026 nm to 1240 nm. Besides, it was detected that the $Mg(OH)_2$ samples obtained using a low dose of hydrazine/nitrate, presented a lower density of defects and the samples synthesized with higher hydrazine/nitrate content developed strong preferential orientations. As the concentration of hydrated hydrazine increases, the growth direction of hexagonal flakes is oriented mainly along the {0001} basal plane. The use of hydrated hydrazine served thus as mineralization template in the hydrothermal process, which induced the specifically orientation of crystallization.
- The effect of electron beam irradiation on the brucite dehydration was to determine differences between two concentrations of hydrazine/nitrate, and their effects on texture, porosity and behavior at atomic level. Then, the changes produced on the microstructure of samples and the generation of interfacial defects, before and after decomposition from $Mg(OH)_2$ to MgO, were discussed. The reaction times and changes in porosity during the exposition to high energy, as a result of the output of hydroxyl ions, were different when brucite samples had been prepared with high

of low doses of reagents. In this way, these results indicated how the dehydration process was faster in samples prepared with high hydrazine/nitrate content. The rapid formation of a porous surface, the amorphized cortex or the presence of highly oriented strains was detected from the very early stage of dehydration in these samples due to the presence of preferential orientations, which increased the reaction kinetic. However, when the $Mg(OH)_2$ samples were prepared with low content of reactants, the porosity changes turn out to be slower. In this way, the understanding of the decomposition reaction mechanism was of key importance to establish significant differences in the kinetics of reaction in both types of routines, and to achieving the reproducibility and control of NPs.

5.1.2. Regarding $Mg(OH)_2$ NPs obtained by sol-gel method

The sol-gel method enabled the synthesis of pure and controlled $Mg(OH)_2$ NPs with a high degree of crystallinity and well defined hexagonal morphologies with particle sizes between 40 to 80 nm, as confirmed by XRD, ESEM-EDS, TEM and SAED analysis.

The investigation of the effect of the synthesis method in the physical and chemical properties of the $Mg(OH)_2$ samples was carried out. Thereby, nanostructured $Mg(OH)_2$ synthesized by sol-gel method were comparatively studied with the brucite samples obtained by hydrothermal method. The research findings showed important differences in the crystallographic structures, the particle sizes and the morphologies of all brucite samples according to the synthesis method:

- While the samples obtained by hydrothermal method exhibited a preferential growth orientation affecting the (0001) plane, the brucite nanoparticles obtained by sol-gel synthesis method showed the obtaining of unoriented NPs. The generation of a strong preferential orientation in the brucite samples obtained by using the hydrothermal method was produced due to the use of hydrated hydrazine as reducing agent, which served as mineralization template in the hydrothermal process. In addition, the higher susceptibility of nuclei to grow at the orientation along the plane (001) detected in these samples could have been produced due to as a consequence of the high pressure and temperature used during the hydrothermal reaction.
- Regarding the particle size of the samples according to the synthesis method, the brucite samples synthesized by hydrothermal method showed the formation of variable particle sizes ranging from 350 nm to 1.8 µm in the largest length and a thickness of around 55-80 nm. In the case of the brucite NPs synthesized by sol-gel method, the particles exhibited smaller and uniform size ranging between 40 to 80 nm and a thickness of 4-9 nm.
- The generation of more uniform and defined hexagonal nanoflakes was also detected in the brucite NPs obtained by sol-gel method, in comparison with the samples synthesized by hydrothermal method, which exhibited more irregular shapes.

The combination of CL analytical technique with the XRD and TEM-ED

analysis resulted especially useful for the study of the different magnesium hydroxide NPs obtained by different synthesis methods. As general findings:

- CL results showed that the luminescence spectra exhibited a strong dependence on the particle orientation. Thus, the luminescence spectra for the samples in oriented along (0001) plane were dominated by emission bands at 3.25 eV, 2.96 eV and 2.66 eV. However, when the CL emission of the samples were registered in the $(11\bar{2}0)$ plane, the luminescence spectra were dominated by an emission band at 3.03 eV, preserving the emission bands at 2.57 eV and at 3.03 eV.
- The CL emissions obtained applying 20 kV accelerating voltage showed the signals corresponding to the presence of magnesite (~ 2.91 eV, ~ 2.54 eV and ~ 1.89 eV), in the inner part of the sample obtained by sol-gel method. This presence of magnesite in the sol-gel sample was produced by carbonation process. In this way, these findings pointed to the sol-gel synthesis method as a potential method to obtain nanoparticles with important physical and chemical properties, highly reactive with a rapid carbonation process.
- The presence of magnesite in the $Mg(OH)_2$ NPs synthesized by sol-gel method was also determined by XRD and SAED analysis.

5.1.3. Regarding the synthesis and morpho-structural characterization of $Mg(OH)_2$ and $Ca(OH)_2$ NPs

The sol-gel synthesis method used in this Ph.D thesis enabled the growth of non-aggregated $Mg(OH)_2$ and $Ca(OH)_2$ NPs with different magnesium and calcium hydroxides weight ratio (10:90 wt%; 90:10 wt% and 50:50 wt%), specifically designed and tailored for application in the dolostone and limestone used in built-heritage.

- The X-Rays diffraction patterns obtained for the magnesium and calcium hydroxides NPs with different weight ratios (10:90 wt%; 90:10 wt% and 50:50 wt%), exhibited the typical diffraction peaks of the brucite and portlandite structures confirming the high purity and the chemical composition of the different hydroxide NPs.
- Quantitative analyses of phase proportions calculated from rietveld refinement of XRD data provided values of: i) 9.21% for $Mg(OH)_2$ and 90.79% for $Ca(OH)_2$, in the $Mg(OH)_2/Ca(OH)_2$ NPs (10:90 wt%) sample; ii) 90.49% for $Mg(OH)_2$ and 9.51% for $Ca(OH)_2$, in the 90:10 wt% sample; iii) 47.94% for $Mg(OH)_2$ and 52.06% for $Ca(OH)_2$, for the 50:50 wt% sample. The calculated lattice parameters for $Mg(OH)_2/Ca(OH)_2$ samples revealed that the $Mg(OH)_2$ presented values slightly high than that of pure $Mg(OH)_2$ NPs. The little increase in cell parameters could be due to an excess structural OH which mostly affects the unit cell dimensions.
- The particle sizes of the $Mg(OH)_2/Ca(OH)_2$ NPs were between ~30 to ~450 nm, with well-defined hexagonal shapes and high crystallinity. It is noted that, while the sample based on $Ca(OH)_2$ exhibited hexagonal shape particles with two particle size distributions: a primary and bigger particle size of around 340.3 ± 123nm, and a smaller particle size of 149.8 nm ± 62 nm corresponding to aggregated particles. Whereas, the $Mg(OH)_2$ and the Mg-Ca hydroxide NPs with weight ratios of 10-90 wt%, 90-10 wt%, and 50-50 wt% showed lower uniform particle size of

around 60.3 ± 19 nm; 64.7 nm ± 34 nm; 34.1 ± 4.7 nm; and 30.13 ± 10 nm, respectively. The findings suggested that $Mg(OH)_2$ could slow down the $Ca(OH)_2$ crystal growth diminishing its particle size up to 78%. The adsorption of impurities on the growing crystal surface could be linked to their crystal growth inhibitory effects, which could reduce the growth of the affected crystal faces.

The dehydration process of nanostructured Mg-Ca hydroxide into Mg-Ca oxide was also studied by TEM-HRTEM. Thus, the changes in morphology, porosity, structural defects, phase transformations and chemistry as a result of the exposition to the electron beam were studied in Mg-Ca hydroxide ($Mg_{0.97}Ca_{0.03}(OH)_2$) nanoparticles by combining TEM, HRTEM, EELS and image analysis. To that respect it can be concluded that:

- Although the $Mg_{0.97}Ca_{0.03}(OH)_2$ nanoparticles had a similar behavior that $Mg(OH)_2$ NPs during the dehydration process, the presence of calcium could affect the transformation time and at the same time cell parameters and hence its specific properties could also be affected. Differences in the ionic radius (Ca^{2+} 0.99Å > Mg^{2+} 0.66Å), could be responsible for the generation of atomic defects, which affect the kinetic of reaction modifying the hydroxide into oxide reaction time.
- The study of the structural changes under electron beam irradiation showed different stages of transformation: i) the progressive changes from brucite to periclase; ii) a mass loss in the Mg-Ca hydroxide particles during the dehydration, marked by a local reduction thickness of 34%; and iii) the formation of an intermediate dehydrated brucite phase.
- The comparison of these results with the findings obtained for the pure $Mg(OH)_2$ nanoparticles showed an increase in the stability of the $Mg_{0.97}Ca_{0.03}(OH)_2$ nanoparticles under electron beam irradiation with slower decomposition reactions. Considering these results, it can be conclude that Calcium ions (Ca^{2+}) could modify different properties of the $Mg(OH)_2$, such as its catalytic performance.

5.1.4. Regarding the application of $Mg(OH)_2$ and $Ca(OH)_2$ as consolidating agents

The Laspra dolostone (Asturias, Spain) was selected to study the effectiveness of hydroxide NPs as consolidating products for stone heritage. This stone substrate was selected because its porosity and mineralogical composition. Particularly, Laspra dolostone is a fossiliferous dolomicrite composed mainly of dolomite (around 90 wt%), and characterized by its open porosity (around 37%) (see *Chapter 3* for more details). The selection of the type of nanoparticles according to the petrophysical properties and chemical composition of the stone substrate was achieved. Thereby, the dolostone substrates were treated with a solution of $Mg(OH)_2$ NPs obtained by hydrothermal method and $Mg(OH)_2$/$Ca(OH)_2$ 50:50 wt% NPs synthesized by sol-gel method. The consolidating action of these nanomaterials in the stone heritage is based on their transformation into carbonate forming through the action of atmospheric CO_2 in the presence of moisture (see *Chapter I*). For this reason, the behavior of these types of nanomaterials when they are exposed under controlled conditions to a high relative humidity of 75% was studied, before being applied to the stone substrates.

- The carbonation reaction of the $Mg(OH)_2$ NPs synthesized by hydrothermal method was confirmed after 15 days of exposition at 75%RH by XRD and HR-TEM, owing to the formation of magnesium carbonate polymorphs, with the detection of a hydromagnesite minority phase ($Mg_5(CO_3)_4(OH)_2 \cdot 4H_2O$). After 31 days of exposition at 75%RH the presence of magnesite phase ($MgCO_3$) was detected in these samples by the replacement of brucite crystals by magnesite via dissolution/precipitation process. Moreover, the monitoring of particle size during the carbonation reaction showed an increase of their magnitude after 31 days at 75%RH, from an average size of around 160 ± 40 nm with a thickness of about 18 nm to a particle size of around 240 ± 30 nm and a thickness of around 20 nm. Therefore, these $Mg(OH)_2$ NPs showed a suitable particle size before and after the exposition to 75 %RH according to the small pore radii (0.2 µm) of the stone to treat, Laspra dolostone.
- The carbonation monitoring of the system composed by $Mg(OH)_2/Ca(OH)_2$ (50:50 %wt) NPs showed the simultaneous presence of both hydroxides ($Mg(OH)_2$ and $Ca(OH)_2$) arranged as interference fringes (Moiré frames). After 31 days of exposition at 75 %RH, it was possible to detect the development of magnesite ($MgCO_3$) as a result of the carbonation, occupying the external crust and the presence of calcite ($CaCO_3$) as stable and well-crystallized mineral. Thereby, the dolomitization process was confirmed as result of the crystallization of dolomite ($CaMg(CO_3)_2$) by partial substitution of Ca^{2+} and Mg^{2+} ions in the calcite structure. This system also showed an optimal particle size after 31 days of exposition at 75 %RH, reaching an increase from 30.13 ± 10 nm to 75.3 ± 20 nm. These results showed a high reactivity of as-prepared $Mg(OH)_2/Ca(OH)_2$ (50:50 %wt) samples, with rapid rates of carbonation and an optimal particle size for their use in the stone heritage consolidation field.

The different types of NPs ($Mg(OH)_2$ and $Mg(OH)_2/Ca(OH)_2$ (50:50 %wt) were applied in Laspra dolostone (Asturias, Spain), and the consolidation process was monitored before and after the treatment under a controlled environmental atmosphere of 75% Relative Humidity.

- After the treatment with $Mg(OH)_2$ NPs obtained by hydrothermal method, the surface appearance of the Laspra dolostone changed slightly due to the formation of a uniform layer over the surface. Moreover, it was possible to see how the pores were partially filled by the nanomaterial without being blocked.
- The penetration depth of the $Mg(OH)_2$ and $Ca(OH)_2$ NPs, and their spatial distribution into the stone matrix was monitored by *in situ* Neutron Radiography (NR). This study was carried out in a controlled sample chamber at 25°C, and 75 %RH at the neutron facilities at Paul Scherrer Institute (PSI, Villigen, Switzerland). Laspra dolostone was thus treated with the different systems of NPs with a concentration of 2.5 g/L in ethanol, by using two common methods of treatment: by brushing and partial capillary absorption. The following conclusions were derived:
  - From the beginning, the application method was found to be crucial to determine the final redistribution of the hydroxide NPs after the treatment. The study

revealed a maximum particle penetration of 0.55 cm after 100 minutes of treatment into the Laspra dolostone substrates treated with a solution of $Mg(OH)_2$/$Ca(OH)_2$ NPs 50:50 wt% 2.5 g/L in ethanol by brushing. However, during the drying phase, radiographs show the accumulation of nanomaterial just underneath the surface, limiting the penetration depth of the NPs into the stone treated.

- For the stone samples treated by partial capillary absorption the neutron radiographs clearly showed the position of the nanomaterial into the treated stones, reaching maximum particles penetration of 1.52 cm for the Laspra dolostone. Moreover, the distribution of the treatment into the lithotypes was preferably accumulated, filling greatly the moldic porosity in lithotypes.
- These results showed that the effectiveness of the NPs as consolidant product of stone is strongly affected by the methodological application of the consolidant product. Therefore, the dispersion of magnesium and calcium hydroxide NPs in ethanol can easily penetrate into the Laspra dolostone substrates treated by brushing and by partial capillary absorption. However, at the drying phase the application method has important implication for the migration of the nanomaterial, limiting the quality of consolidation in the treated stone. Moreover, the NR has proven to be an excellent tool to monitor clearly the NPs diffusion into porous carbonatic stone non-destructively.

Regarding the consolidant effectiveness of the ethanol dispersions of $Mg(OH)_2$/$Ca(OH)_2$ 50:50 wt% NPs (2.5 g/L) on the Laspra dolostone, a decrease in total porosity was detected in the dolostone substrates after the treatment due to the filling of pores by the consolidating product, giving an increase of the inner cohesion of the stone. Furthermore, an increase of 3% in ultrasonic velocity was produced after the treatment with the mixed formulation of NPs. This increase in the ultrasonic velocity values was related to the decrease in total porosity in stones due to the filling of pores by the consolidating product. Moreover, the surface hardness of the treated stones was also increased and the NPs were detected filling the pores and inter-crystalline dolomite grain contacts, without being blocked. This increase of hardness implied a higher cohesion degree of the stone substrates because the surface hardness was related to the mineral composition and their degree of cohesion.

Therefore, the designed inorganic nanomaterial based on $Mg(OH)_2$ and $Ca(OH)_2$ NPs constituted thus stable products with enhanced chemical-physical affinities for natural stone.

5.2. Summary of new antifungal materials based on Zn-doped MgO ($Mg_{1-x}Zn_xO$) NPs

In the present research work the combination of the strong antimicrobial activity of ZnO with the safe-to-use antimicrobial effectiveness and good compatibility of MgO with dolostone was taken as the starting point to develop new antifungal coatings highly compatible with the built-stone heritage. In this way, the obtaining of an effective antifungal treatment based on Zn-doped MgO ($Mg_{1-x}Zn_xO$) NPs with multifunctional

photocatalytic and antifungal properties for calcareous stone heritage was achieved. The morphological microstructural and chemical analysis of the different metal oxides NPs revealed:

- Pure MgO, ZnO and Zn-doped MgO ($Mg_{1-x}Zn_xO$) NPs were successfully processed via sol-gel method. Whereas the MgO, and ZnO NPs showed the typical diffraction peaks corresponding to the planes of MgO phase (periclase structure), and ZnO phase (zincite, wurtzite structure), a negligible shift was found in the diffraction peaks for the Zn-doped MgO NPs. This shift coupled with an increased intensity observed in the (111) plane of periclase was due to the substitution-diffusion of Zn^{2+} ions into the MgO lattice to form $Mg_{1-x}Zn_xO$ (x=0.096) phase. A little increase in cell parameters was also detected in the Zn-doped MgO NPs. Thus, this sample showed that the MgO was slightly high (a=b=c= 4.2283 Å) than that of pure MgO NPs (a=b=c=4.2249 Å) due to the incorporation of Zn^{2+} into the MgO lattice by substitution process.
- The MgO NPs exhibited thin plates with average sizes of around 39 nm ± 10 nm, and the ZnO NPS showed well-defined pseudo-hexagonal shape particles with a bigger particle size of around 130 ± 40 nm. Meanwhile, the Zn-doped MgO NPs showed the formation of quasi-spherical shape NPs with a uniform particle size of about 52 ± 13 nm. These differences suggested that the MgO could reduce or inhibit the ZnO crystal growth.
- The simultaneous presence of MgO and ZnO lattices were observed in adjacent 15- to 20-nanometer particles, which growth as aggregates mostly rotated with structures in parallel orientations, generating point defects, mostly dislocations, as was studied by HR-TEM. The relevant presence of structural defects was also confirmed by PL measurements. The PL excitation spectrum showed three bands, at 327, 379, and 392 nm, attributed to low coordinated surface oxygen ions, and a blue light emission peak centered at 437 nm was observed in the PL emission spectrum, which was ascribed to the structural defects, such as oxygen vacancies or Mg interstitials.

The photocatalytic experiments revealed that ZnO significantly improved the catalytic efficiency of MgO under UV light irradiation (MB removing higher than 80%, after 60 minutes of irradiation). The development of a high surface defects content detected in this sample changed its surface morphology, structural properties and defect density producing thus increased photocatalytic effectiveness in comparison with pristine MgO and ZnO NPs.

The *in Vitro* antifungal activity of NPs was evaluated against different fungal species: *Aspergillus niger*, *Penicillium oxalicum*, *Paraconiothyrium* sp., and *Pestalotiopsis maculans.* These microorganisms are of substantial concern because they have shown to be potentially active in solubilizing limestone through the production of oxalic acids.

- The *In Vitro* evaluation of the antifungal activity was first determined by the agar diffusion method in terms of zone of inhibition of fungal growth. These results revealed revealed that MgO and Zn-doped MgO NPs exhibited an increased activity in comparison with ZnO NPs, with well defined inhibition halos, presenting the

maximum activity the Zn-doped MgO NPs.

- The MIC was studied to determine the lowest concentration of metal oxide NPs that could completely inhibit mycelial growth and conidia germination of fungi. The MICS of MgO and Zn-doped MgO NPs against *A. niger* and *Paraconiothyrium* sp. were found to be 1.25 mg/mL, whereas the MICs against *P.maculans* were found to be 5 mg/mL for both types of NPs. Moreover, it was observed that the MIC against *P. oxalicum* was 0.625 mg/mL with Zn-doped MgO NPs, resulting more effective against *P. oxalicum* than other fungi.
- Importantly, the antifungal activity against *A. niger* and *P. oxalicum* of the metal oxide NPs as coating was studied firstly using treated glass slides as model substrates. The application of MgO and Zn-doped MgO NPs presented antifungal properties, inhibiting successfully the growth of *A.niger* and *P. oxalicum*. Fungal growth was clearly detected on noncoated glass slides as indicated by the presence of colonies. However no colony was observed on coated surfaces with MgO and $Mg_{1-x}Zn_xO$ NPs.

The application of the MgO and Zn-doped MgO NPs as protective coating was carried out in Laspra dolostone and Conchuela limestone.

- The results showed that the fungi-stone interactions are potentially conditioned by the petrograhic features of the stone substrates. Thus, the Laspra dolostone showed an increase bioreceptivity to fungal growth in comparison with Conchuela limestone. The higher porosity and increased microporosity detected in the Laspra dolostone would allow a greater bioreceptivity.
- The research findings revealed that the coatings substantially decreased the epilithic fungal growth of the dolostone and limestone substrates, indicating greater antifungal effectiveness on Zn-doped MgO NPs with a limited impact on their surface color. Thus, the increased antifungal efficiency of Zn-doped MgO NPs was also confirmed.
- For the endolithic colonization for Laspra dolostone and Conchuela limestone. The $Mg_{1-x}Zn_xO$ NPs-based treatment prevented the invasive microbial colonization on calcareous stone substrates. The improved antifungal activity detected in the $Mg_{1-x}Zn_xO$ NPs was attributed to their high superficial defects content produced due to the introduction of Zn ions into MgO.
- The successful antifungal properties of the Zn-doped MgO NPs revealed the use of this type of metal oxide NPs as promising agents to protect the stone heritage from colonization of lithic microorganisms. Moreover, the research work highlights the potential of surface defects for engineering advanced nanomaterials for stone cultural heritage.

5.3. Summary of the $Mg(OH)_2$ NPs for the production of ageint-resistant paper.

An additional application of the $Mg(OH)_2$ NPs synthesized by hydrothermal method was explored. Thereby, the idea to develop highly-age resistant cellulose fiber sheets with different chemical composition and refining degree by their modification with brucite NPs was explored. The following conclusions were derived:

- Pine cellulose fiber sheets were fabricated from bleached with low lignin content (<0.5%) and refined unbleached with high lignin content (22.5%) fibers, as well as their 50%/50% mixture. The structural and morphological analysis showed that the refined cellulose fibers exhibited pronounced fibrillation and the presence of fines together with the gel like layer throughout the cellulose network. At the same time, the most compact sheets were obtained with the mixture of the fibers. This could be due to the stronger inter-fiber interactions detected in these cellulose samples, which improved the mechanical strength and smoothness with respect to the cellulose sheets prepared from the single fiber type.
- The selection of $Mg(OH)_2$ NPs to produce a protective coating from aging in cellulose samples were obtain at 180 $^\circ$C for 12 h and with low dose of hydrazine/nitrate content. The selection was made according to: i) their large average particle size of around 160 $\pm$ 40nm with a thickness of around 18 nm, which allow their deposition over the cellulose surfaces, and; ii) their homogeneity and purity considered suitable for paper conservation. The NPs were applied over the cellulose samples by using two methods widely used for the modification of the paper surface with inorganic dispersions: spraying and immersion.
- The methodological application of the $Mg(OH)_2$ NPs played an important role in the modification of cellulose sheets. Whereas the treatment of brucite NPs by the spray-deposition method generated the deposition of the NPs mainly on the surface of fibers, most of the NPs were distributed into the cellulose samples treated by immersion.
- Besides, the findings showed that the physical and chemical properties of the pine cellulose samples can be modified by the joint action of the presence of residual lignin and heteropolysaccharides in the pulp, the low consistency of refining process and the application of $Mg(OH)_2$ NPs. Specially, the refining degree of cellulose played an important role in the treatment of cellulose with brucite NPs. The presence of microfibrillated residual cell wall polymers in refined fibers improved the interaction and the adsorption of brucite NPs into the cellulose samples. In addition, the brucite NPs facilitated the inter-fiber bonding and consequently improved the smoothness of the paper cellulose sheets and induced an increase in the pH of the sheets to values slightly basic (pH around 8).
- The different untreated and treated cellulose samples were exposed to thermo-hygrometric accelerated ageing. It was found that the physical properties of the treated cellulose samples were not significantly dependent on the environmental factors.

5.4. Outlook.

In this Ph.D thesis, different types of inorganic nanomaterials were explored. This was done to evaluate if these new formulations could bring answers to specific issues of crucial importance for the conservation of cultural heritage: i) the development of consolidating products based on $Mg(OH)_2$ and $Ca(OH)_2$ NPs for the consolidation of stone heritage; ii) the engineering of metal oxides based on $Mg_{1-x}Zn_xO$ NPs and designed for the antifungal protection of stone heritage, and iii) the application of brucite NPs on cellulose fibers in order to create high aging-resistant cellulose fiber sheets. In spite of the promising properties of the new nanomaterials developed for the cultural heritage preservation presented in this research work, additional aspects need to be considered.

The durability of the different inorganic NPs-based treatments on stone substrates need to be studied toward artificial aging (salt crystallization, wetting-drying, and freezing-thawing cycles) in order to determine and quantify their capability to enhance the durability of carbonatic stones. In this sense, it is also essential to study the factors that can influence the effectiveness of the innovative nanomaterials as consolidating and antifungal protective treatments for stone works of art in real outdoor conditions. Thereby, although these new nanomaterials have been specifically designed and tailored for their application in cultural heritage conservation, showing promising properties as consolidating, antifungal, and protective agents in laboratory conditions, more research work is needed about their behavior, effectiveness, and durability in an outdoor environment. Therefore, due to the high complexity of real aged stone surfaces, future research should focus on the analysis of the long-term treatment effectiveness after the application on real cases of stone building surfaces.

Additionally, more studies are needed in order to address the stability behavior of the developed inorganic nanomaterials being exposed to several thermohygrometric conditions (mainly different cycles of temperature, relative humidity, and/or rainfall), with emphasis on their effect on the crystallization kinetics and the development of structural modifications, which may affect the success of stone treatments. These studies should be conducted with the aid of advanced characteristics techniques (such as neutron scattering, three-dimensional atom probe tomography, HR-TEM), in multidisciplinary approaches. The advances in the optimization and non-destructive techniques is expected to strengthen the understanding and consequently, the effectiveness of new nanostructured materials for stone. In this direction, future studies will be conducted about the need of any binding agent to ensure an optimal adhesion of the nanoparticles applied to real deteriorated surfaces. This is specially important in theses cases in which stone surfaces are exposed to outdoor conditions for creating functional coatings able to exhibit several properties simultaneously, to simplify and improve the conservative treatments. At same time, as was shown, high surface defects content can play important roles on the mechanism of photocatalytic and antifungal properties of the NPs. Thereby, to explore the incorporation of metal oxide NPs into coating matrix in order to induce controlled defect sites could be an interesting goal to reach.

Furthermore, the antimicrobial activity of the metal oxide NPs will be studied against yeast (such as *Candida albicans*), gram positive (*Staphylococcus aureus*), and

gram negative (*Escherichia coli*) bacteria to determine another important spectrum of activity of the different metal oxide NPs.

It should be mentioned that promising results have been showed in different studies about the use of the $Mg(OH)_2$ as a smoking- and toxic-free additive in polymeric materials. This is why the exploration of the use of $Mg(OH)_2$ NPs coatings for cellulose samples to induce additional flame-retardant properties could be carried out by Limiting Oxygen Index Testing & Analysis (LOI).

Future research is also necessary to shed light on the human health risks and environmental implications resulting from the use of new nanomaterials for stone cultural heritage preservation.

The importance and application of the developed inorganic nanomaterials may also extend to other additional areas, such as geological, industrial and technological, showing an important impact of this thesis on different areas. The carbonation has interesting implication in CO_2 sequestration, being an excellent way to reduce greenhouse gas emissions, as alternative to carbon capture systems for power plants and other large point sources. To this extent, the different $Mg(OH)_2$ and $Ca(OH)_2$ NPs developed could be studied as environmentally friendly chemical due to the high capacity that have shown to absorb CO_2. Additionally, the different inorganic nanoparticles could be also used as additives in construction materials (e.g. mortars, renders, plasters) to modify and enhance its performance, its thermal and mechanical properties or to induce additional properties, such as antifungal and/or self-cleaning capacities.

Finally, the results derived from this thesis are expected to introduce new knowledge and nanomaterials to improve the conservation of world cultural heritage, developing an innovative approach in search of strategies for the cultural heritage preservation.